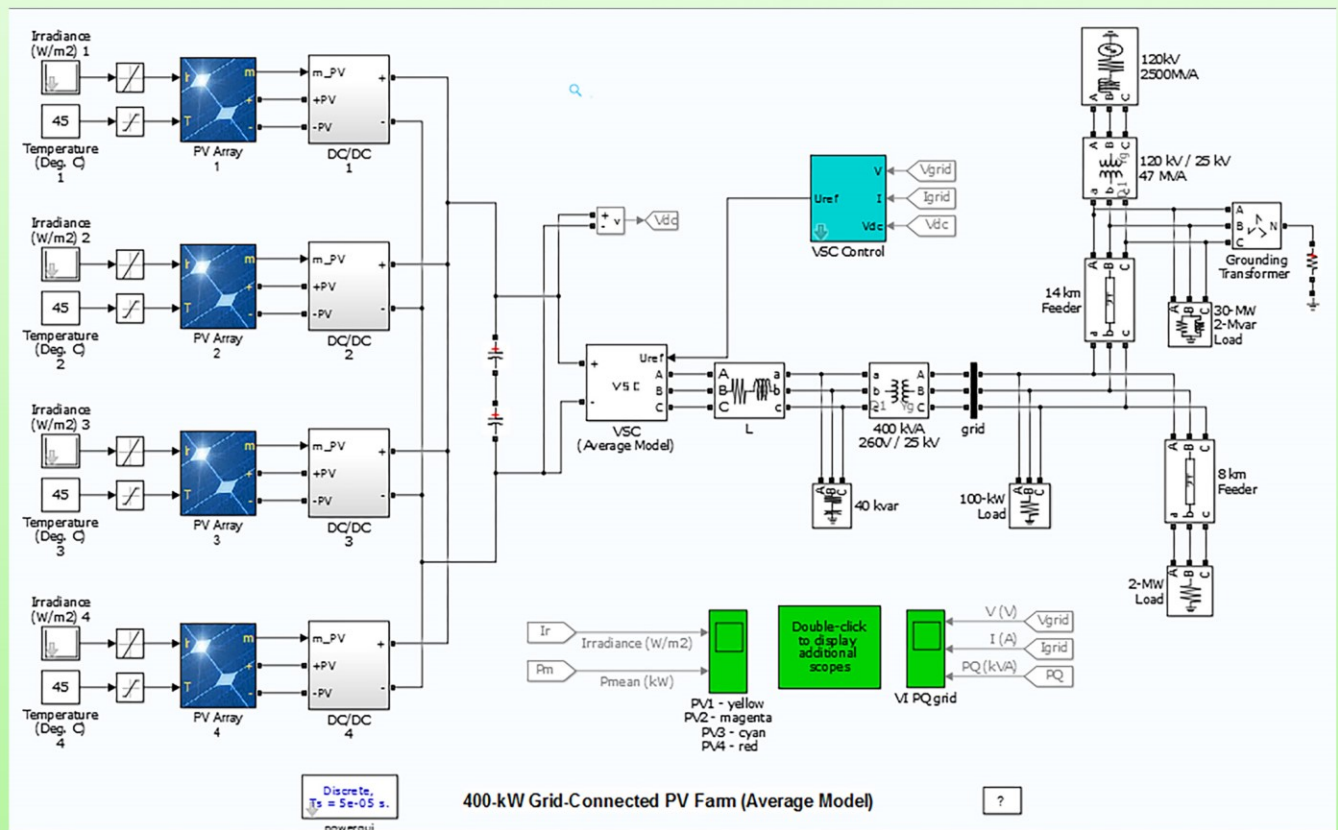


Trends in Renewable Energy

Volume 4, Issue 1, June 2018



Trends in Renewable Energy

ISSN: 2376-2136 (Print) ISSN: 2376-2144 (Online)

<http://futureenergysp.com/>

Trends in Renewable Energy is an open accessed, peer-reviewed semi-annual journal publishing reviews and research papers in the field of renewable energy technology and science.

The aim of this journal is to provide a communication platform that is run exclusively by scientists working in the renewable energy field. Scope of the journal covers: Bioenergy, Biofuel, Biomass, Bioprocessing, Biorefinery, Biological waste treatment, Catalysis for energy generation, Energy conservation, Energy delivery, Energy resources, Energy storage, Energy transformation, Environmental impact, Feedstock utilization, Future energy development, Green chemistry, Green energy, Microbial products, Physico-chemical process for Biomass, Policy, Pollution, Renewable energy, Smart grid, Thermo-chemical processes for biomass, etc.

The Trends in Renewable Energy publishes the following article types: peer-reviewed reviews, mini-reviews, technical notes, short-form research papers, and original research papers.

The article processing charge (APC), also known as a publication fee, is fully waived for the Trends in Renewable Energy.

Editorial Team of Trends in Renewable Energy

EDITOR-IN-CHIEF

Dr. Bo Zhang

P.E., Prof. of Chemical Engineering, Editor, Trends in Renewable Energy, United States

HONORARY CHAIRMEN

Dr. Yong Wang

Voiland Distinguished Professor, The Gene and Linda Voiland School of Chemical Engineering and Bioengineering, Washington State University, United States

Dr. Mahendra Singh Sodha

Professor, Lucknow University; Former Vice Chancellor of Devi Ahilya University, Lucknow University, and Barkatulla University; Professor/Dean/HOD/Deputy Director at IIT Delhi; Padma Shri Award; India Professor of Industrial Chemistry, CEO of Eurochem Engineering srl, Italy

Dr. Elio Santacesaria

VICE CHAIRMEN

Dr. Mo Xian

Prof., Assistant Director, Qingdao Institute of BioEnergy and Bioprocess Technology, Chinese Academy of Sciences, China

Dr. Changyan Yang

Prof., School of Chemical Engineering & Pharmacy, Wuhan Institute of Technology, China

EDITORS

Dr. Yiu Fai Tsang,

Associate Prof., Department of Science and Environmental Studies, The Education University of Hong Kong

Dr. Melanie Sattler

Dr. Syed Qasim Endowed Professor, Dept. of Civil Engineering, University of Texas at Arlington, United States

Dr. Attila Bai

Associate Prof., University of Debrecen, Hungary

Prof. Christophe Pierre Ménézo

University of Savoy Mont-Blanc, France

Dr. Moinuddin Sarker

MCIC, FICER, MInstP, MRSC, FARSS., VP of R & D, Head of Science/Technology Team, Natural State Research, Inc., United States Associate Prof., Biomass Processing Laboratory, Centre for Biofuel and Biochemical Research, Green Technology Mission Oriented Research, Universiti Teknologi PETRONAS, Malaysia

Dr. Suzana Yusup

Global Technology Development, Monsanto Company, United States

Dr. Zewei Miao

Pfizer Inc., United States

Dr. Hui Wang

North Carolina Agricultural and Technical State University, United States

Dr. Shuangning Xiu

Associate Prof., Institute of Chemical Industry of Forest Products, China

Dr. Junming XU

Academy of Forest, China

Dr. Hui Yang

Prof., College of Materials Science and Engineering, Nanjing Tech University, China

Dr. Ying Zhang

Associate Prof., School of Chemistry and Materials Science, University of Science and Technology of China, China

Dr. Ming-Jun Zhu

Prof., Assistant Dean, School of Bioscience & Bioengineering, South China University of Technology, China

MANAGING EDITOR

Dr. Bo Zhang

P.E., Prof. of Chemical Engineering, Editor, Trends in Renewable Energy, United States

EDITORIAL BOARD

Dr. Risabh Dev Shukla	Dean and Associate Prof., Department of Electrical Engineering, Budge Budge Institute of Technology Kolkata, India
Dr. Neeraj Gupta	Indian Institute of Technology Roorkee, India
Dr. Elena Lucchi	Politecnico di Milano, Italy
Dr. Muhammad Mujtaba Asad	Faculty of Technical and Vocational Education, Universiti Tun Hussein Onn Malaysia, Malaysia
Dr. Afzal Sikander	Associate Prof., Department of Electrical Engineering, Graphic Era University, India
Dr. Padmanabh Thakur	Professor and Head, Department of Electrical Engineering, Graphic Era University, India
Dr. K. DHAYALINI	Professor, Department of Electrical and Electronics Engineering, K. Ramakrishnan College of Engineering, Tamilnadu, India
Shangxian Xie	Texas A&M University, United States
Dr. Tanmoy Dutta	Sandia National Laboratories, United States
Dr. Efstathios Stefanos	Pontifical Catholic University of Ecuador, Faculty of Exact and Natural Sciences, School of Physical Sciences and Mathematics, Ecuador
Dr. Xin Wang	Miami University, United States
Dr. Rami El-Emam	Assist. Prof., Faculty of Engineering, Mansoura University, Egypt
Dr. Rameshprabu Ramaraj	School of Renewable Energy, Maejo University, Thailand
Dr. ZAFER ÖMER ÖZDEMİR	Kirklareli University, Technology Faculty, Turkey
Dr. Vijay Yeul	Chandrapur Super Thermal Power Station, India
Dr. Mohanakrishna Gunda	VITO - Flemish Institute for Technological Research, Belgium
Dr. Shuai Tan	Georgia Institute of Technology, United States
Shahabaldin Rezania	Universiti Teknologi Malaysia (UTM), Malaysia
Dr. Madhu Sabnis	Contek Solutions LLC, Texas, United States
Dr. Qiang Yan	Mississippi State University, United States
Dr. Mustafa Tolga BALTA	Associate Prof., Department of Mechanical Engineering, Faculty of Engineering, Aksaray University, Turkey
Dr. María González Alriols	Associate Prof., Chemical and Environmental Engineering Department, University of the Basque Country, Spain
Dr. Nattaporn Chaiyat	Assist. Prof., School of Renewable Energy, Maejo University, Thailand
Dr. Nguyen Duc Luong	Institute of Environmental Science and Engineering, National University of Civil Engineering, Vietnam
Mohd Lias Bin Kamal	Faculty of Applied Science, Universiti Teknologi MARA, Malaysia
Dr. N.L. Panwar	Assistant Prof., Department of Renewable Energy Engineering, College of Technology and Engineering, Maharana Pratap University of Agriculture and Technology, India
Dr. Caio Fortes	BASF, Brazil
Dr. Flavio Praticco	Department of Methods and Models for Economics, Territory and Finance, Sapienza University of Rome, Italy
Dr. Wennan ZHANG	Docent (Associate Prof.) and Senior Lecturer in Energy Engineering, Mid Sweden University, Sweden
Dr. Ing. Stamatis S. Kalligeros	Assistant Prof., Hellenic Naval Academy, Greece
Carlos Rolz	Director of the Biochemical Engineering Center, Research Institute at Universidad del Valle, Guatemala
Ms. Liliash Makashini	Copperbelt University, Zambia
Dr. Ali Mostafaeipour	Assistant Prof., Industrial Engineering Department, Yazd University, Iran
Dr. Camila da Silva	Prof., Maringá State University, Brazil
Dr. Anna Skorek-Osikowska	Silesian University of Technology, Poland
Dr. Shek Atiqure Rahman	Sustainable and Renewable Energy Engineering, College of Engineering, University of Sharjah, Bangladesh
Dr. Emad J Elnajjar	Associate Prof., Department of Mechanical Engineering, United Arab Emirates University, United Arab Emirates

Dr. Kenneth Okedu	Caledonian College of Engineering, Oman
Dr. Cheng Zhang	Sr. Materials Engineer, Medtronic, Inc., United States
Dr. Chandani Sharma	Assistant Prof., Department of Electrical Engineering, Graphic Era University, India
Dr. Kashif Irshad	Assistant Prof., Mechanical Engineering Department, King Khalid University, Saudi Arabia
Dr. Abhijit Bhagavatula	Principal Lead Engineer, Southern Company Services, United States
Dr. S. Sathish	Associate Prof., Department of Mechanical Engineering, Hindustan University, India
Mr. A. Avinash	Assistant Prof., KPR Institute of Engineering & Technology, India
Mr. Bindeshwar Singh	Assistant Prof., Kamla Nehru Institute of Technology, India
Dr. Yashar Hashemi	Tehran Regional Electric Company, Iran
Dr. Navanietha Krishnaraj R	South Dakota School of Mines and Technology, United States
Dr. SANDEEP GUPTA	JECRC University, India
Dr. Shwetank Avikal	Graphic Era Hill University, India
Dr. Xianglin Zhai	Poochon Scientific LLC, United States
Dr. Rui Li	North Carolina Agricultural and Technical State University, United States
Dr. Adam Elhag Ahmed	National Nutrition Policy Chair, Department of Community Services, College of Applied Medical Sciences, King Saud University, Saudi Arabia
Dr. Jingbo Li	Massachusetts Institute of Technology, United States
Dr. Srikanth Mutnuri	Associate Prof., Department of Biological Sciences, Associate Dean for International Programmes and Collaboration, Birla Institute of Technology & Science, India
Dr. Bashar Malkawi	S.J.D., Associate Prof., College of Law, University of Sharjah, United Arab Emirates
Dr. Simona Silvia Merola	Istituto Motori - National Research Council of Naples, Italy
Dr. Hakan Caliskan	Faculty of Engineering, Department of Mechanical Engineering, Usak University, Turkey

Table of Contents

Volume 4, Issue No. 1, June 2018

Reviews

Towards Sustainable Development: A Review of Green Technologies

Zaffar Ahmed Shaikh.....1-14

Articles

Main Line Fault Localization Methodology (MLFLM) in Smart Grid – The Underground Medium- and Low-Voltage Broadband over Power Lines Networks Case

Athanasios G. Lazaropoulos15-42

Broadband Performance Metrics and Regression Approximations of the New Coupling Schemes for Distribution Broadband over Power Lines (BPL) Networks

Athanasios G. Lazaropoulos43-73

Enhancement of the Rooftop Photovoltaic Array Characteristic Interconnected by the Grid under Partial Shading Condition by using Cascaded DC/DC Converter (WITHDRAWN)

Ahmed M. Mohamed, Salah M. Saffan, Ahmed M. Attalla, Hamdy Elgohary.....74-89

Mini-Reviews

Sustainable Management of Spent Hydroprocessing Catalyst

Changyan Yang, Jinlong Wu, Wei Wang, Bo Li, Bo Zhang, Yigang Ding.....90-95

Towards Sustainable Development: A Review of Green Technologies

Zaffar A. Shaikh *

Faculty of CS & IT, Benazir Bhutto Shaheed University, Lyari, Karachi, Pakistan

Received October 17, 2017; Accepted November 23, 2017; Published November 24, 2017

In recent years, climatic changes, global warming, energy depletion and other environment-related concerns have led to the emergence of green technologies. Researchers believe that the increase in the level of sustainable development will result in sustainable economics and societies. It will also have a very positive impact on sustainability in the future. Technical advancements in the modern society mark human creativeness and innovations. However, those technologies have resulted in the disruption of ecology from local to global level. Green technologies have a promising future in meeting the needs of economic sustainability. But, environmental and social sustainability factors need to be reinforced in a mutual manner. Both environmental and economic impact and efficiency of a technology should be analyzed before the implementation of technologies. It should be a win-win situation when economic and sustainable growths are highly emphasized. This paper reviews green technologies and discusses the challenges faced in advancing and implementing green technologies and trends that lead to sustainability. The paper also delineates regulatory policies and finance-related issues.

Keywords: Green Technologies; Clean Technologies; Sustainable Development; Sustainability; Review

Introduction

Green technologies are eco-friendly technologies that result in economic and social sustainability [1,2]. Green technologies may sound a sophisticated name, but it means no other than clean technology. In the earlier days, green technologies were known as environmental technologies [3]. From Information System perspectives, green technologies encompass environmentally friendly products that reduce the production of Greenhouses Gases (GHGs). They have in the past been viewed as a costly alternative to cheaper, unsustainable technology which has been in use all through.

Sustainability through green technologies means coming up with nature-friendly or eco-friendly technologies that not only meet human needs but at the same time minimize waste generation and support life today and in future [4,5]. Therefore, sustainable development must be met in all the three dimensions, i.e., social, economic and environment [6,7]. In this paper, we provide an overview of green technologies. The challenges faced in advancing and implementing green technologies and current trends that lead to sustainability are discussed. This paper also delineates regulatory policies and finance-related issues.

The rest of paper is organized as follows. The 'Review of Green Technologies' section explores application areas of green technologies. Next, in 'Challenges faced by Green Technologies' section, we discuss issues faced in advancing and implementing

green technologies. Further, the potential benefits of green technologies are delineated in ‘Opportunities for Green Technology Markets’ section. Finally, the study conclusions, author perspectives, and future research directions have been provided in ‘Conclusions’ section.

Review of Green Technologies

This section provides an overview of thirteen application areas of green technologies where they have been implemented successfully. Systematic and best evidence reviews have a methods section. This section enables motivated researchers to repeat the review. Narrative reviews do not have a methods section but should include some information about applied methods at the end of the introduction.

Water Treatment

Water is an essential element in life. In our world, several regions suffer from water contamination and scarcity. Water treatment is the act of removing undesirable contaminants from water. Undesirable substances may include biological, chemicals and even physical pollutants making it viable to be used in other applications. Water treatment is the solution preferred by many developing countries to reduce water stress. This solution may be focused on different perspectives depending on applications such as industrial and human activity [8].

Stages of water treatment

Today, the most common methods of water treatment include coagulation and flocculation, sedimentation, filtration, and disinfection (Figure 1).

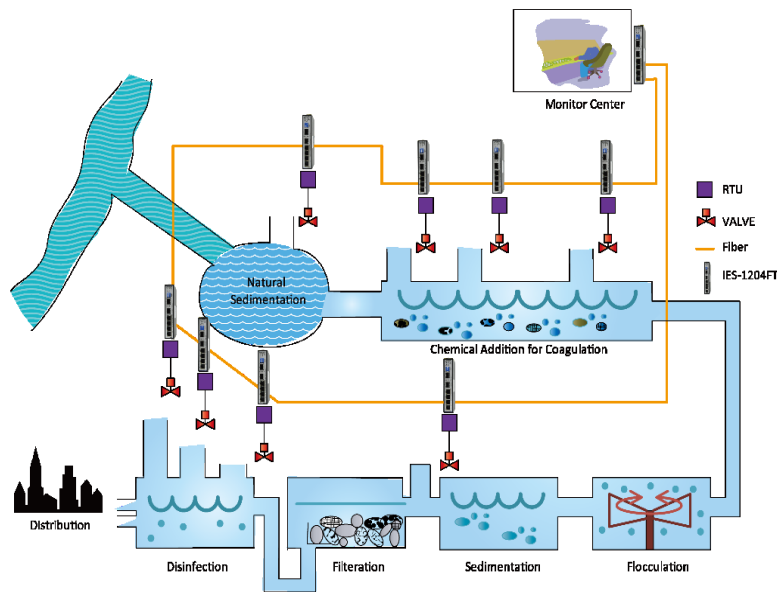


Figure 1. Basic model of water treatment scheme.

Coagulation and flocculation in most cases are often the first steps in water treatment. During this stage, a chemical with a positive charge is added to the water and the negative charge is attached to the dirt. This process detaches foreign proteins from water that form large particles called Floc [9]. Those large particles are then removed through sedimentation. The filters trap small particles that escape in the filtration stage. With current green technologies being implemented in water treatment process, most water treatment plants use advanced filtering systems such as Nano filters and membrane filters [7,10]. These filters trap minute particles [11].

The last stage is disinfection. The step removes biological organisms such as parasites, bacteria, viruses, and protozoa [9]. In the modern treatment plants, the commonly available disinfectants are chlorine and chlorimide. However, this method has proven to cause a carcinogenic effect. Thus, Ozonating is a process that is being encompassed by many developing countries [7].

Safe water is required to sustain life. Since clean water cannot be determined by physical examination only, chemical tests are done to determine its standard. The essential elements must be available and in the right quality [6]. The World Health Organization (WHO) and the United States Environmental Protection Agency regulate the quality of the water. After treatment, water is not piped to the households and industries, but the qualitative tests are done until the water meets the standard required by those bodies. These agencies have set regulatory policies that state the number of contaminants that can be found in the water of any specific area [12]. Every water treatment system must meet those Safe Drinking Water Act standards.

The WHO is laying out regulatory laws almost every year. In 2005, it was estimated that around 94% of the diarrhea cases reported could have been reduced by treating water for consumption [7]. The remedy was to use green technologies such as chlorination, safe can storage, filtration and solar treatment. Such a sustainability of water has been achieved in many countries [1,10,11].

Sewerage Treatment

This section portrays technology advancements at present that bring sustainable wastewater treatments.

Wastewater treatment can be termed as the process of removing solids, organics, and nutrients from the effluents of households and businesses. The knowledge of the sewerage treatment has evolved from early centuries. In the modern society, green technologies have been encompassed in this field to help removing physical, biological and chemical contaminants from the effluents to make them eco-friendly [11]. Wastewater treatment has a significance in that it allows the water from the industries to be treated before being discharged back to the environment [8,9]. It is believed that the wastewater contains harmful compounds that will not only interfere with the quality of the environment but have adverse human health complications [3,5]. While designing a wastewater treatment plant, the following factors are put into the consideration [7]:

- remove organic and biodegradable materials
- extract the part that is solid
- get rid of pathogenic microbes

A systematic modeling of the treatment plant is shown in Figure 2 on next page. Wastewater primarily occurs in four stages: screening, primary treatment, secondary treatment, and final treatment

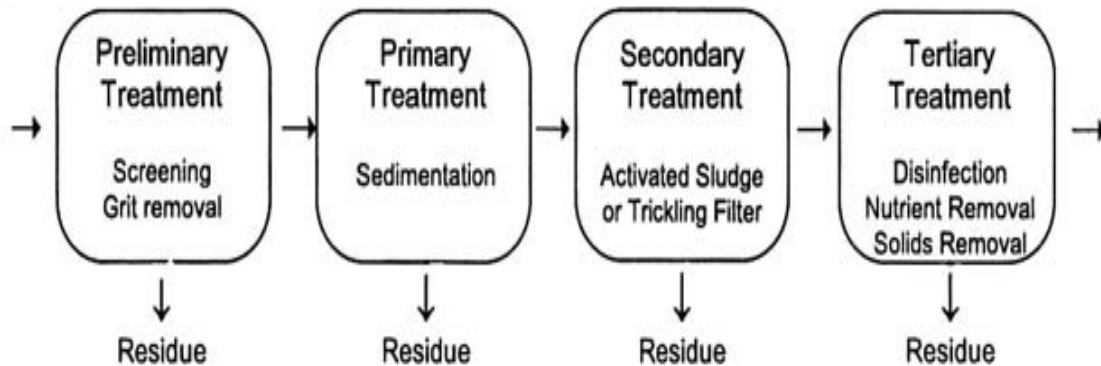


Figure 2. Common steps involved in wastewater treatment

Screening is the first stage of wastewater treatment. It removes large solids and objects from wastewaters. The primary steps separate the organic part of the waste through sedimentation tanks where they sink and settle into the ground. The effluent that leaves the main treatment contains high levels of Biochemical Oxygen Demand. Thus, secondary treatment proceeds to break down the organic matter using biological processes [6]. Wastewater contains a numerous number of nutrients. The final stage reduces the level of nutrients before discharging the wastewater into the rivers [5].

Eutrophication is one of the adverse effects that leads to environmental degradation. The growth of plants in the water affects the level of oxygen and carbon dioxide in the water causing the death of the aquatic animals [9].

The increasing level of environmental awareness has led to various industries and homesteads to deploy green technology techniques for reusability of wastewater [9,13]. The regulatory rules set by the government and environment conservative bodies force the industry to seek technologies that minimize wastewater being produced and ensure recycling [3].

Green technologies have ensured that the wastewater produced by the industry and homesteads can be used in other areas such as irrigation and livestock watering in arid and semi-arid areas after the treatment [11]. As manufacturing industries are being designed, many have found the importance of creating a recycling plant within the same plant to cut on the cost of wastewater management [6,10]. The final water effluent may be reused in the manufacturing process. The consensus is that it is easier to treat wastewater than to formulate new plans for obtaining fresh water from underground sources [5].

The technology advancements such as the use of Microbial Fuel Cells have a promising future in sustainable wastewater management [8,13]. Though technology has aroused some hitches in the universal application and economic viability of the project, further research is ongoing on how to make the technology the part of the future prototypes of the sustainable wastewater treatment [4,7,13].

Solid Waste Treatment and Management

Solid waste is one of the major aspects of sustainability that has been focused in the recent past [1,14]. The government-supported solid waste management schemes have resulted in the creation of innovative technologies that reduce waste generation [5,15].

In accordance with Product Stewardship Bill 2011 of Australia [16], there is an urge for every business to maintain responsibility and keep the environment free from hazardous waste. These regulations and codes played a pivotal role in economic and social development sustainability [1,2]. The waste disposals into the landfills go against sustainable development. The guidelines for a sustainable development are designed to cover six steps as shown in Figure 3 below, *i.e.*, Reduce, Reuse, Recycle, Recover, Incinerate and Landfill [5]. Disposing waste into landfills goes against the principles and means that new products will be processed from scratch. The end results are that there will be an increase in the demand for fuel, energy and other resources. Also, as the waste breaks into these landfills, the production of GHG emissions such as carbon dioxide and methane increases [17,18]. The technology used in waste management differ in developing and developed countries, rural to urban areas, and residential to industrial zones [8,15].

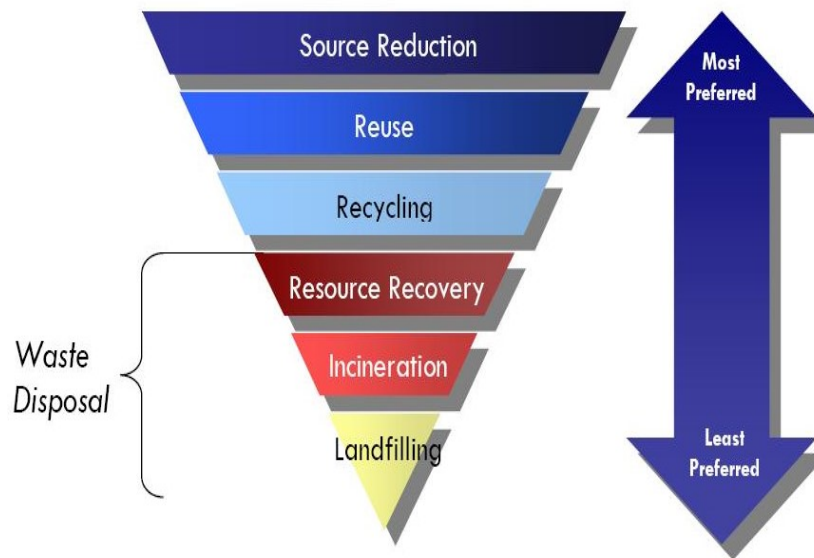


Figure 3. Solid waste management hierarchy.

The old technologies adopted by waste recovery industries saw the waste disposed of in the landfill's compost to form fertilizers. However, the latest green innovations have led to the development of aerobic digesters such as bioreactors that encompass in-vessel treatment of waste [15]. The new advancements in technologies not only does it manage waste but act as a source of renewable energy. Other waste management includes gasification and plasma synthesis, and zero waste programs [19].

Air Purification

Air pollution is largely becoming a technical issue. Air pollution is the introduction of harmful chemicals and GHGs into the air. They result in human and animal diseases and

end results are a damage to the atmosphere [11,17]. Air pollution is believed to be because of human struggle to achieve development. The common pollutants are industries and transportation devices. Various gasses such as sulfur dioxide, nitric oxide, carbon monoxide and more toxic gasses are emitted in large amounts. Air pollution has become an escalating factor after the GHGs have led the depletion of the Ozone layer [9].

Air filtration using green technologies has been encouraged in most industries. Most of the companies reduce air pollution by filtering GHGs during the emission process [18]. An example of technologies to reduce air pollution includes lead-free fuel and the introduction of catalytic converters. The introduction of such green technologies to trucks, buses and small vehicles will lead to significant reduction of air pollutants [11].

In the modern world, more fuel-efficient vehicles and hybrid electric cars have seen the reduction of air pollutants. These cars saw the reduction of gasoline intake by 50%. The technologies which have largely been implemented in most cities have seen air pollution reduction in the urban sector [7,8]. In power plant productions and industrial areas, filters in the emission chimneys have reduced gas pollution. Although no current technology has been put in place to deal with GHGs such as carbon dioxide, many industries have found a way to reuse gasses such as anaerobic bioreactors [20].

Environmental Remediation

Environmental remediation is an important focus of the green technologies aimed at maintaining sustainability [2,14]. This section focuses on green technologies that aid in the treatment of waste, help in the reuse, eliminate or reduce hazardous waste from the environment [5]. Environmental remediation knowledge has been evolving since the 20th century. Environmental remediation can be termed as the removal of pollutants or other contaminants from soil and waters. These pollutants can accumulate in living organisms and result to carcinogenic effects and other toxicity. In some cases, remediation actions can be because of a regulatory requirement, after assessment of human health and overall economic conditions of the environment [3].

Energy Conservation

Energy conservation refers to the effective production of energy that meets current needs without compromising on future availability [4]. Green technologies have brought a motivation to innovate new sources of energy including renewable sources while that replace fossil fuels. The energy crisis has never been an issue with green technologies. In fact, they have led to the introduction of devices that require minimum energy. In other words, energy conservation can be termed as energy efficiency and is a major pillar of sustainable development [11].

Energy conservation will see an increase in economics, financial and social security. Improved energy efficiency in homesteads, businesses, and transportation is expected to reduce energy demands by 2050s [21]. The green technologies have proven to be useful in some countries as it has slowed the rate of import and relying on the energy produced domestically.

Renewable Energy

Energy has become a vital factor in economic growth and social development of any country. With rapid power consumption becoming a global challenge, the need to find alternative and energy efficient technologies have been put in place. Fossil fuels are used as a source of energy for centuries. In definition, fossil fuel is a substance where solar

power is obtained, turned into chemical energy and stored in plants and animals who have been dead for decades [7]. When plants are acted on to produce energy, they emit GHGs. The GHGs result in adverse effects on the environment and future generation [3,17].

From a research study conducted in Malaysia in 2002 [18], fossil fuels are recorded as the primary source of electricity generation as shown in Table 1 below.

Table 1. Emission Factors of Fossil Fuels for Electricity Generation [18].

Fuels	Emission Factor (kg/kWh)			
	Carbon Dioxide	Sulphur Dioxide	Nitrogen Oxide	Carbon Monoxide
Coal	1.1800	0.019	0.0052	0.0002
Petroleum	0.8500	0.0164	0.0025	0.0002
Gas	0.5300	0.0005	0.0009	0.0005

Renewable energy sources (such as hydro, solar, geothermal and biomass) are of great significance to economic and environmental sustainability [1,2]. These clean technologies can lead to the production of large kWh with less emission of GHGs [11,17]. The International Energy Agency confirms that over 50% of electricity energy by 2050 will come from renewable energy sources [21]. However, a long-term grid is required to achieve sustainable renewable energy [22].

Capture and Storage Technology

Capture and Storage (CCS) is aimed at reducing GHGs emission. CCS captures carbon dioxide from environment and stores it in a viable surface. It follows a 3-step process as explained in Figure 4 below. The process involves capturing carbon dioxide from power plants, transporting carbon dioxide through pipes and the storage of carbon dioxide [23]. CCS technology sees carbon dioxide deposited in oil and gas recovery sites or un-mine-able coal sites.

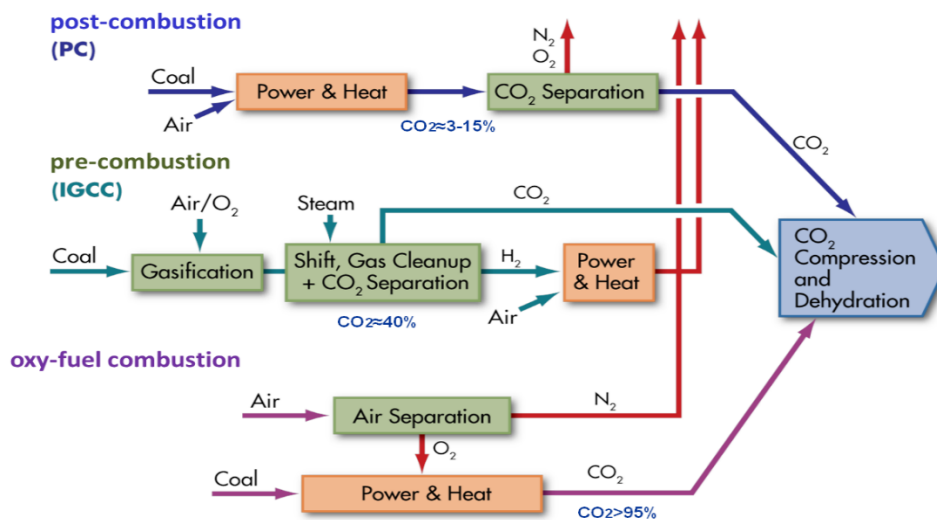


Figure 4. Summary of Carbon Dioxide Capture Technologies [17].

Though CCS technology seems to bring about sustainability, it has only been partially integrated on a commercial scale [1,17].

Green Building Practices

Conventional buildings are the number one contributors of GHGs. However, this sector has focused on coming up with green buildings [24,25]. In the wake of climatic changes such as global warming, Green Building Practices (GBPs) are receiving global acceptance [7,9]. The GBPs are environmentally friendly and more economically reliable. Industries have come up with a new technology of building houses that are eco- and nature-friendly.

The GBPs is a new technology in both developing and least developed countries. The research to determine how GBPs contribute to environmental sustainability is still substantial [1,2,11]. However, since they are economically productive, the countries especially the least developed countries have embraced the technology as a sustainable development [19].

Green buildings generally cost 2-7% more than the normal conventional buildings regarding the capital. The difference in money can be suggested to arise from modeling and designing cost. Green technologies require a sophisticated design which is costly. The rise of capital could also be because of green materials and green technologies used in the project [24]. Even though green buildings are costly, there are economic productivities that result from GBPs. As noted earlier, green technologies are eco-friendly, have more property values, are more energy-efficient and above all, they are energy efficient [24].

The impact of green buildings on the environment and social life [3,15,24,25] is attained by:

- efficient and efficient use of resources such as energy and water
- minimization of waste, water and reduction in environmental degradation
- providing occupation to employees, thus improving health and overall productivity

Sustainable Transportation

Sustainable transportation is a transport system that results in a positive impact on the environment. With current green technology being utilized in the manufacture of green vehicles, there will be less emission of GHGs compared to standard cars, thus leading to a sustainable environment [7,11]. Environment Protection Agency defines sustainable transport system as [26]:

- a transport system that allows society to quickly fulfill the urge or development at the individual level, company or even community level sustaining social-economic and environmental health
- a transport system that is efficient and supports the competitive economy and may result in economic advancement
- a sustainable system that reduces GHGs emission by utilizing a renewable source of energy and has reduced impact on a waste generation.

The introduction of electric hybrid cars leads to a reduction in carbon dioxide emitted during transport. The structure of hybrid cars is an internally designed combustion

engine with an electrical engine that helps in achieving sustainable transportation system [23].

Clean Industries

Clean industry is a term referred to industries that minimize environmental degradation. Clean industries encompass green technologies in the manufacture of products and in the long run activities that result in sustainability [1,2]. The term clean industry is used interchangeably with green industry and may also refer to the companies that function to solve environmental challenges [3].

It's hard to say the size of the distribution of green technologies worldwide as different countries are in a race to see who's winning the clean energy race [11]. For example, a report analyzed by Pew Charitable Trusts demonstrated that China's \$34.6 billion budget is leading in clean technology followed by United States' \$18.6 billion budget [27]. Also, there are policy laws that have contributed to the increase in efficient production of clean products.

Hydrogen and Fuel Cells

Hydrogen is a very rare element in the universe. Hydrogen can be extracted from different sources such as coal, crude oil, natural gas, and water. But, water is the only source known to be pollution free [6,28]. With modern technologies, internal combustion engines in most cars can be modified to run on arrays of fuels including hydrogen fuels. Vehicles that use hydrogen cell fuels are three times more efficient than those that burn gassed fuels in their engines [13,28,29].

The first hydrogen fuel was discovered by William Robert Grove, a Welsh physicist, in 1842 [30]. Later, NASA used fuel cells to launch its shuttle into a space mission. Hydrogen and Fuel cells have transformed industrial and social fabrics of most countries worldwide [13,31]. Today, many people believe that fuel cell technology will have a significant impact on a new technological renaissance. These innovations are expected to be environmentally friendly and will positively impact economy [31]. William Clay Ford Jr. (Executive Chairman, Ford Motor Company) said, "In today's world, solving environmental problems is an investment, not an expense". The significant features that make hydrogen cells more preferred over conventional fuel are that they have no emission, and they are quiet and free from vibration [13,28].

Agricultural Technology

Conventional agricultural technologies take a toll on the environment. There is the emission of GHGs, pollution of waterways and utilization of tangible resources [18]. Clean agricultural technologies range from drip irrigation to reduced water usage and from machinery farming to natural pesticides. Investment in agricultural sectors is likely to be influenced by cost-effectiveness, consumer demands, regulatory mandatory and public interest [17,29].

The green technologies are being used to improve the efficiency of crop planting and harvesting, use of chemicals for managing pests and weeds, making of fertilizers for covering water pollution and mitigating soil erosions [11]. Research institutes are investigating eco-farming practices for reducing the emission of methane, replenish soil carbon made and replace fossil fuels with fuel made from plant biomass [18].

Challenges Faced by Green Technologies

Technologies have impacted our society and its environment in many ways and helped in developing more advanced economies such as today's global economy [31]. Green technologies are environment healing technologies. They minimize environmental damages brought by technologies created by humans for their conveniences [8]. However, green technologies have been facing challenges that make it harder to realize their set goals. Such challenges include marketing challenges, economies of scales, financing problems, and regulatory and technical challenges [9]. Below we discuss major challenges faced today in implementing green technology initiatives, design and manufacture.

Development Challenges

Green technologies have experienced unreliability and disruption of fuel resource supplies. They make it difficult to have a lasting fuel contract as many small renewable energy programs lack palm oil plantations and mills [10]. Interconnections between other electricity providers and green technologies are not high enough to enable them to access energy supplies provided by renewable materials. The use of renewables has been limited by the price point. The renewable energy materials are costlier than available fossil fuel energy sources. Besides, natural gas availability presents a significant competition to the development of green technology advances [29].

Examining the effects and implications of national policy in making recommendations for appropriate technology extension has been a challenge. There are no sufficient advancements to examine these implications. This has delayed green technology development programs since some of the national policy influences are not well known [11].

Market Challenges

Expanding the occupation of green technologies in developing countries is most disadvantaged by the hurdles encountered during the trade development. There is inadequate knowledge about worldwide available environment-friendly technologies and the associated services in the market. This insufficient worldwide know-how about green technology suppliers slows down the manufacture of nature-friendly green products. Also, there are environmental and industrial concerns and views incorporated in devising of international policies on environment and trade.

The complex regulations of entering world's green technology markets keep out small and medium-sized businesses. Additionally, on the supply chain side of marketing a new product, it takes the consumers a lot of time to switch from old products to the new ones. This process can be challenging and long [10]. The green chemistry products have faced resistance and barriers to full acceptance. There is a lack of agreement on products to be considered safer for human use [8,11,32].

Technology Challenges

The world lacks adequate professionals with skills and knowledge matches green technologies and the values it stands for. For instance, in green buildings, professionals do not appreciate all components of green buildings. These include ventilation, temperature, and lighting control as well as efficient methods of obtaining energy that minimizes environmental damages [3,9,24].

As green technologies keep advancing, it must keep up with the latest technologies to meet demands to outgrow previous ways of handling their businesses. For effective communication across multiple countries, green technologies need real-time methods to access their data. Advancements in Information and Communication Technologies is a challenge that green technologies must continuously innovate for them to thrive and achieve their set goals [25].

Financing Challenges

Financing renewable energy projects have been a significant challenge. To fund renewable energy projects the small renewable energy project developers must have a firm financial standing. And they should be financially capable of doing so through equity injection rather than depending mostly on commercial loans. The developers lack adequate funds to finance their projects hence they start to stagnate. The Government should consider giving out a soft loan to sponsor renewable energy projects as national projects.

In agriculture field, green technologies have encountered challenges of identifying suitable technologies for generating income through sustainable agriculture, like rural renewable energy and ecological agriculture [9].

Regulatory Challenges

Managing global regulatory compliances regarding green technologies are a hurdle that slows down the development of green technologies. While massive investments are taking place within the US, there are extensive opportunities for renewable energy projects in other countries [19]. Getting those countries to comply with green technology regulations has proved impossible.

Organizations driven by green technology projects face challenges of identifying, meeting and managing regulations which vary widely from country to country [9]. Complex rules and regulations of entry into the green technology global markets make it difficult for medium-sized and small enterprises to penetrate the market via green technologies [2]. The effectiveness in implementing energy regulations differs significantly from one country to another. Some countries lack enforcement of government regulations to thrust ahead of green technology initiatives. For example, in Asia, there are no regulations on green building creativities. Some countries have green building agenda, but not all are supplemented with proper incentives or rules to spur growth [19,24].

Opportunities for Green Technology Markets

Green technologies consist of complicated and expensive but simplest technology advancements. They serve basic human needs and can explore new possibilities of exploring and improving comfort and leisure in human lives [8]. Green technologies offer new and interesting opportunities in the construction and development of extra durable, energy efficient materials to provide a reliable energy source [8,11]. New eco-friendly products and services can be created aiming at increasing growth rate while using minimum resources and causing minimum damage to the environment [3].

Reducing the number of resources used in developing green products would significantly reduce adverse impacts, hence avoiding economic and environmental collapse. Green technology market has identified renewable energy, water recycling and treatment services, the most substantial factors for export opportunities and growth. Green

technologies have a chance to open a competitive, powerful green technology sector in developing countries. This can be vital in spreading and extending green technology advancements and help minimize damages created by industrial growth [9].

CONCLUSIONS

The understanding of green technology challenges is making related technology sustainable and competitive. The green technology innovations solve or minimize problems especially in agricultural and manufacture sector.

We can overcome most of these problems through slowing down green technology developments if necessary steps are considered. For instance, the governments should offer to fund renewable energy projects when the owner is stuck because of the financial constraints. Or the government should put in place targeted financial enticements. They may include lowering local government taxes to encourage the import of renewable materials for energy and promoting adoption of green buildings in the market [2,24]. Moreover, removing fossil fuel subsidies would strengthen economic incentives for green technology advances. Educating public and training personnel dealing with green technology advances can provide the necessary knowledge required for technologies to work efficiently. If humans can manage to overcome challenges encountered by green technologies, it can have many beneficial purposes such as waste management, incineration through recycling, water and air purification and use of energy conserving devices. They will give people the comfort they need to live their lives comfortably.

From the above details, we can conclude that green technologies are a must in today's world. Since conventional technology is challenging sustainability, green technologies should be carried out to ensure sustainability of the eco-social environment. Though there are some shortcomings in the implementation of clean technology, but, if we see its long-term benefits, we and our future generations will surely benefit [4]. Also, technology will help us conserve our limited sources. Thus, the easiest way to maintain economic, environmental and social sustainability is education.

CONFLICTS OF INTEREST

The author declares that there is no conflict of interests regarding the publication of this paper.

REFERENCES

- [1] Davison, A. (2001). *Technology and the contested meanings of sustainability*. SUNY Press.
- [2] Klimova, A., Rondeau, E., Andersson, K., Porras, J., Rybin, A., & Zaslavsky, A. (2016). An international Master's program in green ICT as a contribution to sustainable development. *Journal of Cleaner Production*, 135, 223-239.
- [3] Huesemann, M., & Huesemann, J. (2011). *Techno-fix: Why technology won't save us or the environment*. New Society Publishers.

- [4] Wheeler, K. A., & Bijur, A. P. (2000). *Education for a sustainable future: A paradigm of hope for the 21st century* (Vol. 7). Springer Science & Business Media.
- [5] Williams, M., & Helm, A. (2011). Waste-to-energy success factors in Sweden and the United States. *Analyzing the Transferability of the Swedish Waste-to-Energy Model to the United States*.
- [6] Ahmed, S., Ahmad, M., Swami, B. L., & Ikram, S. (2016). A review on plants extract mediated synthesis of silver nanoparticles for antimicrobial applications: A green expertise. *Journal of advanced research*, 7(1), 17-28.
- [7] Biac (2010), 'Technology development and deployment to address green growth challenges', Business and Industry Advisory Committee to the OECD, 2010, Paris.
- [8] Clark, J. H., & Macquarrie, D. J. (Eds.). (2008). *Handbook of green chemistry and technology*. John Wiley & Sons.
- [9] Aithal, P. S., & Aithal, S. (2016). Opportunities & Challenges for Green Technology in 21st Century.
- [10] Dubey, R., Gunasekaran, A., Papadopoulos, T., Childe, S. J., Shibin, K. T., & Wamba, S. F. (2017). Sustainable supply chain management: framework and further research directions. *Journal of Cleaner Production*, 142, 1119-1130.
- [11] Jagarajan, R., Asmoni, M. N. A. M., Mohammed, A. H., Jaafar, M. N., Mei, J. L. Y., & Baba, M. (2017). Green retrofitting—A review of current status, implementations and challenges. *Renewable and Sustainable Energy Reviews*, 67, 1360-1368.
- [12] Weinmeyer, R., Norling, A., Kawarski, M., & Higgins, E. (2017). The Safe Drinking Water Act of 1974 and Its Role in Providing Access to Safe Drinking Water in the United States. *AMA Journal of Ethics*, 19(10), 1018.
- [13] Garland, N. L. (2010, May). US Department of Energy Fuel Cell Technologies Program. In *18th World Hydrogen Energy Conference 2010—WHEC 2010 Proceedings Speeches and Plenary Talks*.
- [14] Klionsky, D. J., Abdelmohsen, K., Abe, A., Abedin, M. J., Abeliovich, H., Acevedo Arozena, A., ... & Adhietty, P. J. (2016). Guidelines for the use and interpretation of assays for monitoring autophagy. *Autophagy*, 12(1), 1-222.
- [15] Paritosh, K., Kushwaha, S. K., Yadav, M., Pareek, N., Chawade, A., & Vivekanand, V. (2017). Food Waste to Energy: An Overview of Sustainable Approaches for Food Waste Management and Nutrient Recycling. *BioMed Research International*, 2017.
- [16] Australian Government. (2011). *Product Stewardship Act 2011*. Available at: <https://www.legislation.gov.au/Details/C2011A00076> (accessed on December 1, 2016).
- [17] Llamas, B., Navarrete, B., Vega, F., Rodriguez, E., Mazadiego, L. F., Cámara, Á., & Otero, P. (2016). Greenhouse Gas Emissions—Carbon Capture, Storage and Utilisation. In *Greenhouse Gases*. InTech.
- [18] Mahlia, T. M. I. (2002). Emissions from electricity generation in Malaysia. *Renewable Energy*, 27(2), 293-300.
- [19] Li, D. H., Yang, L., & Lam, J. C. (2013). Zero energy buildings and sustainable development implications—A review. *Energy*, 54, 1-10.
- [20] Centi, G., & Perathoner, S. (Eds.). (2014). *Green Carbon Dioxide: Advances in CO2 Utilization*. John Wiley & Sons.
- [21] International Energy Agency. (2014). *World Energy Outlook*. Paris, France: OECD Publishing, IEA.
- [22] International Energy Agency. (2014). *Energy Technology Perspectives*. Paris, France: OECD Publishing, IEA.

- [23] Leung, D. Y., Caramanna, G., & Maroto-Valer, M. M. (2014). An overview of current status of carbon dioxide capture and storage technologies. *Renewable and Sustainable Energy Reviews*, 39, 426-443.
- [24] Cassidy, R. (2003). *White paper on sustainability: A report on the Green Building Movement*. Supplement to Building Design and Construction. Available at: <https://www.usgbc.org/Docs/Resources/BDCWhitePaperR2.pdf> (accessed on November 23, 2017).
- [25] GhaffarianHoseini, A., Dahlan, N. D., Berardi, U., GhaffarianHoseini, A., Makaremi, N., & GhaffarianHoseini, M. (2013). Sustainable energy performances of green buildings: A review of current theories, implementations and challenges. *Renewable and Sustainable Energy Reviews*, 25, 1-17.
- [26] Mihyeon Jeon, C., & Amekudzi, A. (2005). Addressing sustainability in transportation systems: definitions, indicators, and metrics. *Journal of infrastructure systems*, 11(1), 31-50.
- [27] Pew Charitable Trusts. (2010). *Who's Winning the Clean Energy Race?* Available at: <http://www.pewtrusts.org/~media/legacy/uploadedfiles/peg/publications/report/g20reportlowresfinalpdf.pdf> (accessed on November 23, 2017).
- [28] Cannon, J. S. (1995). *Harnessing Hydrogen: The Key to Sustainable Transportation*. Available at: <https://www.afdc.energy.gov/pdfs/3033.pdf> (accessed on November 23, 2017).
- [29] Richhariya, G., Kumar, A., Tekasakul, P., & Gupta, B. (2017). Natural dyes for dye sensitized solar cell: A review. *Renewable and Sustainable Energy Reviews*, 69, 705-718.
- [30] Wisniak, J. (2015). Electrochemistry and Fuel Cells: The Contribution of William Robert Grove. *Indian Journal of History of Science*, 50, 476-490.
- [31] McDowall, W., & Eames, M. (2006). Forecasts, scenarios, visions, backcasts and roadmaps to the hydrogen economy: A review of the hydrogen futures literature. *Energy Policy*, 34(11), 1236-1250.
- [32] Clark, J. H., & Macquarrie, D. J. (Eds.). (2008). *Handbook of green chemistry and technology*. John Wiley & Sons.

Article copyright: © 2018 Zaffar A. Shaikh



This work is licensed under a [Creative Commons Attribution 4.0 International License](https://creativecommons.org/licenses/by/4.0/).

Main Line Fault Localization Methodology (MLFLM) in Smart Grid – The Underground Medium- and Low-Voltage Broadband over Power Lines Networks Case

Athanasios G. Lazaropoulos*

School of Electrical and Computer Engineering / National Technical University of Athens / 9 Iroon Polytechniou Street / Zografou, GR 15780

Received November 24, 2017; Accepted December 22, 2017; Published December 29, 2017

This paper assesses the performance of the main line fault localization methodology (MLFLM) when its application is extended to underground medium- and low-voltage broadband over power lines (UN MV and UN LV BPL) networks, say UN distribution BPL networks.

This paper focuses on the localization of main distribution line faults across UV MV and UN LV BPL networks. By extending the MLFLM procedure, which has successfully been applied to overhead medium-voltage (OV MV) BPL networks, the performance assessment of MLFLM is investigated with respect to the nature of the main distribution line faults, the intensity of the measurement differences and the fault location across the main distribution lines of the underground distribution power grid (either MV or LV grid).

Keywords: Smart Grid; Intelligent Energy Systems; Broadband over Power Lines (BPL) Networks; Power Line Communications (PLC); Faults; Fault Analysis; Fault Localization; Distribution Power Grids

1. Introduction

Thanks to the broad coverage of power grids and the low cost deployment of broadband over powerlines (BPL) system architecture, broadband over powerlines (BPL) networks act as a convenient technology solution in the emerging cooperative communications network of Smart Grid [1]. Compared against the other wired and wireless communications technologies that already interoperate in the Smart Grid, BPL networks can more easily deal with the “last mile” and “last-inch” problems since BPL networks are capable of providing broadband communications access to isolated places with significant broadband speeds by exploiting the already installed power grid infrastructure [2]. Another strong argument of the BPL technology is that its network components are already standardized systems by IEEE Std 1901 [3], which defines a standard for all BPL devices that are deployed across the transmission, distribution and indoor power grids including BPL devices used for various smart grid applications.

Since the transmission and distribution power grids were not originally intended for conveying high frequency signals, several adversarial factors, such as high frequency-selective channel attenuation and noise, foment the venture of communications signal propagation and transmission by severely deteriorating the quality of the supported

*Corresponding author: AGLazaropoulos@gmail.com

smart grid applications [4]-[10]. Apart from the inherent deficiencies of BPL networks, whose impact has thoroughly been examined in [4]-[8], [11]-[23], measurement differences, faults and instabilities of the power grid further deteriorate the broadband performance of BPL networks.

Until now, significant efforts have been made to counteract measurement differences and identify / localize faults and instabilities that may occur across the transmission and distribution power grids. Initially, a great convenience towards the aforementioned problems has been offered by the combined operation of the well-established hybrid method [4]-[8], [11]-[23] with piecewise monotonic data approximations (PMAs), such as L1PMA, L2WPMA and L2CXCV [24]-[32]. Their application to measurement data, such as channel attenuations and reflection coefficients, has allowed the restoration of theoretical transfer functions and the reflection coefficients, respectively, even if measurement differences of various intensities may occur [21], [33]-[36]. On the basis of the mitigation of measurement differences and the retrieval of the transfer functions and reflection coefficients for a given BPL topology, Topology Identification Methodology (TIM) suggests that the determination of the topological characteristics of the examined topology is a straightforward process through an identification procedure that compares PMA approximated data with the respective ones of a detailed BPL topology database [22], [37]. Another recently proposed smart grid application, which is supported by BPL networks and the combined operation of the hybrid method with PMAs, is the Fault and Instability Identification Methodology (FIIM) that deals with the identification and localization of various faults and instabilities that may occur across the transmission and distribution power grids, such as faults in branch lines, instabilities in branch interconnections and instabilities in branch terminations [37]. However, the only case that cannot be examined by FIIM is the identification and localization of main distribution line faults that have been covered by the Main Line Fault Localization Methodology (MLFLM) presented in [33], [34], [38].

Utilities employ either overhead or underground lines for implementing their distribution power grids for new urban, suburban and rural installations in accordance with different criteria like cost requirements, existing grid topology and urban plan constraints [8]. Until now, the previous smart grid applications have mainly applied to overhead transmission and distribution BPL networks. The main interest of this paper is the application and assessment of MLFLM to UN distribution power grids that are supported by BPL networks. In this paper, the pieces of experience concerning the identification and localization of main distribution line faults across overhead medium-voltage (OV MV) BPL networks is here extended in UN BPL networks, namely: (i) The extended TM2 method of [33], which is suitable for determining the reflection coefficients during the main distribution line fault cases, is here applied. (ii) The application of PMAs, such as L1PMA, that is used in order to mitigate the destructive role of measurement differences during the identification / localization of main distribution line faults of UN BPL networks is also done [34]. Anyway, the identification procedure through the application of the main distribution line fault identification percentage metric (MDLFI) is omitted in this paper, since a main distribution line fault across UN BPL network is assumed de facto; and (iii) all the properties of MLFLM, which have been thoroughly presented in [38], are also adopted in this paper. In order to push forward the knowledge frontier of [33], [34], [38], the following innovations are made in this paper: (a) the detailed database of coupling reflection coefficients and respective MDLFIs of [38] are reconstructed for all

the possible UN MV and UN LV BPL topologies. As in OV MV BPL networks of [33], [34], [38], the database also takes into account the nature of the main distribution line faults; (b) MLFLM procedure is tailored to UN BPL networks. Three new submethods, that accompany MLFLM and MDLFIs, are proposed in order to cope with the more challenging cases that can arise in UN distribution BPL networks during the localization of main distribution line faults; and (c) the MLFLM efficiency is evaluated while MLFLM results of UN BPL networks against measurement differences and main distribution line faults are compared versus the respective ones of OV MV BPL networks.

The rest of this paper is organized as follows: In Sec.II, the findings of [33], [34], [38], which concern UN BPL networks, PMAs and MDLFI, that are used in this paper are briefly outlined. In Sec.III, the required modifications concerning MLFLM application are demonstrated. Sec.IV assesses MLFLM efficiency in UN MV and UN LV BPL networks when measurement differences and main distribution line faults occur. Finally, the results of MLFLM application in UN BPL networks are compared against the respective ones of OV MV BPL networks. Sec.V concludes this paper.

2. Brief Presentation of UN BPL Networks, PMAs and MDLFI

2.1 MTL Configurations of UN MV and UN LV Lines

As concerns the MTL configuration of the examined UN MV BPL networks of this paper, the UN MV distribution line is the three-phase sector-type PILC distribution-class cable of Fig. 1(a). The cable arrangement consists of the three-phase three-sector-type conductors ($n^{\text{UNMV}}=3$), one shield conductor and one armor conductor. To electrostatically and magnetostatically protect the inner conductors, both the shield and the armor are grounded at both ends [6], [14], [39]-[43]. Apart from the aforementioned protection, the analysis in UN MV configurations is based on the consideration of the shield conductor as the reference one thus allowing the analysis to be focused only on the inner MTL set that consists of the three phases and the shield. Details about the exact dimensions of the UN MV MTL configuration of Fig. 1(a) are given in [14].

As concerns the MTL properties of the UN LV configuration, the UN LV distribution line that is examined is the three-phase four-conductor ($n^{\text{UNLV}}=3$) core-type XLPE distribution cable of Fig. 1(b). This cable arrangement consists of the three-phase three-core-type conductors, one core-type neutral conductor and one shield conductor. As it has already been assumed in the UN MV case, the shield is grounded at both ends and considered as the reference conductor permitting the analysis of UN LV configuration to be exclusively concentrated on the inner set of the UN LV cable [19], [20], [42]-[48]. The exact dimensions of the UN LV MTL configuration, which is used in the present work, are given in [14].

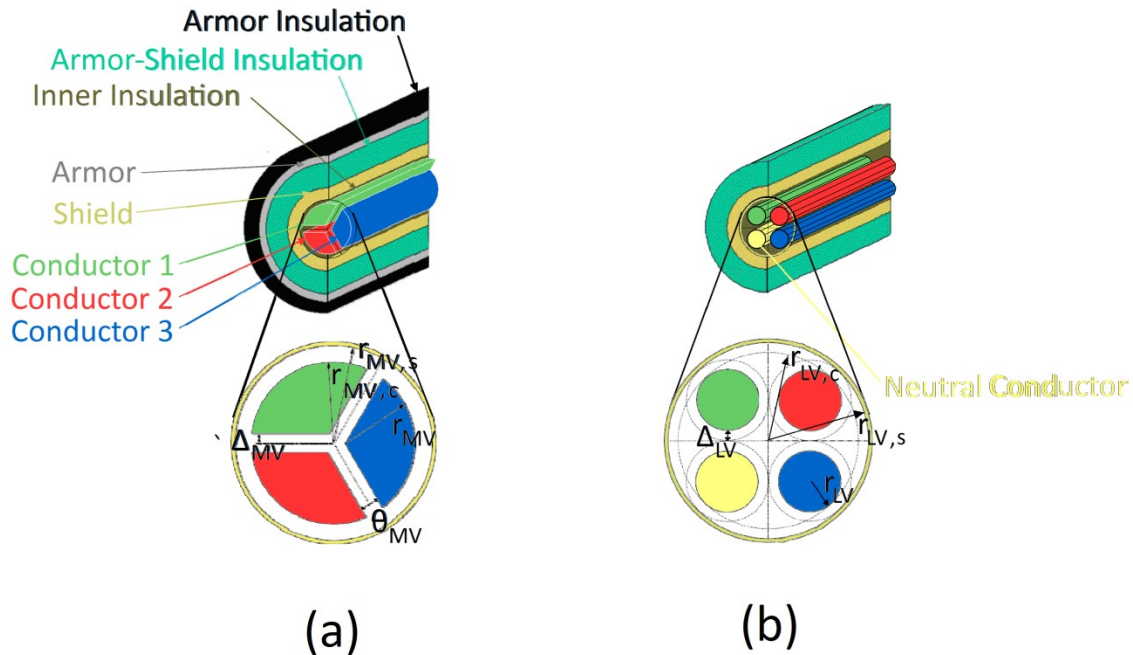


Fig. 1. Typical MTL structures [14], [43]. (a) UN MV. (b) UN LV.

The analytical formulation, which is adopted in this paper for the signal propagation analysis in UN distribution BPL systems, considers high frequency transmission in the general case of UN power lines consisting of multiple conductors surrounded by one common shield [6], [7], [19], [20], [42], [47], [49].

2.2 Topologies of UN MV and UN LV BPL Networks

The typical UN BPL topology of Fig. 2, being bounded by transmitting and receiving end and having N branches, is considered for the examined UN BPL connections of this paper. With reference to Fig. 2, average path lengths of the order of 200m are considered in UN MV and UN LV topologies [6], [7], [11], [12]. In fact, the definition of a maximum path length in UN BPL networks prevents high channel attenuations that may eliminate the broadband potential of BPL networks. Depending on the number of branches and their allocation across the transmission path, five indicative UN BPL topologies are defined that act as representative topologies of the respective UN BPL classes, namely [14]:

- (i) A typical underground urban topology (urban case A) with $N=3$ branches ($L_1=70\text{m}$, $L_2=55\text{m}$, $L_3=45\text{m}$, $L_4=30\text{m}$, $L_{b1}=12\text{m}$, $L_{b2}=7\text{m}$, $L_{b3}=21\text{m}$).
- (ii) An aggravated underground urban topology (urban case B) with $N=5$ branches ($L_1=40\text{m}$, $L_2=10\text{m}$, $L_3=20\text{m}$, $L_4=40\text{m}$, $L_5=60\text{m}$, $L_6=30\text{m}$, $L_{b1}=22\text{m}$, $L_{b2}=12\text{m}$, $L_{b3}=8\text{m}$, $L_{b4}=2\text{m}$, $L_{b5}=17\text{m}$).
- (iii) A typical underground suburban topology (suburban case) with $N=2$ branches ($L_1=50\text{m}$, $L_2=100\text{m}$, $L_3=50\text{m}$, $L_{b1}=60\text{m}$, $L_{b2}=30\text{m}$).
- (iv) A typical underground rural topology (rural case) with only $N=1$ branch ($L_1=50\text{m}$, $L_2=150\text{m}$, $L_{b1}=100\text{m}$).

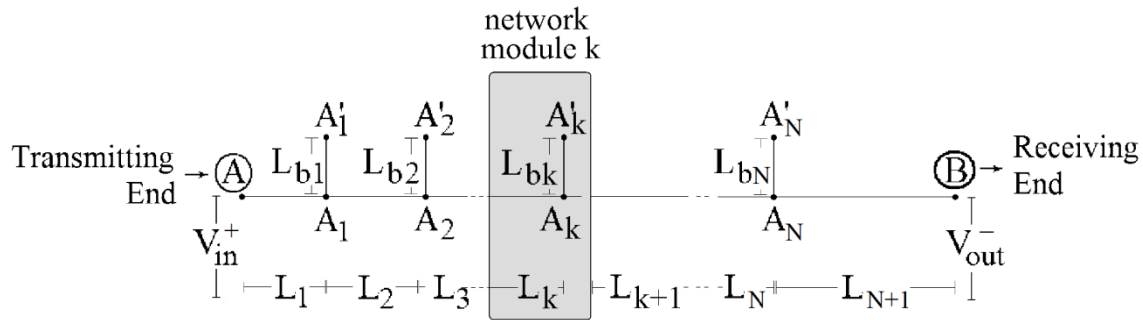


Fig. 2. Typical UN BPL topology with N branches.

- (v) The underground “LOS” transmission (“LOS” case) along the same end-to-end distance $L = L_1 + \dots + L_{N+1} = 200\text{m}$ when no branches are encountered.

Here, it should be noted that the aforementioned five indicative UN BPL topologies remain common either in UN MV or in UN LV BPL connections. Apart from the topological properties of UN BPL connections, the circuitual parameters need to be detailed. In accordance with [4], [5]-[7], [14], [16], [18], [19], [39], [44], [45], [47], [48], [50]-[52], the branching cables are assumed identical to the main distribution cables and the interconnections between the main distribution and branch conductors are fully connected. Also, the transmitting and the receiving ends are assumed matched to the characteristic impedance of the modal channels whereas the branch terminations are assumed open circuit.

Since the MTL configuration and the topological characteristics of UN BPL networks are already known, the well-established hybrid method that consists of: (i) a bottom-up approach that is based on the MTL theory and eigenvalue decomposition (EVD); and (ii) a top-down approach that is denoted as TM2 method and is based on the concatenation of multidimensional chain scattering matrices; is applied in order to determine the coupling channel attenuation and coupling reflection coefficients of UN BPL channels. More specifically, to cope with the main distribution line faults, the extended TM2 method has been proposed in [33] and tested in [34], [38]. Extended TM2 method is the required extension of the well-verified original TM2 method [4]-[8], [11]-[20], [47], [53], [54] since original TM2 method only deals with the transmission properties of BPL networks during their normal operation and not at the fault cases. While extended TM2 method receives the same inputs with original TM2 method, it gives as output the coupling reflection coefficients of an UN BPL network at its transmitting end when a main distribution line fault occurs across its transmission path.

2.3 Main Distribution Line Faults and Measurement Differences

Similarly to OV MV grids of [33], [34], [38], critical problematic conditions, such as the main distribution line faults, can occur across the UN distribution power grids having as primary result the electric power distribution blackout to consumers and as secondary result the interruption of smart grid broadband services that are based on the BPL networking. In accordance with [38], since a main distribution line fault occurs at a specific distance from the transmitting end, the original UN BPL topology is then divided into two new modified UN BPL topologies with each path length being equal or shorter

than 200m but the path length sum being equal to 200m. These two modified UN BPL topologies maintain as the only common point between them the point of the main distribution line fault. In order to study the propagation and transmission behavior of the modified UN BPL topologies, the main distribution line fault point is treated as a termination load that behaves as either short- or open-circuit termination depending on the fault nature. Here, it should be noticed that the original UN BPL topologies are characterized by terminal loads that are matched to the characteristic impedances of the modes examined. As proven in [38], the localization of main distribution line faults by using MLFLM becomes more effective when both modified UN BPL topologies are examined. Therefore, pairs of complementary modified UN BPL topologies to the original one are used whose topological characteristics primarily depend on the location of the main distribution line fault and the fault nature.

As presented in [34], [38], the identification and localization of main distribution line faults remain an easy and straightforward task only in the cases of zero measurement differences. However, this case remains rather a theoretical and special situation since measurement differences of various intensities occur that vary from time to time and location to location even across the same UN BPL topology.

Apart from the main distribution line faults, the existence of measurement differences may jeopardize the fault localization of MLFLM as indicated in [38]. In accordance with [22], the causes of the presented measurement differences can be grouped into six categories, namely: (i) Isolation difficulties of specific MTL parameters in time- and frequency-domain; (ii) Low accuracy and sensitivity of the used equipment during measurements; (iii) Cross-talk and resonant phenomena due to the parasitic capacitances and inductances of lines; (iv) The weakness of including specific wiring and grounding practices; (v) Practical impedance deviations of lines, branches, terminations and transmitting/receiving ends; and (vi) The isolation lack of the noise effect during the transfer function computations.

The strong point of MLFLM towards the mitigation of measurement differences is the adoption of PMAs during the process of measurement data of channel attenuation and coupling reflection coefficient in BPL networks [21]-[23], [33]-[38]. The application of PMAs, such as L1PMA [24]-[30], L2WPMA [31] and L2CXCVC [32], drastically improve the fault localization efficiency even in the case of significant measurement differences. When MLFLM is going to be applied, MLFLM receives as inputs for its PMA module the coupling reflection coefficient data of UN distribution BPL topologies, the measurement frequencies and the number of monotonic sections while MLFLM gives as output the main distribution line fault identification percentage metric (MDLFI) with respect to the distance from the transmitting end for the complimentary modified UN BPL topologies. In fact, MDLFI is a MLFLM accompanying performance metric, has been proposed in [23], [34], [37], [38] and is suitable for the identification and localization of main distribution line faults across BPL networks. On the basis of MDLFI minima, the localization of main distribution line faults is going to be accomplished in UN BPL networks.

2.4 MDLFI, MLFLM Database and Localization Procedure

According to the results of [33], [38], the main distribution line fault localization efficiency of MLFLM depends on the magnitude of the measurement differences and the complexity of the examined BPL topology. In fact, one main advantage of MLFLM is the

application of MDLFI metric to each pair of the available modified BPL topologies of MLFLM database bypassing the inherent drawback of MDLFI that is the MDLFI selective behavior with respect to the fault distance from the transmitting end (for more details see [33]).

Using both the available two coupling reflection coefficient measurement sites, which are the transmitting and receiving ends of the examined original UN BPL topology, to define the respective modified UN BPL topologies, the simultaneous minimization of the two MDLFIs (say, MDLFI₁ and MDLFI₂) leads to the exact localization of the main distribution line fault. Similarly to MDLFI of [38], MDLFI_k, $k=1 \dots 2$ of the respective two modified UN BPL topologies are given by

$$MDLFI_k = \frac{\sum_{k_{\text{sect}}=1}^{20} MDLFI_{\text{par},k}(k_{\text{sect}})}{600}, k=1 \dots 2 \quad (1)$$

where

$$MDLFI_{\text{par},k}(k_{\text{sect}}) = \sum_{i=1}^{30} \frac{\left| \overline{\Gamma_{\text{meas},k}^{\text{WtG}}(f_i, k_{\text{sect}})} - \overline{\Gamma_{\text{theor},k}^{\text{WtG}}(f_i, k_{\text{sect}})} \right|}{\left| \overline{\Gamma_{\text{theor},k}^{\text{WtG}}(f_i, k_{\text{sect}})} \right|}, k=1 \dots 2 \quad (2)$$

, $\overline{\Gamma_{\text{theor},k}^{\text{WtG}}}$, $k=1 \dots 2$ are the PMA approximated theoretical UN BPL coupling reflection coefficient column vectors of the respective two modified UN BPL topologies, $\overline{\Gamma_{\text{meas},k}^{\text{WtG}}}$, $k=1 \dots 2$ are the PMA approximated measured UN BPL reflection coefficient column vectors of the respective two modified UN BPL topologies, f_i , $i=1, \dots, 30$ are the measurement frequencies and k_{sect} is the number of monotonic sections considered in this paper, which ranges from 1 to 20.

As detailed in [38], PMA approximated theoretical UN BPL coupling reflection coefficient column vectors are computed for all the available modified UN BPL topologies when the original UN BPL topology is known. In order to implement the MLFLM database that consists of all these pairs of modified UN BPL topologies as well as their coupling reflection coefficients, the first step is the consideration of the length spacing L_s of main distribution line faults. Since the average transmission length is equal to 200m and the length spacing L_s that defines the database accuracy is assumed equal to 10m in this paper, there are $\left(\frac{200\text{m}}{10\text{m}}\right) + 1 = 21$ pairs of modified UN BPL topologies for given original UN BPL topology. Except for the database properties regarding the number of the considered UN BPL topologies, a set of database specifications is here given [22], [38]:

- $k_{\text{sect},\text{min}}$ is the lower monotonic section bound, which is assumed to be equal to 1 in this paper, and $k_{\text{sect},\text{max}}$ is the upper monotonic section bound, which is assumed to be equal to 20 in this paper.
- The operation frequency range and the flat fading subchannel frequency spacing are assumed equal to 1-30MHz and 1MHz, respectively. Therefore, the number of subchannels u in the examined frequency range is equal to 30.

- Arbitrarily, the WtG³ coupling scheme is applied during the following simulations [6], [18], [55]-[58].
- For each UN BPL topology that is considered in the database, the two cases of termination loads that are short- and open-circuit terminations are considered.

Based on the measured coupling reflection coefficients of the modified OV MV BPL topologies, the theoretical coupling reflection coefficients of all the available modified OV MV BPL topologies of the MLFLM database and MDLFIs of the set of the respective modified OV MV BPL topologies, MLFLM has achieved to exactly localize the main distribution line faults across original OV MV BPL topologies [33], [34], [38]. Here, MLFLM is applied to UN MV and UN LV BPL networks by exploiting the validated strong points concerning the handling of MDLFIs; say, the double coupling reflection coefficient measurement sets (i.e., the first set from the transmitting end side and the other one from the receiving end side of the original UN BPL topology) of the MLFLM database and the simultaneous minimization of MDLFIs. Since each set of coupling reflection coefficients accompanies the topological characteristics of the respective set of modified UN BPL topologies in the database, the exact location of the main distribution line fault across the original UN BPL topology is a straightforward process. Visually, the exact location of the main distribution line fault is found by studying the graphical representation of MDLFIs versus the distance from the transmitting end and spotting the location where MDLFIs simultaneously present their minimum value.

3. Numerical Results and Discussion

The five original UN BPL topologies of Sec. 2.2, which remain common for both UN MV and UN LV cases, are simulated with the purpose of evaluating the MLFLM performance when main distribution line faults occur and require to be localized across UN distribution power grids. A number of factors such as the type of distribution power grid (say, either UN MV or UN LV), the complicity of the original UN BPL topology, the nature of the terminal load and the location of main distribution line fault are examined. Similarly to [38], the combined impact of measurement differences and main distribution line faults is examined. In order to study this combined result, the following conditions concerning the measurement differences and main distribution line faults are considered, namely:

- The measurement differences that occur during the determination of coupling reflection coefficients in UN MV and UN LV topologies are described by continuous uniform distributions (CUDs) with maximum CUD value a_{MD} . In accordance with [38], three different measurement difference CUDs are taken into account:
 - CUD with $a_{MD}=0$ (no measurement differences are assumed while this CUD case is denoted as CUD case A);
 - CUD with $a_{MD}=0.1$ (denoted as CUD case B); and
 - CUD with $a_{MD}=0.2$ (denoted as CUD case C).
- To study the impact of main distribution line faults on the MLFLM performance, three representative fault locations are given:
 - Fault located at 20m from the transmitting end (denoted as Fault case A);

- Fault located at 90m from the transmitting end (denoted as Fault case B); and
- Fault located at 190m from the transmitting end (denoted as Fault case C).

Prior to assess the MLFLM performance, it is assumed that the existence of a main distribution line fault across the UN distribution power grid has been already identified but not localized.

3.1 The Impact of the Maximum CUD Value of Measurement Differences on the Fault Localization by Applying MLFLM

As indicated in [38], the successful application of MLFLM is achieved by spotting the simultaneous minimization of MDLFIs across the transmission path. The location of the previous simultaneous minimization defines the main distribution line fault location. Although MLFLM is very accurate when no measurement differences are considered, MLFLM satisfactorily localizes main distribution line faults even if measurement differences of various CUD magnitudes are assumed. MLFLM performance of fault localization in UN MV and UN LV BPL networks is investigated in this subsection.

In Fig. 3(a), MDLFIs of the urban UN MV BPL topology of case A are plotted versus the distance from the transmitting end when the terminal load is assumed to be short-circuit during the main distribution line fault case A for CUD case A, B and C. In Fig. 3b, same plots are drawn with Fig. 3(a) but for the case of an open-circuit terminal load. In Figs. 4(a) and 4(b), same plots with the respective Figs. 3(a) and 3(b) are given but for the case of the urban UN LV BPL topology of case A.

It is obvious that the localization of main distribution line faults across UN distribution BPL networks becomes easier when measurement differences remain low. From Figs. 3(a), 3(b), 4(a) and 4(b), it is verified that the fault localization performance remains high even if decent measurement differences occur (i.e., measurement differences with maximum CUD magnitude up to 0.2). Hence, MLFLM performance towards the localization of main distribution line faults presents relative immunity against the factors that affect the accuracy of measurement equipment.

As presented in [38], MDLFIs of UN distribution BPL networks present similar behavior with the respective one of MDLFIs of OV BPL networks. When measurement differences are negligible, both MDLFIs achieve their minimum values that are equal to 0. As the measurement differences increase so do MDLFIs but their values at the position of the main distribution line fault remain the lowest in comparison with the other MDLFI values for given maximum CUD magnitude. Here, it should be noted that significant measurement differences can deteriorate MLFLM performance since the localization of the main distribution line faults in these cases may affect the simultaneous minimization of MDLFIs.

According to [6], [11], [12], [16], by comparing channel attenuations of UN distribution BPL channels, it is evident that the channel attenuation of UN MV BPL channels is significantly higher than the one of UN LV BPL channels. This channel attenuation difference is primarily due to the insulation characteristics of the considered UN MV cables –i.e., paper-insulated lead covered (PILC) distribution cables–. Apart from the channel attenuation, coupling reflection coefficients and the respective

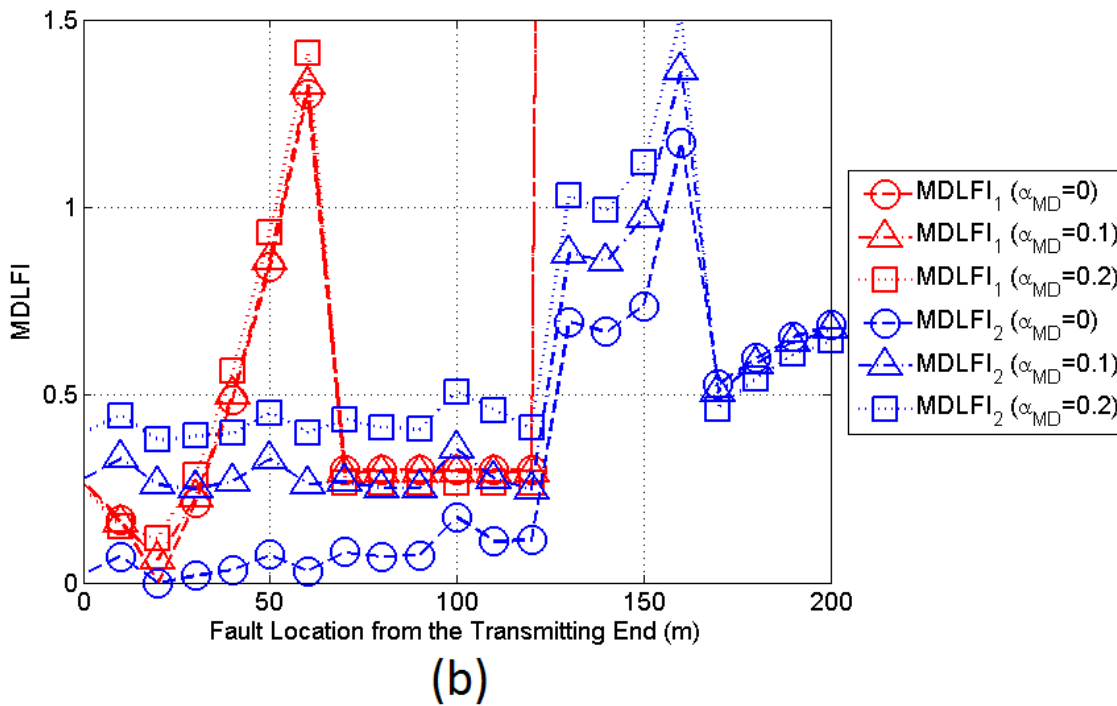
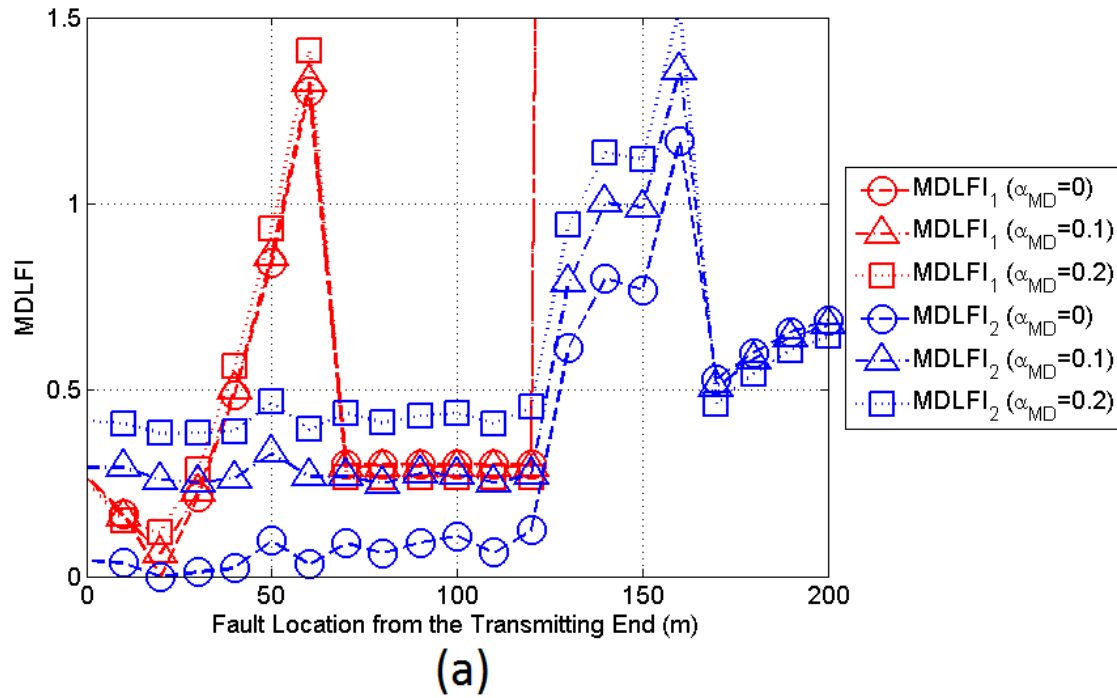


Figure 3. MDLFIs of the urban UN MV BPL topology versus the fault location from the transmitting end for various CUD magnitudes when fault case A is applied (fault location at 20m). (a) Short-circuit terminal load (b) Open-circuit terminal load.

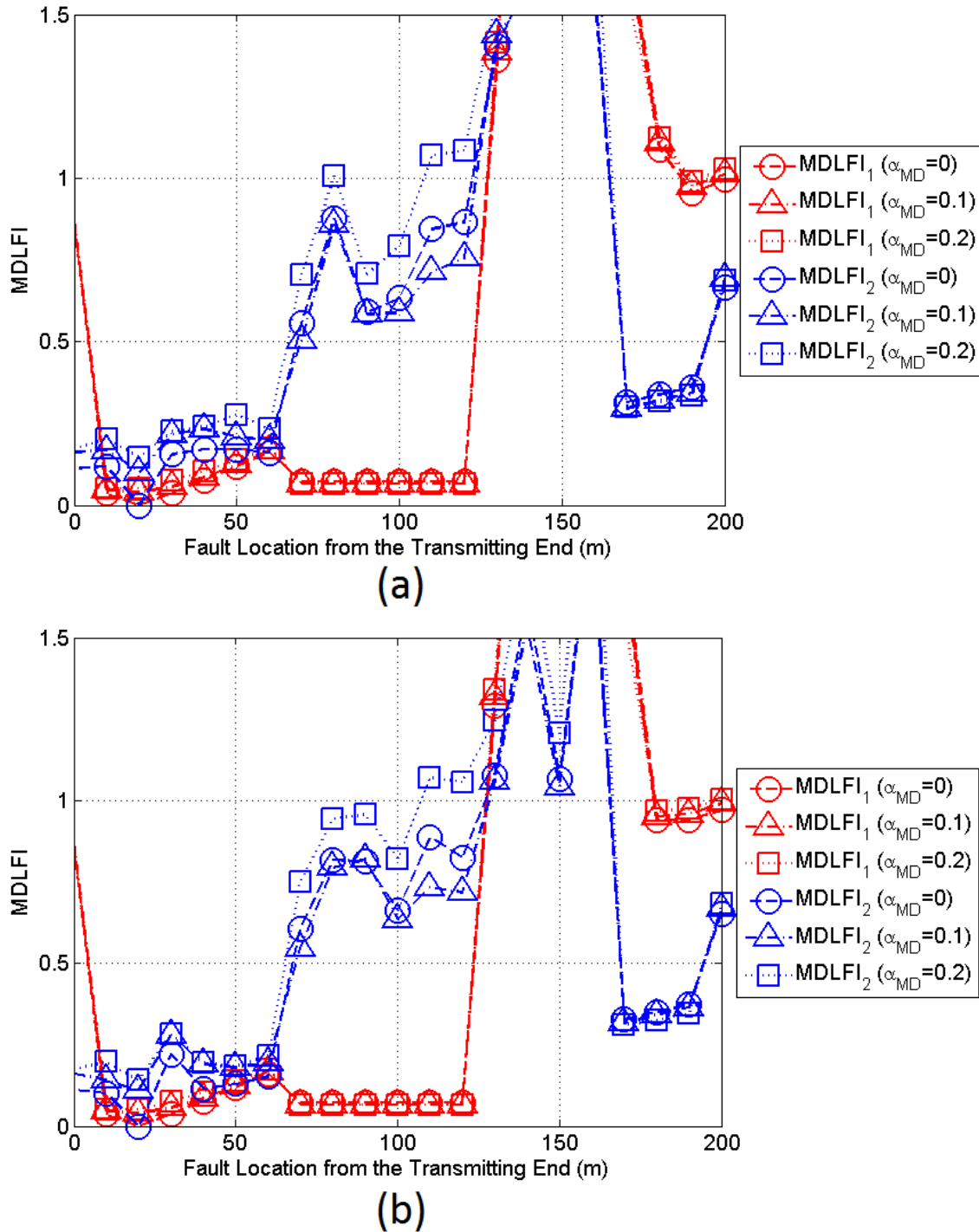


Figure 4. Same curves with Figure 3 but for the case of the urban UN LV BPL topology.

MDLFIs are also affected by the insulation characteristics of the considered UN MV BPL cables; MDLFIs of UN LV BPL topologies present lower values than the respective ones of UN MV BPL topologies. Since coupling reflection coefficients of UN MV BPL channels are low enough, the measurement differences that are superimposed to the coupling reflection coefficients have strong effect to the overall coupling reflection coefficients. Hence, measurement differences become less critical during the localization

of main distribution line faults in UN LV BPL topologies and, for that reason, MDLFIs of UN LV BPL topologies achieve better simultaneous MDLFI minimizations for different intensities of measurement differences –compare MDLFI₁ and MDLFI₂ curves of Figs. 3(a) and 3(b) with the respective ones of 4(a) and 4(b)–.

Regardless of the type of the examined UN distribution power grid, the minima of MDLFIs define the location of the main distribution line fault through their simultaneous appearance. It is clear that the simultaneous minimization of MDLFIs at the location of the main distribution line faults is secured when the measurement differences remain low. Divergences may occur only in the cases of measurement differences that are characterized by high intensities –see MDLFI₂ of Fig. 3(a) and 3(b) when maximum CUD magnitude is equal to 0.2–. In these cases, the location of the main distribution line fault can be fulfilled by using two newly proposed submethods that cooperatively act with MLFLM:

- *MDLFI area method.* In accordance with this method, the main distribution line fault lies in the area that is bounded by the two minima of MDLFIs. Example of the MDLFI area case is given in Figs. 3(a) and 3(b) for maximum CUD magnitudes exceeding 0.1 where MDLFI₁ gives the exact location of the main distribution line fault (left bound of the MDLFI area) while minimum of MDLFI₂ offers the right bound of the MDLFI area.
- *MDLFI sum minimization.* The general form of the MDLFI curves may reveal the fault location. In these cases, the minimum of the sum of MDLFI₁ and MDLFI₂ indicates the location of the main distribution line fault.

Also, a rule of thumb that is suitable for the localization of the main distribution line faults when significant differences between MDLFI₁ and MDLFI₂ occur is given in Sec. 3.3 and is based on the MDLFI that is closer to the main distribution line fault.

Finally, the nature of the main distribution line fault, as reflected on the terminal load, slightly affects the MLFLM performance. In fact, the main distribution line faults across UN distribution BPL networks can be either short- or open-circuit terminal load depending on the fault nature. Since MLFLM performance remains almost immune with respect to the nature of the terminal load, this event indicates that the topological properties of the examined UN distribution BPL topology and the maximum CUD magnitude of measurement differences remain the most important factor concerning MLFLM performance. For that reason, the impact of the topological complexity of UN distribution BPL topologies on MLFLM performance is first examined in the following subsection. Also, since no significant MLFLM performance deviations are presented for different terminal loads, only one case (say, the case of short-circuit terminal load) is considered in the rest of this paper. Anyway, this is a typical procedure during the examination of MLFLM for the sake of the manuscript size reduction [33], [34], [38].

3.2 The Impact of the Main Distribution Line Fault Location on MLFLM Performance

Although each MDLFI presents strong dependence on the fault location [33], their combined operation under the aegis of MLFLM offers protection against the localization selectivity. Since each MDLFI offers safer results when the fault location lies near to its measurement site, the application of MDLFIs at the transmitting and receiving

ends of the original UN distribution BPL topologies allows the cross check of the fault location as presented in Sec. 3.1 through the simultaneous minimization of MDLFIs.

Until now, only the fault case A has been examined where the main distribution line fault lies at 20m from the transmitting end. In accordance with the previous MDLFI property description, it is expected that MDLFI₁ gives a more accurate localization through its minimization in comparison with the respective one of MDLFI₂ because the main distribution line fault lies near to MDLFI₁ measurement point that is the transmitting end of the original UN distribution BPL topology. This event is valid either for the UN MV or for the UN LV BPL topologies.

In this subsection, the behavior of MDLFIs and consequently MLFLM is investigated for different location of main distribution line faults. In order to assess the performance of MDLFIs and MLFLM, Fault case B and C are applied where the fault location lies at 90m and 190m from the transmitting end, respectively. Indeed, in Fig. 5(a), MDLFIs are plotted versus the distance from the transmitting end when the terminal load is assumed to be short-circuit during the main distribution line fault for all the CUD cases examined so far (i.e., CUD case A, B and C). Note that the original urban MV BPL topology of Sec 2.2 and the Fault case B are assumed. In Fig. 5(b), same plots with Fig. 5(a) are drawn but for the case of the original UN LV BPL topology of Sec. 2.2. In Figs. 6(a) and 6(b), same curves with the respective Figs. 5(a) and 5(b) are given but for the Fault case C.

In all the cases, which have been examined in Figs. 3(a), 3(b), 5(a), 5(b), 6(a) and 6(b), MLFLM achieves to localize the main distribution line fault through the simultaneous minimization of MDLFIs regardless of the fault location. Actually, when main distribution line fault lies near to the transmitting end, MDLFI₁ more easily identifies the fault location in comparison with MDLFI₂ –see Fault case A of Figs. 3(a) and 3(b)–. Conversely, when main distribution line fault lies near to the receiving end of the original UN distribution BPL topology MDLFI₂ more easily copes with this case due to the aforementioned inherent MDLFI property of the fault distance selectivity –see Fault case C of Figs. 6(a) and 6(b)–. Finally, if main distribution line faults lie near to the middle of the original UN distribution BPL topology then the combined operation of MDLFIs is required –see Fault case B of Figs. 5(a) and 5(b)–. Also, MLFLM performance remains approximately the same either for UN MV BPL topologies or UN LV BPL ones.

During the localization of main distribution line faults, MDLFIs can be treated as filters of different types. When main distribution line faults lie near to the transmitting or receiving end, MDLFI₁ resembles to a low pass or high pass filter, respectively. When main distribution line faults occur near to the middle of the examined UN distribution BPL topology, both MDLFIs can be considered as bandpass filters. This observation is very useful when intense measurement differences occur since then the localization of main distribution line faults comes from the matching of the pass regions of MDLFIs. In fact, this matching of the two MDLFI pass areas allows the determination of a region where the main distribution line faults lie and defines the general concept of the aforementioned MDLFI area method. Therefore, it is evident that the localization of main distribution line faults that lie near to the middle of UN distribution BPL networks remains the most difficult case of fault localization.

Apart from the fault location, MDLFI performance should be examined when different UN distribution BPL topologies are applied. Similarly to the OV MV BPL

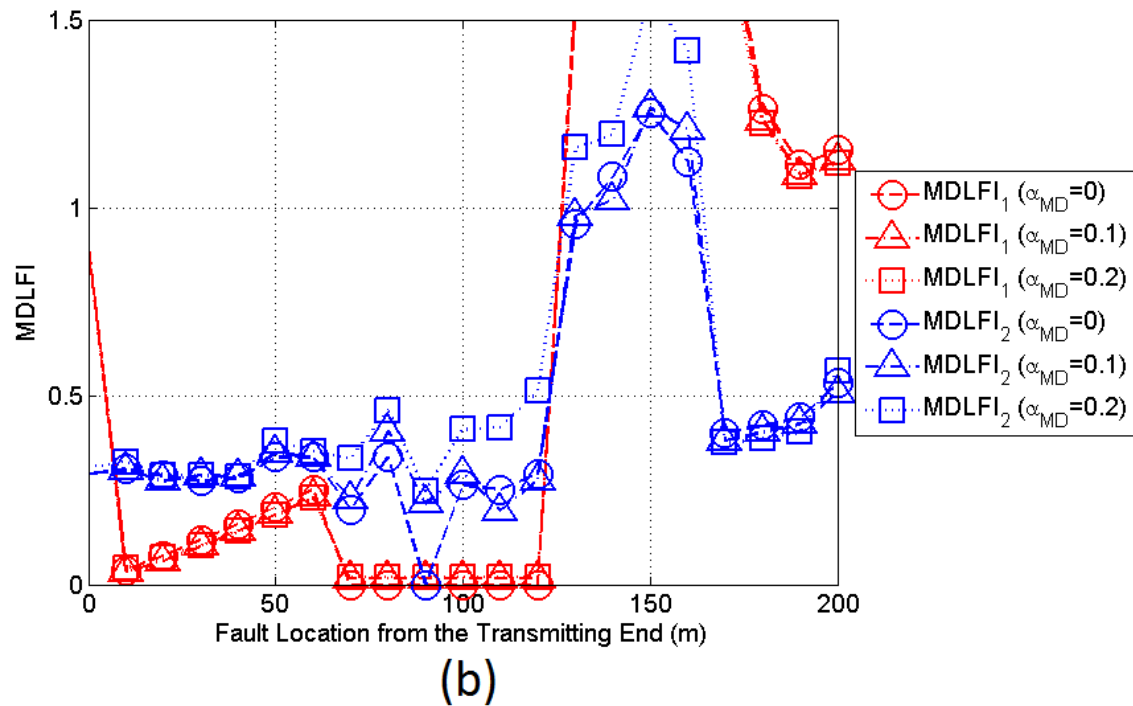
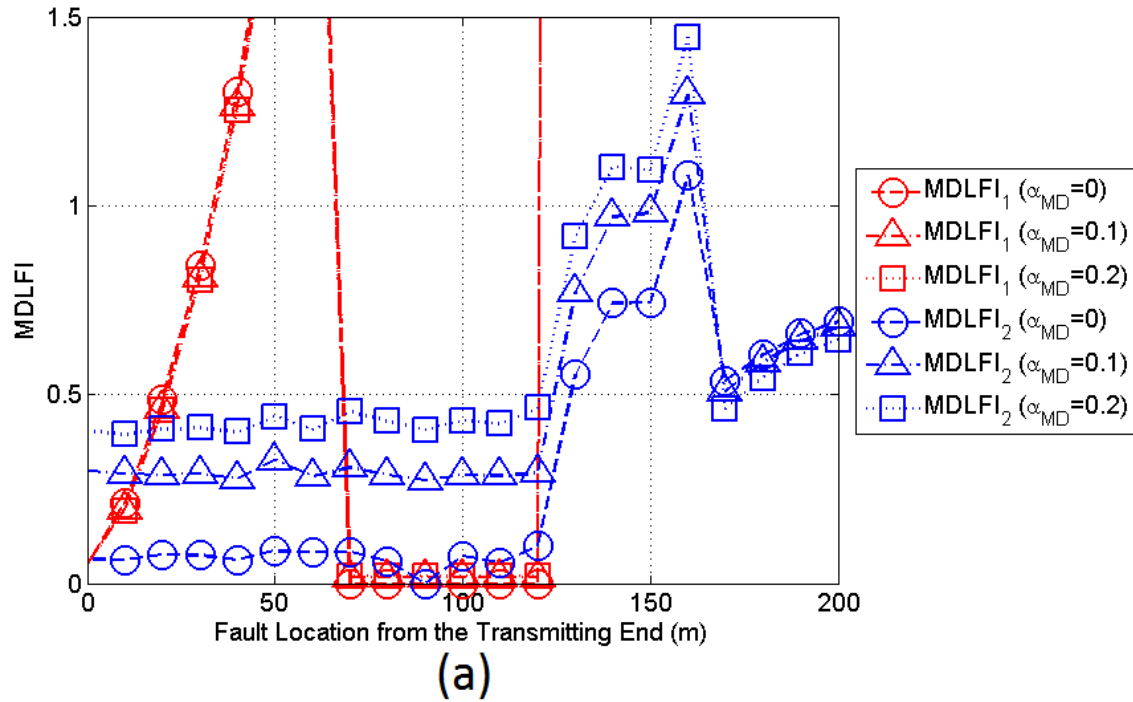


Figure 5. MDLFIs of the urban UN distribution BPL topologies versus the fault location from the transmitting end for various CUD cases when Fault case B occurs (the terminal load is assumed to be a short-circuit termination load and the fault location is at 90m). (a) MV. (b) LV.

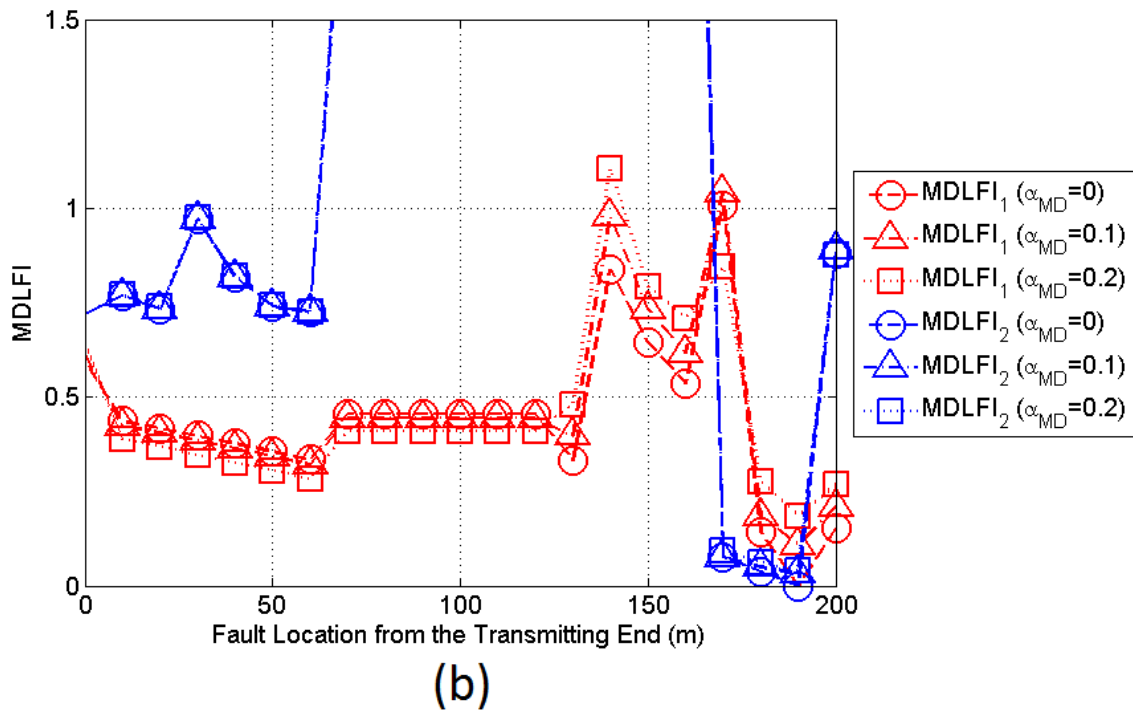
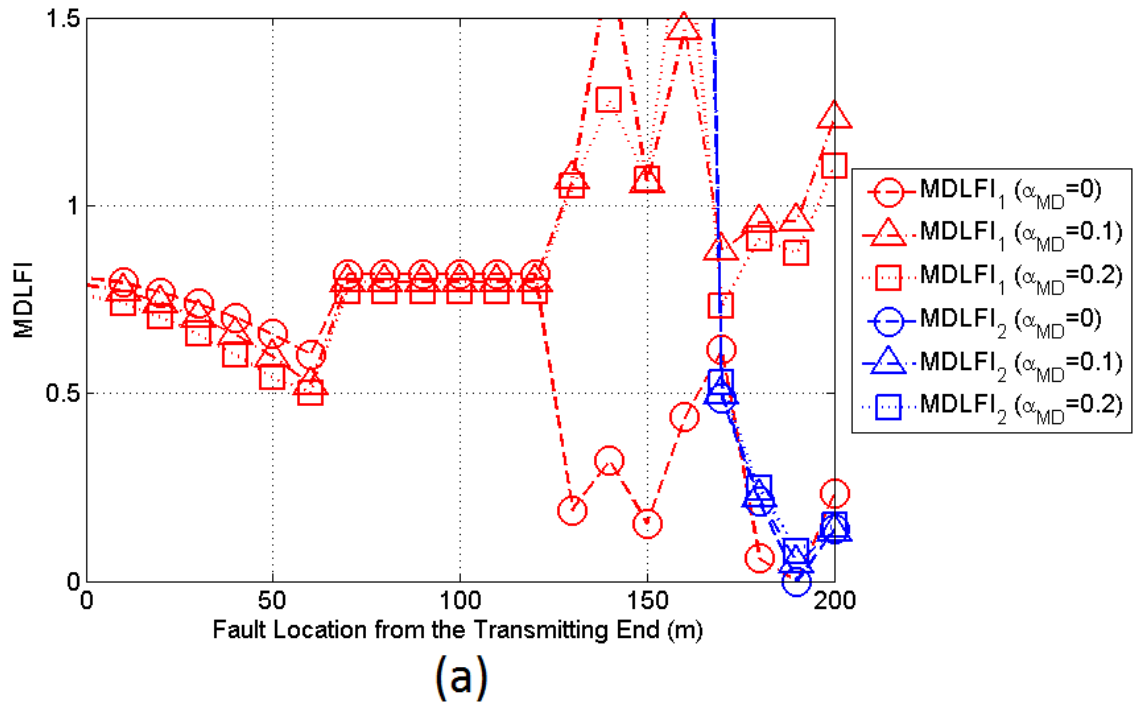


Figure 6. Same curves with Figure 5 but for the Fault case C (the fault location is at 190m).

topologies [33], [34], [38], the topological complexity of UN distribution BPL topologies concerning their number and their length of branches affects either the measured coupling reflection coefficients or the form of MDLFIs or the minima of MDLFIs.

3.3 The Impact of the Original UN Distribution BPL Topologies on MLFLM Performance

In this subsection, MLFLM performance is assessed for the other four indicative original UN distribution BPL topologies described in Sec. 2.2 –say, urban case B, suburban case, rural case and “LOS” case–.

Indeed, in Fig. 7(a), MDLFIs are plotted versus the distance from the transmitting end of the original UN MV BPL topology of urban case B when the terminal load is assumed to be short-circuit. Note here that the Fault case A is assumed and all the available CUD cases are considered. In Fig. 7(b), same curves with Fig. 7(a) are given but for the case of the original UN LV BPL topology of urban case B. In Figs. 8, 9 and 10, same plots are drawn with Fig. 7 but for the suburban, rural and “LOS” cases, respectively.

From Figs. 3(a), 3(b), 7(a), 7(b), 8(a), 8(b), 9(a), 9(b), 10(a) and 10(b), the following conclusions regarding the MLFLM performance can be deduced:

- When CUD magnitude of measurement differences is equal to zero the exact localization of main distribution line faults occurs regardless of the type of UN distribution BPL network (i.e., MV or LV) and the examined BPL topology. In all the cases examined, there is a simultaneous minimization of MDLFIs at the fault position.
- When the CUD magnitude of measurement differences increases, MDLFIs start to take values greater than zero at the fault location. MDLFI₁ acts as the primary MDLFI metric while MDLFI₂ acts as the secondary one whether the examined main distribution line fault lies near to the transmitting end. It is clear from the previous figures that MDLFI₁ minima always define the exact location of the main distribution line fault, which is located at 20m from the transmitting end regardless of the examined UN distribution BPL topology. MDLFI₂ presents its curve minima at 20m in the majority of the cases examined.
- When measurement differences occur, MLFLM more easily localizes the occurred main distribution line faults in UN LV BPL networks than in UN MV BPL networks. As already been mentioned, measurement differences significantly affect coupling reflection coefficients of UN MV BPL topologies since their values have already been affected by the intense intrinsic characteristics of UN MV MTL configurations.
- When the examined BPL topologies are characterized by relative topological complexity (i.e., high number of branches of short branch lengths), the localization of the main distribution line faults more easily occurs. Since the terminations of the short branches critically influence the coupling reflection coefficients across the transmission path in accordance with the transmission theory [11], [16], the measurement differences can be easily detected due to their superimposition to an already existing coupling reflection coefficient pattern.
- Conversely, in BPL topologies that are characterized by low number of short branches, such as rural and “LOS” topologies of the UN distribution BPL topologies, the superimposed measurement differences drastically deteriorate the performance of MLFLM. In fact, when measurement differences start to present

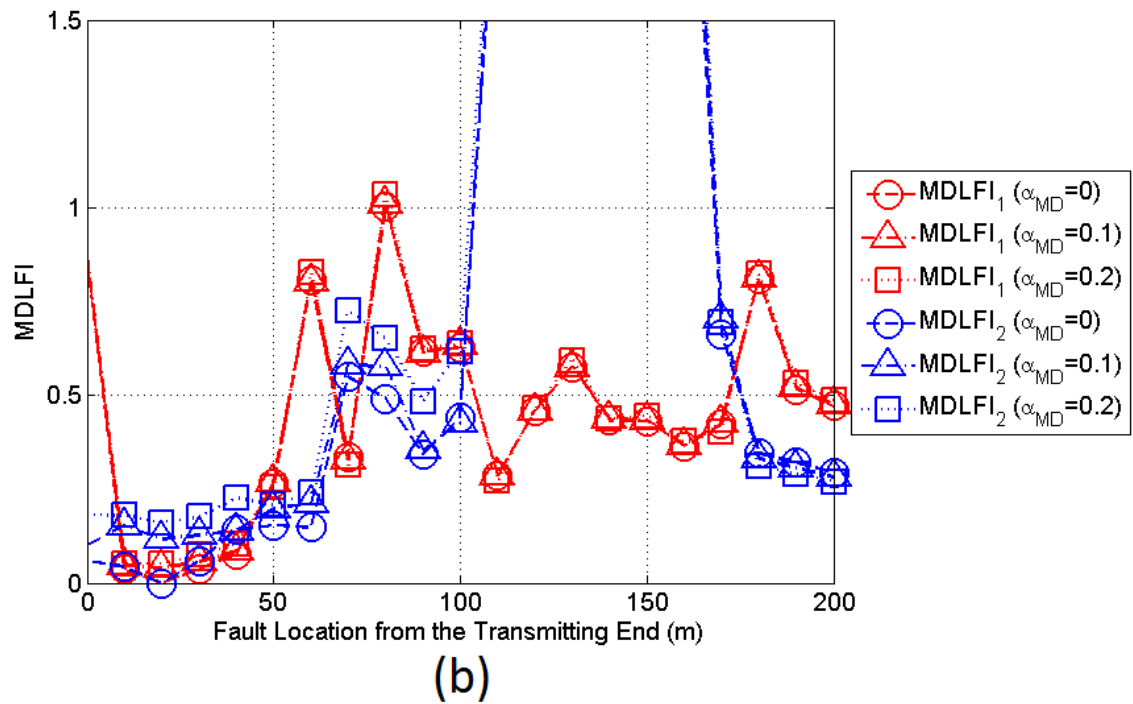
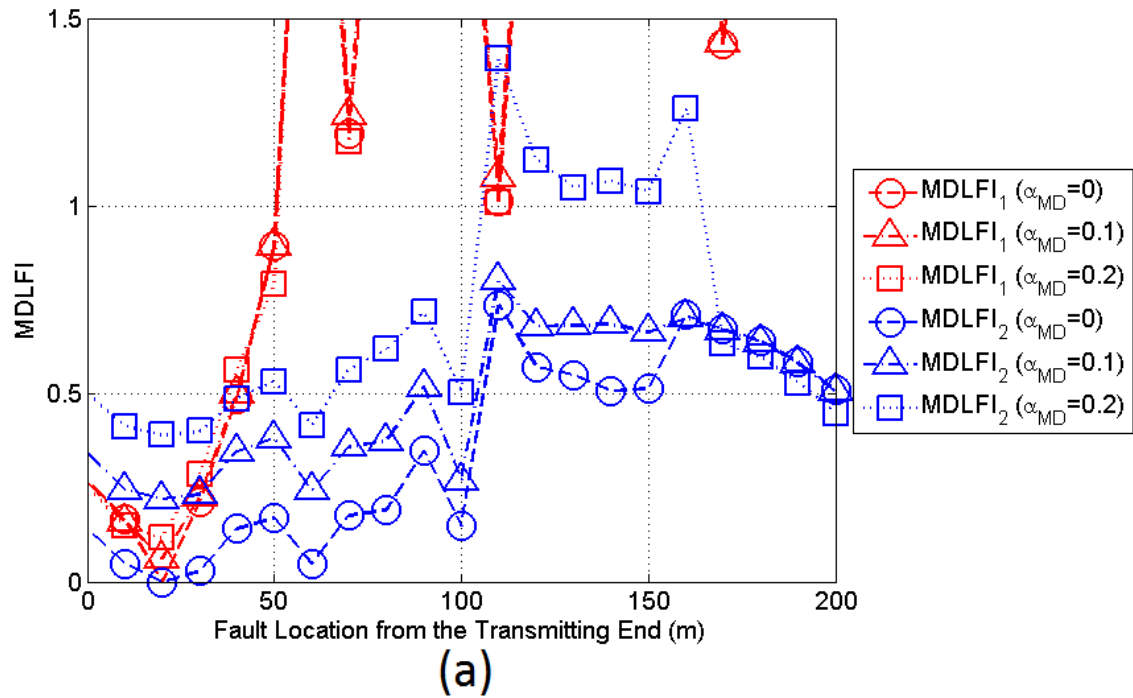


Figure 7. MDLFIs of the original UN BPL topology of urban case B versus the fault location from the transmitting end for various CUD cases when Fault case A occurs (the terminal load is assumed to be a short-circuit termination load). (a) MV. (b) LV.

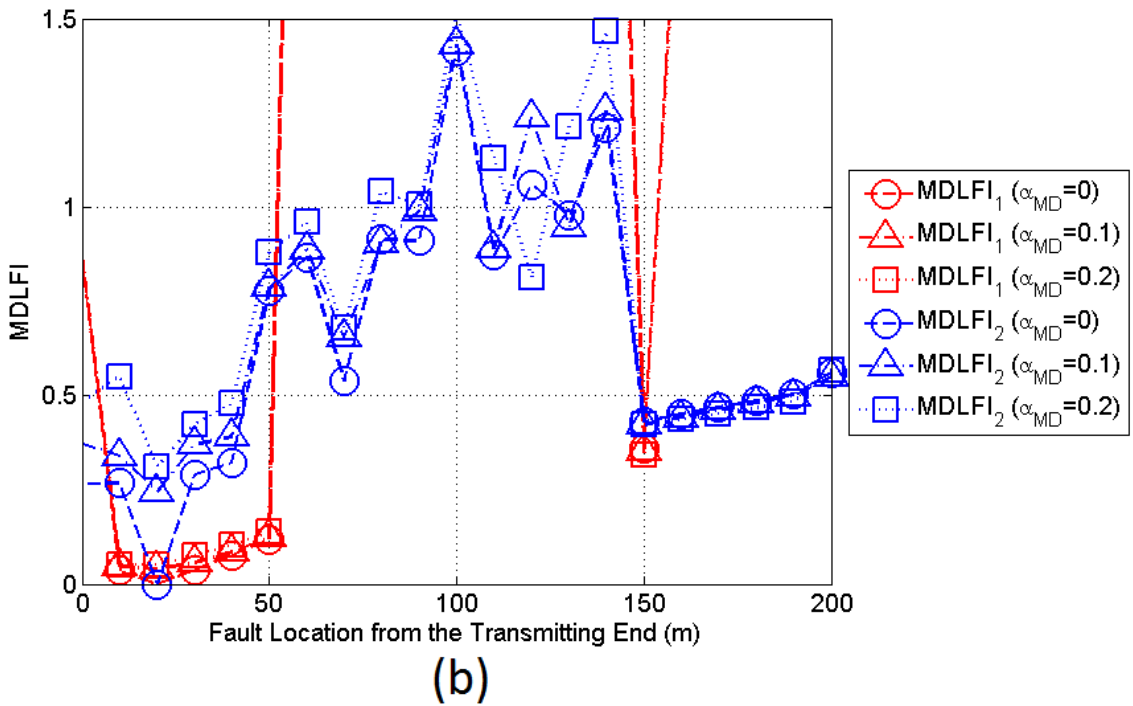
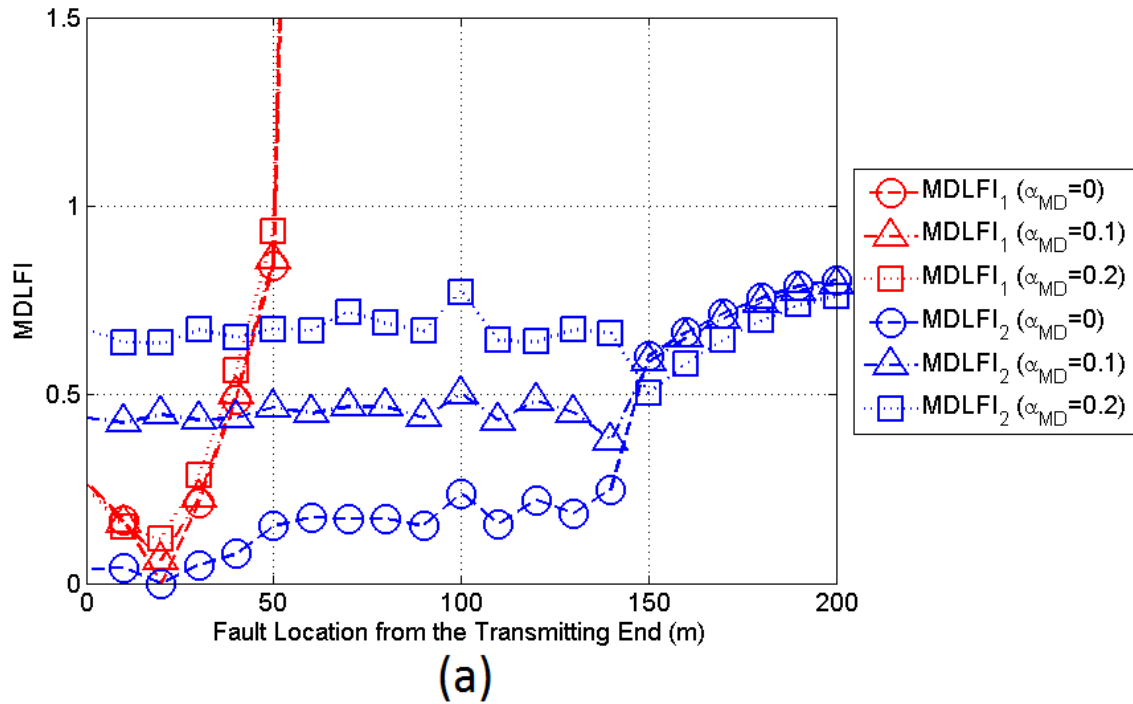
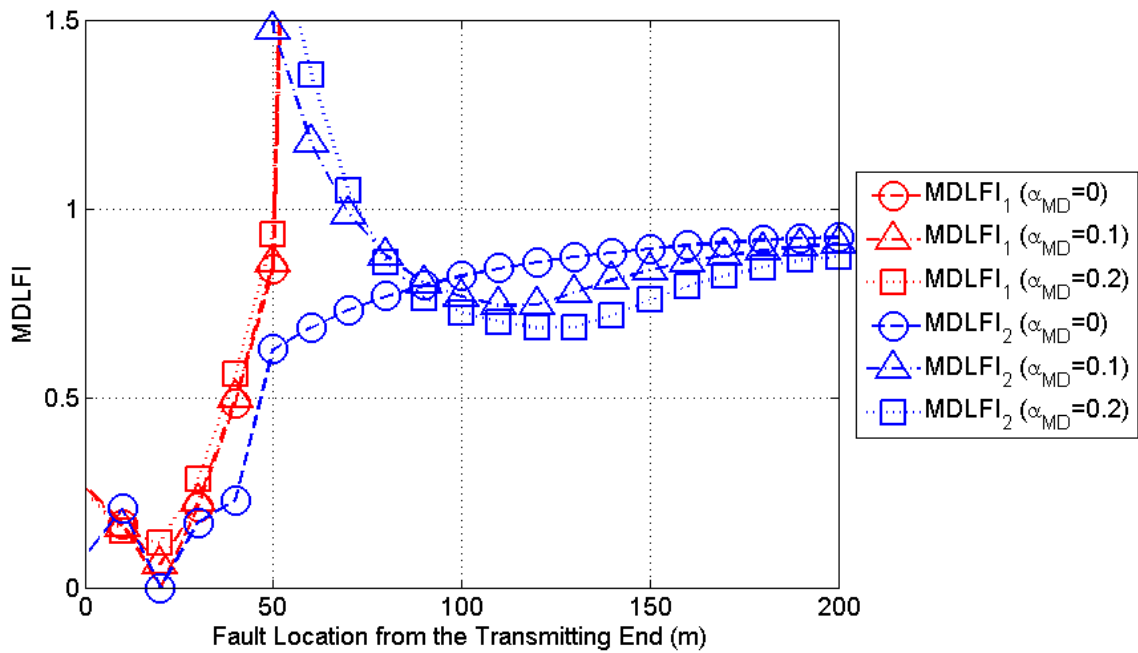
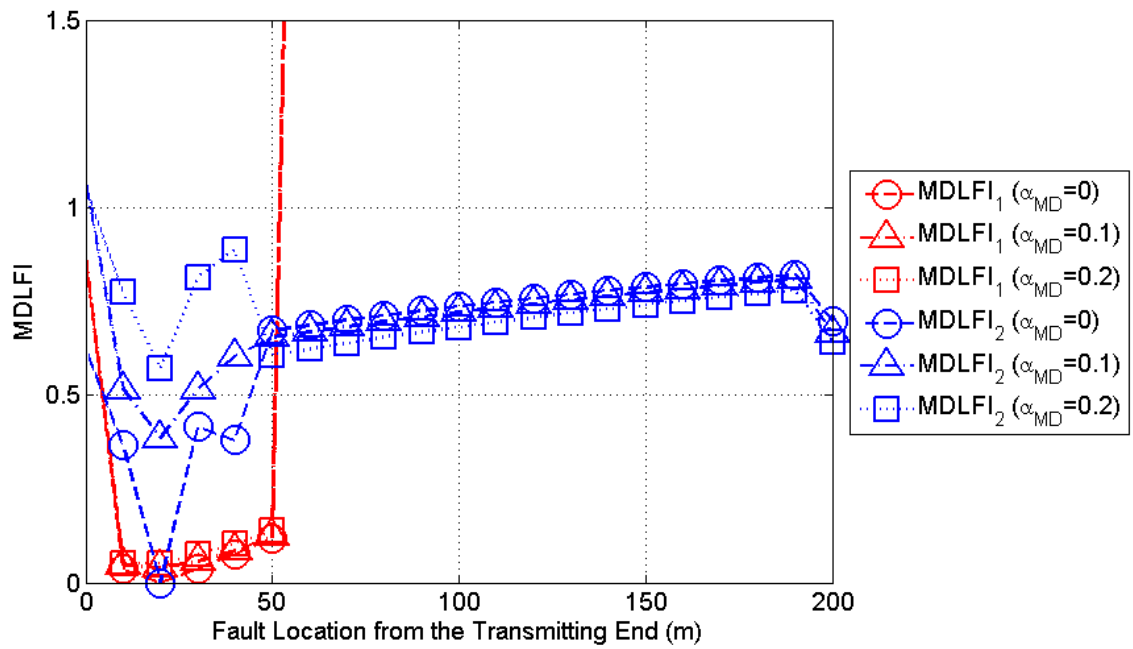


Figure 8. Same curves with Figure 7 but for the suburban case.



(a)



(b)

Figure 9. Same curves with Figure 7 but for the rural case.

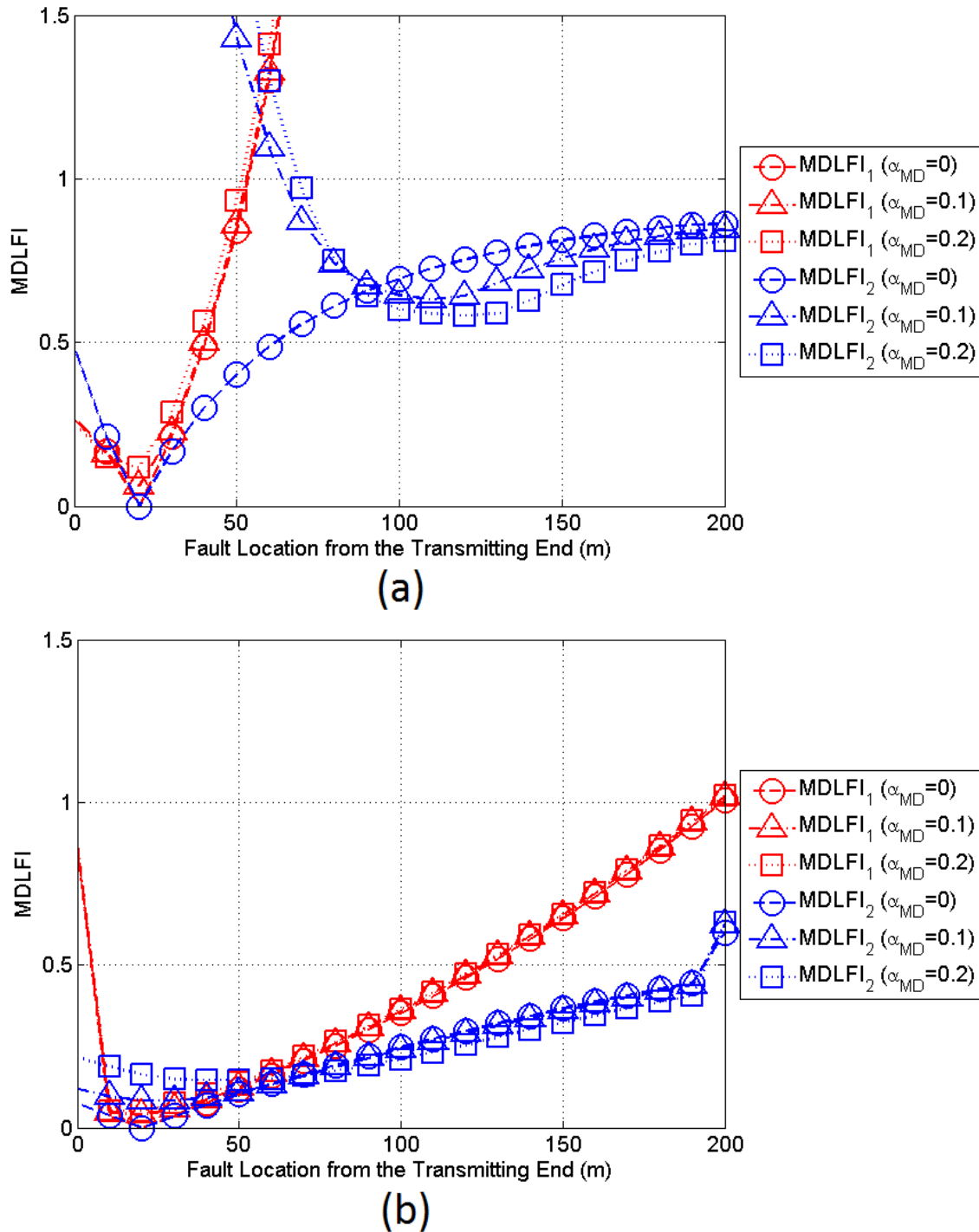


Figure 10. Same curves with Figure 7 but for the “LOS” case.

high CUD magnitudes, MDLFI of the measurement site that is the most distant to the main distribution line fault starts to present deviations. These deviations depend on the CUD magnitude and the type of distribution power grid. However, MDLFI that is the closest to the main distribution line fault steadily localizes the main distribution line fault through its minimization regardless of the maximum CUD value. Actually, the worst case scenario is given in Figs. 9(a) and 10(a)

where it is clear that MDLFI₂ of the rural and “LOS” topologies of UN MV grid fails to localize the main distribution line fault when maximum CUD value exceeds 0.1. The main distribution line fault can be localized by neither MDLFI area method nor MDLFI sum minimization. Therefore, in the cases of rural and “LOS” topologies of high channel attenuations, MLFLM is based on the MDLFI that presents a notch-type minimization (single MDLFI minimization case). Note here that the last proposed submethod includes only the case of UN MV grid when intense measurement differences occur. Synoptically, the localization of main distribution line faults through the simultaneous minimization of MDLFIs is safe in rural and “LOS” BPL topologies of UN distribution power grids when: (i) low maximum CUD values occur regardless of the UN distribution power grid type; and (ii) MLFLM is applied to UN LV grid.

3.4 MLFLM Performance in OV and UN Distribution Power Grids

Comparing findings of this paper that concern the MLFLM performance in UN distribution power grids with the respective ones of [38] that concern the MLFLM performance in OV distribution power grids, several similarities but also differences can be outlined during the application of MLFLM, namely:

- In all the cases examined where the measurement differences have been neglected, MLFLM have successfully localized main distribution line faults by the simultaneous minimization of MDLFI₁ and MDLFI₂ regardless of the distribution power grid. In fact, both MDLFIs receive zero value at the location of the main distribution line fault.
- Regardless of the location of a main distribution line fault, MLFLM can localize the faults through the simultaneous minimization of MDLFIs. Even if the main distribution line fault is located at the middle of the original BPL topology and measurement differences are considered, the minimization of MDLFIs occurs at this position in a band pass filter way. The simultaneous minimization of MDLFIs defines the normal operation of MLFLM that deals with the main distribution line faults in the majority of the BPL topologies in OV and UN distribution power grids.
- As measurement differences increase so do the minima of MDLFIs at the location of the main distribution line fault. The values of minima differ from zero.
- In the cases of intense measurement differences, MDLFIs may not present simultaneous minimization at the location of the main distribution line fault. In these cases, the general form of MDLFIs entails the location of the main distribution line fault. Anyway, the MDLFI that is closer to the main distribution line fault present a notch type minimization and MLFLM decision is based on this regardless of the intensity of the occurred measurement differences (single MDLFI minimization case). Note that both MDLFIs present notch type minimization regardless of the intensity of the occurred measurement differences when the main distribution line fault is located near to the middle of the transmission path of the examined BPL topology.
- Even if measurement differences occur, the localization of the main distribution line faults remains safer in the cases of aggravated BPL topologies, such as urban and suburban topologies, due to the inherent intense changes of coupling

- reflection coefficients. Actually, MDLFIs of these cases present notch type minimization at the location of the main distribution line faults and this is explained by the operation of PMAs.
- The localization of main distribution line faults in rural and “LOS” cases becomes a challenging issue for MLFLM especially when significant measurement differences occur and the channel attenuation of the examined BPL topologies is high.
 - OV MV and UN LV BPL topologies are treated by MLFLM in the same way since their channel attenuation remains low. If measurement differences are low, the localization of the main distribution line faults comes from the simultaneous minimization of MDLFIs. If measurement differences become high, the localization of the main distribution line fault is based on either the MDLFI area method or the MDLFI sum minimization.
 - Due to the UN MV MTL configuration considered in this paper, UN MV BPL topologies present significant higher channel attenuations in comparison with the respective ones of OV MV and UN LV BPL topologies. The absence of a rich multipath environment has as a result the performance deterioration of MLFLM when a main distribution line fault needs to be localized. Therefore, in rural and “LOS” topologies, when measurement differences remain low, the localization of the main distribution line faults comes from the simultaneous minimization of MDLFIs. If measurement differences are intense and the main distribution line fault lies near to either the transmitting end or the receiving end, the single MDLFI minimization is adopted. If measurement differences are intense but the main distribution line fault lies near to the middle of the examined topology, either the MDLFI area method or the MDLFI sum minimization can be adopted.

In accordance with [33], [34], [38], these three papers have achieved to cover the identification and localization methodology of main distribution line faults through the proposal and application of MLFLM methodology in OV distribution BPL networks. In this paper, MLFLM methodology has been extended by incorporating three submethods in order to cope with the localization problem of main distribution line faults in UN distribution BPL networks. A complete methodology of identifying and localizing possible faults and instabilities across distribution power grids is now available.

4. Conclusions

In this paper, which extends the application of MLFLM from OV MV BPL networks to UN distribution BPL networks, the detailed presentation and the performance assessment of MLFLM have been demonstrated. Given the existence of a random main distribution line fault, MLFLM has successfully localized its location across the transmission path of various UN MV and UN LV BPL topologies despite the imposed performance deterioration that is added by the measurement differences.

In accordance with [38], this paper has briefly outlined the required steps to create MLFLM database, define MDLFIs and apply MDLFIs to MLFLM database in order to localize the main distribution line faults. After the theoretical presentation of MLFLM, a number of case scenarios has been reported so that MLFLM performance is

evaluated. During these case scenarios, the impact of some critical parameters, such as the type of UN distribution power grid (i.e., UN MV and UN LV power grid), the intensity of measurement differences, the location of the main distribution line fault and the nature of the main distribution line fault (i.e., short- or open- circuit terminal load), on the MLFLM performance has been assessed indicating the localization accuracy of MLFLM in the vast majority of the cases examined.

Synopsizing the results, MLFLM can very accurately localize main distribution line faults regardless of their location across the transmission path of UN distribution BPL topologies due to the combined used of MDLFIs. In addition, as it is obvious, MLFLM performance mainly depends on the intensity of the occurred measurement differences allowing the accurate localization of measurement differences even if maximum CUD magnitudes reach up to 0.2. Also, MLFLM can more easily localize main distribution line faults in more complex UN distribution BPL topologies (i.e., urban, aggravated urban and suburban BPL topologies) rather in less complex ones (i.e., rural and “LOS” BPL topologies). This is due to the fact that MLFLM accuracy is based on the pattern recognition of coupling reflection coefficients since MDLFIs are related with PMAs. Furthermore, MLFLM performance depends on the type of the UN distribution power grid since it remains higher in the cases of low overall channel attenuation (such as UN LV BPL topologies and the majority of UN MV BPL topologies).

Although MLFLM can very accurately localize main distribution line faults in the vast majority of the cases examined during its normal operation (i.e., simultaneous minimization of MDLFIs), three new submethods, which accompanies MLFLM, have been proposed in order to cope with some special cases where MLFLM presents deviations. More specifically, the first two submethods, which are the MDLFI area method and the MDLFI sum minimization, have been proposed in order to localize main distribution line faults when measurement differences are equal or greater than 0.2. The third submethod, that is the single MDLFI minimization and is treated as the last-resort method, has been proposed in order to localize main distribution line faults when the following extreme conditions coexist: (i) UN distribution BPL topologies of high channel attenuation and low topological complexity (e.g., rural and “LOS” UN MV BPL topologies); (ii) measurement differences with maximum CUD magnitudes that are equal or greater than 0.1; and (iii) main distribution line faults that lie near to the transmitting or receiving end of the original BPL topology.

A complete methodology of localizing main distribution line faults in OV and UN distribution BPL networks has been proposed. The already accurate MLFLM has been enriched with three additional submethods in order to localize main distribution line faults in the most challenging cases of distribution power grids.

CONFLICTS OF INTEREST

The author declares that there is no conflict of interests regarding the publication of this paper.

References

- [1] S. Ezzine, F. Abdelkefi, J. P. Cances, V. Meghdadi, and A. Bouallégué, "Evaluation of PLC Channel Capacity and ABER Performances for OFDM-Based Two-Hop Relaying Transmission," *Hindawi Wireless Communications and Mobile Computing*, vol. 2017, ArticleID 4827274, pp. 1-12, 2017.
- [2] F. A. Pinto-Benel, M. Blanco-Velasco, and F. Cruz-Roldán, "Throughput Analysis for Wavelet OFDM in Broadband Power Line Communications," 2017. [Online]. Available: <https://pdfs.semanticscholar.org/55ee/c64f1b4533f1be2d21db993b48eda3d96f38.pdf> (accessed on 12/28/2017).
- [3] IEEE P1901, "Draft Standard for Broadband over Power Line Networks: Medium Access Control and Physical Layer Specifications", 2010. [Online]. Available: <http://grouper.ieee.org/groups/1901/index.html> (accessed on 12/28/2017).
- [4] A. G. Lazaropoulos and P. G. Cottis, "Transmission characteristics of overhead medium voltage power line communication channels," *IEEE Trans. Power Del.*, vol. 24, no. 3, pp. 1164-1173, Jul. 2009.
- [5] A. G. Lazaropoulos and P. G. Cottis, "Capacity of overhead medium voltage power line communication channels," *IEEE Trans. Power Del.*, vol. 25, no. 2, pp. 723-733, Apr. 2010.
- [6] A. G. Lazaropoulos and P. G. Cottis, "Broadband transmission via underground medium-voltage power lines-Part I: transmission characteristics," *IEEE Trans. Power Del.*, vol. 25, no. 4, pp. 2414-2424, Oct. 2010.
- [7] A. G. Lazaropoulos and P. G. Cottis, "Broadband transmission via underground medium-voltage power lines-Part II: capacity," *IEEE Trans. Power Del.*, vol. 25, no. 4, pp. 2425-2434, Oct. 2010.
- [8] A. G. Lazaropoulos, "Broadband transmission characteristics of overhead high-voltage power line communication channels," *Progress in Electromagnetics Research B*, vol. 36, pp. 373-398, 2012. [Online]. Available: <http://www.jpier.org/PIERB/pierb36/19.11091408.pdf>
- [9] A. G. Lazaropoulos, "Capacity Performance of Overhead Transmission Multiple-Input Multiple-Output Broadband over Power Lines Networks: The Insidious Effect of Noise and the Role of Noise Models," *Trends in Renewable Energy*, vol. 2, no. 2, pp. 61-82, Jan. 2016. [Online]. Available: <http://futureenergysp.com/index.php/tre/article/view/23>
- [10] Homeplug, AV2 Whitepaper, 2011, [Online]. Available: <http://www.homeplug.org/techresources/resources/>
- [11] A. G. Lazaropoulos, "Factors Influencing Broadband Transmission Characteristics of Underground Low-Voltage Distribution Networks," *IET Commun.*, vol. 6, no. 17, pp. 2886-2893, Nov. 2012.
- [12] A. G. Lazaropoulos, "Towards broadband over power lines systems integration: Transmission characteristics of underground low-voltage distribution power lines," *Progress in Electromagnetics Research B*, 39, pp. 89-114, 2012. [Online]. Available: <http://www.jpier.org/PIERB/pierb39/05.12012409.pdf>
- [13] A. G. Lazaropoulos, "Broadband transmission and statistical performance properties of overhead high-voltage transmission networks," *Hindawi Journal of Computer Networks and Commun.*, 2012, article ID 875632, 2012. [Online]. Available: <http://www.hindawi.com/journals/jcnc/aip/875632/>

- [14] A. G. Lazaropoulos, "Towards modal integration of overhead and underground low-voltage and medium-voltage power line communication channels in the smart grid landscape: model expansion, broadband signal transmission characteristics, and statistical performance metrics (Invited Paper)," *ISRN Signal Processing*, vol. 2012, Article ID 121628, 17 pages, 2012. [Online]. Available: <https://www.hindawi.com/journals/isrn/2012/121628/>
- [15] A. G. Lazaropoulos, "Review and Progress towards the Common Broadband Management of High-Voltage Transmission Grids: Model Expansion and Comparative Modal Analysis," *ISRN Electronics*, vol. 2012, Article ID 935286, pp. 1-18, 2012. [Online]. Available: <http://www.hindawi.com/isrn/electronics/2012/935286/>
- [16] A. G. Lazaropoulos, "Review and Progress towards the Capacity Boost of Overhead and Underground Medium-Voltage and Low-Voltage Broadband over Power Lines Networks: Cooperative Communications through Two- and Three-Hop Repeater Systems," *ISRN Electronics*, vol. 2013, Article ID 472190, pp. 1-19, 2013. [Online]. Available: <http://www.hindawi.com/isrn/electronics/aip/472190/>
- [17] A. G. Lazaropoulos, "Green Overhead and Underground Multiple-Input Multiple-Output Medium Voltage Broadband over Power Lines Networks: Energy-Efficient Power Control," *Springer Journal of Global Optimization*, vol. 2012 / Print ISSN 0925-5001, pp. 1-28, Oct. 2012.
- [18] P. Amirshahi and M. Kavehrad, "High-frequency characteristics of overhead multiconductor power lines for broadband communications," *IEEE J. Sel. Areas Commun.*, vol. 24, no. 7, pp. 1292-1303, Jul. 2006.
- [19] T. Sartenaer, "Multiuser communications over frequency selective wired channels and applications to the powerline access network" Ph.D. dissertation, Univ. Catholique Louvain, Louvain-la-Neuve, Belgium, Sep. 2004. [Online] Available: https://dial.uclouvain.be/pr/boreal/en/object/boreal%3A5010/datastream/PDF_12/view (accessed on 12/28/2017).
- [20] T. Calliacoudas and F. Issa, "Multiconductor transmission lines and cables solver," An efficient simulation tool for plc channel networks development," presented at the *IEEE Int. Conf. Power Line Communications and Its Applications*, Athens, Greece, Mar. 2002.
- [21] A. G. Lazaropoulos, "Best L1 Piecewise Monotonic Data Approximation in Overhead and Underground Medium-Voltage and Low-Voltage Broadband over Power Lines Networks: Theoretical and Practical Transfer Function Determination," *Hindawi Journal of Computational Engineering*, vol. 2016, Article ID 6762390, 24 pages, 2016. doi:10.1155/2016/6762390. [Online]. Available: <https://www.hindawi.com/journals/jcengi/2016/6762390/cta/>
- [22] A. G. Lazaropoulos, "Measurement Differences, Faults and Instabilities in Intelligent Energy Systems – Part 1: Identification of Overhead High-Voltage Broadband over Power Lines Network Topologies by Applying Topology Identification Methodology (TIM)," *Trends in Renewable Energy*, vol. 2, no. 3, pp. 85 – 112, Oct. 2016.
- [23] A. G. Lazaropoulos, "Measurement Differences, Faults and Instabilities in Intelligent Energy Systems – Part 2: Fault and Instability Prediction in Overhead High-Voltage Broadband over Power Lines Networks by Applying Fault and Instability Identification Methodology (FIIM)," *Trends in Renewable Energy*, vol.

- 2, no. 3, pp. 113 – 142, Oct. 2016. [Online]. Available: <http://futureenergysp.com/index.php/tre/article/view/27/33>
- [24] I. C. Demetriou and M. J. D. Powell, “Least squares smoothing of univariate data to achieve piecewise monotonicity,” *IMA J. of Numerical Analysis*, vol. 11, pp. 411-432, 1991.
- [25] I. C. Demetriou and V. Koutoulidis, “On Signal Restoration by Piecewise Monotonic Approximation”, in *Lecture Notes in Engineering and Computer Science: Proceedings of The World Congress on Engineering 2013*, London, U.K., Jul. 2013, pp. 268-273.
- [26] I. C. Demetriou, “An application of best L_1 piecewise monotonic data approximation to signal restoration,” *IAENG International Journal of Applied Mathematics*, vol. 53, no. 4, pp. 226-232, 2013.
- [27] I. C. Demetriou, “L1PMA: A Fortran 77 Package for Best L_1 Piecewise Monotonic Data Smoothing,” *Computer Physics Communications*, vol. 151, no. 1, pp. 315-338, 2003.
- [28] I. C. Demetriou, “Data Smoothing by Piecewise Monotonic Divided Differences,” *Ph.D. Dissertation*, Department of Applied Mathematics and Theoretical Physics, University of Cambridge, Cambridge, 1985.
- [29] I. C. Demetriou, “Best L_1 Piecewise Monotonic Data Modelling,” *Int. Trans. Opt Res.*, vol. 1, no. 1, pp. 85-94, 1994.
- [30] <http://cpc.cs.qub.ac.uk/summaries/ADRF>
- [31] I. C. Demetriou, “Algorithm 863: L2WPMA, a Fortran 77 package for weighted least-squares piecewise monotonic data approximation,” *ACM Transactions on Mathematical Software (TOMS)*, vol. 33, no.1, pp. 6, 2007.
- [32] I. C. Demetriou, “L2CXCV: A Fortran 77 package for least squares convex/concave data smoothing,” *Computer physics communications*, vol. 174, no.8, pp. 643-668, 2006.
- [33] A. G. Lazaropoulos, “Main Line Fault Localization Methodology in Smart Grid – Part 1: Extended TM2 Method for the Overhead Medium-Voltage Broadband over Power Lines Networks Case,” *Trends in Renewable Energy*, vol. 3, no. 3, pp. 2 – 25, 2017. [Online]. Available: <http://futureenergysp.com/index.php/tre/article/view/36/pdf>
- [34] A. G. Lazaropoulos, “Main Line Fault Localization Methodology in Smart Grid – Part 2: Extended TM2 Method, Measurement Differences and L_1 Piecewise Monotonic Data Approximation for the Overhead Medium-Voltage Broadband over Power Lines Networks Case,” *Trends in Renewable Energy*, vol. 3, no. 3, pp. 26 – 61, 2017. [Online]. Available: <http://futureenergysp.com/index.php/tre/article/view/37/pdf>
- [35] A. G. Lazaropoulos, “Power Systems Stability through Piecewise Monotonic Data Approximations – Part 1: Comparative Benchmarking of L1PMA, L2WPMA and L2CXCV in Overhead Medium-Voltage Broadband over Power Lines Networks,” *Trends in Renewable Energy*, vol. 3, no. 1, pp. 2 – 32, Jan. 2017. [Online]. Available: <http://futureenergysp.com/index.php/tre/article/view/29/34>
- [36] A. G. Lazaropoulos, “Power Systems Stability through Piecewise Monotonic Data Approximations – Part 2: Adaptive Number of Monotonic Sections and Performance of L1PMA, L2WPMA and L2CXCV in Overhead Medium-Voltage Broadband over Power Lines Networks,” *Trends in Renewable Energy*, vol. 3, no.

- 1, pp. 33 – 60, Jan. 2017. [Online]. Available: <http://futureenergysp.com/index.php/tre/article/view/30/35>
- [37] A. G. Lazaropoulos, “Improvement of Power Systems Stability by Applying Topology Identification Methodology (TIM) and Fault and Instability Identification Methodology (FIIM) – Study of the Overhead Medium-Voltage Broadband over Power Lines (OV MV BPL) Networks Case,” *Trends in Renewable Energy*, vol. 3, no. 2, pp. 102 – 128, Apr. 2017. [Online]. Available: <http://futureenergysp.com/index.php/tre/article/view/34/pdf>
- [38] A. G. Lazaropoulos, “Main Line Fault Localization Methodology in Smart Grid – Part 3: Main Line Fault Localization Methodology (MLFLM),” *Trends in Renewable Energy*, vol. 3, no. 3, pp. 62 – 81, 2017. [Online]. Available: <http://futureenergysp.com/index.php/tre/article/view/38/pdf>
- [39] OPERA1, D5: Pathloss as a function of frequency, distance and network topology for various LV and MV European powerline networks. IST Integrated Project No 507667, Apr. 2005.
- [40] P. C. J. M. van der Wielen, “On-line detection and location of partial discharges in medium-voltage power cables” Ph.D. dissertation, Tech. Univ. Eindhoven, Eindhoven, the Netherlands, Apr. 2005.
- [41] P. C. J. M. van der Wielen, E. F. Steennis, and P. A. A. F. Wouters, “Fundamental aspects of excitation and propagation of on-line partial discharge signals in three-phase medium voltage cable systems,” *IEEE Trans. Dielectr. Electr. Insul.*, vol. 10, no. 4, pp. 678-688, Aug. 2003.
- [42] M. Tang, and M. Zhai, “Research of transmission parameters of four-conductor cables for power line communication,” in *Proc. Int. Conf. on Computer Science and Software Engineering*, Wuhan, China, Dec. 2008, vol. 5, pp. 1306–1309.
- [43] A. G. Lazaropoulos, “A Panacea to Inherent BPL Technology Deficiencies by Deploying Broadband over Power Lines (BPL) Connections with Multi-Hop Repeater Systems,” *Bentham Recent Advances in Electrical & Electronic Engineering*, vol. 10, no. 1, pp. 30-46, 2017.
- [44] A. G. Lazaropoulos, “Underground Distribution BPL Connections with (N + 1)-hop Repeater Systems: A Novel Capacity Mitigation Technique,” *Elsevier Computers and Electrical Engineering*, vol. 40, pp. 1813-1826, 2014.
- [45] A. G. Lazaropoulos, “Broadband over Power Lines (BPL) Systems Convergence: Multiple-Input Multiple-Output (MIMO) Communications Analysis of Overhead and Underground Low-Voltage and Medium-Voltage BPL Networks (Invited Paper),” *ISRN Power Engineering*, vol. 2013, Article ID 517940, pp. 1-30, 2013. [Online]. Available: <http://www.hindawi.com/isrn/power.engineering/2013/517940/>
- [46] DLC+VIT4IP, D1.2: Overall system architecture design DLC system architecture. FP7 Integrated Project No 247750, Jun. 2010.
- [47] T. Sartenaer and P. Delogne, “Deterministic modelling of the (Shielded) outdoor powerline channel based on the multiconductor transmission line equations,” *IEEE J. Sel. Areas Commun.*, vol. 24, no. 7, pp. 1277-1291, Jul. 2006.
- [48] OPERA1, D44: Report presenting the architecture of plc system, the electricity network topologies, the operating modes and the equipment over which PLC access system will be installed, IST Integr. Project No 507667, Dec. 2005.
- [49] N. Theethayi, “Electromagnetic interference in distributed outdoor electrical systems, with an emphasis on lightning interaction with electrified railway

- network,” Ph.D. dissertation, Uppsala Univ., Uppsala, Sweden, Sep. 2005, [Online]. Available: <http://uu.diva-portal.org/smash/get/diva2:166746/FULLTEXT01>
- [50] J. Anatory, N. Theethayi, R. Thottappillil, M. M. Kissaka, and N. H. Mvungi, “The influence of load impedance, line length, and branches on underground cable Power-Line Communications (PLC) systems,” *IEEE Trans. Power Del.*, vol. 23, no. 1, pp. 180-187, Jan. 2008.
- [51] J. Anatory, N. Theethayi, and R. Thottappillil, “Power-line communication channel model for interconnected networks-Part II: Multiconductor system,” *IEEE Trans. Power Del.*, vol. 24, no. 1, pp. 124-128, Jan. 2009.
- [52] J. Anatory, N. Theethayi, R. Thottappillil, M. M. Kissaka, and N. H. Mvungi, “The effects of load impedance, line length, and branches in typical low-voltage channels of the BPLC systems of developing countries: transmission-line analyses,” *IEEE Trans. Power Del.*, vol. 24, no. 2, pp. 621-629, Apr. 2009.
- [53] A. G. Lazaropoulos, “Designing Broadband over Power Lines Networks Using the Techno-Economic Pedagogical (TEP) Method – Part II: Overhead Low-Voltage and Medium-Voltage Channels and Their Modal Transmission Characteristics,” *Trends in Renewable Energy*, vol. 1, no. 2, pp. 59-86, Jun. 2015. [Online]. Available: <http://futureenergysp.com/index.php/tre/article/view/6/16>
- [54] A. G. Lazaropoulos, “Designing Broadband over Power Lines Networks Using the Techno-Economic Pedagogical (TEP) Method – Part I: Overhead High Voltage Networks and Their Capacity Characteristics (Invited Review Article),” *Trends in Renewable Energy*, vol. 1, no. 1, pp. 16-42, Mar. 2015. [Online]. Available: <http://futureenergysp.com/index.php/tre/article/view/2>
- [55] A. Canova, N. Benvenuto, and P. Bisaglia, “Receivers for MIMO-PLC channels: Throughput comparison,” in *Proc. IEEE Int. Symp. Power Line Communications and Its Applications*, Rio de Janeiro, Brazil, Mar. 2010, pp. 114–119.
- [56] D. Schneider, J. Speidel, L. Stadelmeier, and D. Schill, “Precoded spatial multiplexing MIMO for inhome power line communications,” in *Proc. IEEE Global Telecommunications Conference*, New Orleans, LA, USA, Nov./Dec. 2008, pp. 1–5.
- [57] M. Zimmermann and K. Dostert, “Analysis and modeling of impulsive noise in broad-band powerline communications,” *IEEE Trans. Electromagn. Compat.*, vol. 44, no. 1, pp. 249-258, Feb. 2002.
- [58] T. Esmailian, F. R. Kschischang, and P. G. Gulak, “In-building power lines as high-speed communication channels: Channel characterization and a test channel ensemble,” *Int. J. Commun. Syst.*, vol. 16, pp. 381–400, May 2003.

Article copyright: © 2018 Athanasios G. Lazaropoulos. This is an open access article distributed under the terms of the [Creative Commons Attribution 4.0 International License](https://creativecommons.org/licenses/by/4.0/), which permits unrestricted use and distribution provided the original author and source are credited.



Broadband Performance Metrics and Regression Approximations of the New Coupling Schemes for Distribution Broadband over Power Lines (BPL) Networks

Athanasios G. Lazaropoulos*

*School of Electrical and Computer Engineering / National Technical University of Athens /
9 Iroon Polytechniou Street / Zografou, GR 15780*

Received February 05, 2018; Accepted March 11, 2018; Published March 15, 2018

This paper assesses the broadband performance of overhead (OV) and underground (UN) low-voltage (LV) and medium-voltage (MV) broadband over power lines (BPL) networks when the new refined Coupling Scheme module (CS2 module) is adopted. The broadband performance of distribution BPL networks is assessed in terms of their Average Channel Gain (ACG), Root-Mean-Square Delay-Spread (RMS-DS), Coherence Bandwidth (CB) and Spectral Efficiency (SE). Also, corresponding regression approximations (*i.e.*, UN1, UN2 and UN3 approaches) are given in the examined BPL frequency range. The aforementioned broadband performance metrics of the application of CS2 module are compared against the relative ones of the vintage CS1 module and of MIMO channels. The analysis and relevant numerical results outline: (i) the important improvement of the aforementioned performance metrics and regression approximations when CS2 module is applied in distribution BPL networks instead of CS1 module; and (ii) the universal role of UN1, UN2 and UN3 approaches for describing coupling scheme channels and MIMO ones.

Keywords: Broadband over Power Lines (BPL); Power Line Communications (PLC); distribution power grids; statistical performance metrics; Smart Grid (SG).

1. Introduction

The evolution of the traditional distribution power grids –*i.e.*, overhead (OV) and underground (UN) low-voltage (LV) and medium-voltage (MV)– to a unified smart grid can become the key to delivering broadband last-mile access and simultaneously to developing of an advanced IP-based power system [1]-[7]. Actually, the smart grid is a systems epitome that embodies the interoperability of several communications technologies [8], [9]. Among the candidate communications solutions, broadband over power lines networks (BPL) networks attract the decision-makers' interest due to their techno-economic advantage of not requiring further investments concerning their network cabling since the infrastructure of distribution power grids acts as the required network communication backbone [10].

*Corresponding author: AGLazaropoulos@gmail.com

However, the propagation and transmission of communications signals along distribution BPL networks remain a challenging issue since distribution power grids were not designed for broadband communications purposes. This rather hostile medium for communications is characterized by high attenuation, multipath due to various reflections, BPL signal coupling losses, noise and electromagnetic interference (EMI) [11]-[16]. It is evident that each of the aforementioned aggravating factors differently influences the performance of distribution BPL networks.

As the attenuation, multipath due to various reflections and coupling losses are concerned, the well-validated hybrid model achieves to accurately describe them in BPL networks [2]-[4], [6], [7], [11], [14], [17]-[25]. Being extensively verified during the performance assessment of various multiconductor transmission line (MTL) configurations in BPL networks, the hybrid model consists of two interconnected methods, namely: (i) a bottom-up method that is based on an appropriate combination of MTL theory and similarity transformations, such as the EigenValue Decomposition (EVD), the Single Value Decomposition (SVD) and the Unified Value Decomposition (UVD); and (ii) a top-down method that is based on the concatenation of multidimensional transmission matrices of the cascaded network BPL connections. Various refinements of the aforementioned two methods have been proposed in the literature in order to cope with the special needs of the various supported smart grid applications (e.g., Multiple Input Multiple Output (MIMO) BPL networks [25], [26], power systems stability [27]-[29], identification and localization of faults across distribution power grids [30] and wireless sensor networks [31], [32]).

However, one recent refinement of the top-down method that can significantly enhance the broadband performance and influence the future architectural design of BPL networks is the proposal of Coupling Scheme module (CS2) module [33]. Similarly to its predecessor CS1 module [3], [6], CS2 method handles with the injection and the extraction of BPL signals across the power lines of distribution power grids. As already been presented in [33], findings concerning channel attenuation and capacity reveal that CS2 module better exploits all the available conductors of the MTL configurations than its predecessor CS1 module through the wiser management of the BPL signal power injection and extraction.

In this paper, the broadband performance metrics of Average Channel Gain (ACG), Root-Mean-Square Delay-Spread (RMS-DS), Coherence Bandwidth (CB) and Spectral Efficiency (SE) of OV and UN MV and LV BPL networks when CS2 module is applied are compared against the respective ones of CS1 module and MIMO channels [17]. Besides the comparison of performance metrics and the relative observations, the regression approximations of [17], *i.e.*, UN1 and UN2 approaches, are again calculated for OV and UN LV and MV BPL networks by taking into account the configuration of CS2 module. In addition, UN3 approach that relates SE with ACG is proposed for OV and UN LV and MV BPL networks. Finally, the detailed UN1 and UN2 approaches of CS2 module are compared against the respective ones of CS1 module and of MIMO channels while UN3 approach is assessed for CS2 and CS1 module. The universal character of these three approaches in describing distribution BPL networks is here validated.

The rest of this paper is organized as follows: In Section II, OV and UN LV and MV configurations used in this paper are briefly presented. Section III synthesizes the basics of the propagation, the transmission and the signal coupling across distribution BPL networks. Here, CS2 module is detailed while its operation and performance are

compared against the ones of CS1 module. Section IV reports the broadband performance statistical metrics as well as UN1, UN2 and UN3 regression approximations, which are applied in this paper. In Section V, a series of numerical results and conclusions are provided, aiming at marking out the impact of various coupling schemes supported by CS2 module on the statistical performance metrics and regression approximations of distribution BPL networks. Section VI concludes this paper.

2. Distribution BPL Network Configurations

2.1 MTL Configurations of OV and UN LV and MV BPL Networks

In Figs. 1(a)-(d) of [6], the MTL configurations of distribution BPL networks that are examined in this paper are demonstrated. More specifically:

- *OV LV MTL Configuration:* With reference to Fig. 1(a) of [6], four parallel non-insulated conductors are suspended one above the other spaced by Δ_{LV} while the lowest conductor is suspended at height h_{LV} above ground ($n^{OVLV} = 4$). The upper conductor is the neutral, while the lower three conductors are the three phases. The exact dimensions for this MTL configuration are detailed in [6].
- *OV MV MTL Configuration:* With reference to Fig. 1(b) of [6], the horizontal arrangement of OV MV distribution lines consists of three parallel non-insulated phase conductors ($n^{OVMV} = 3$) spaced by Δ_{MV} that are hang at typical height h_{MV} above ground. There is no neutral conductor. The exact properties of this MTL configuration are given in [6].
- *UN LV MTL Configuration:* With reference to Fig. 1(c) of [6], the cable arrangement of UN LV MTL configuration consists of the three-phase three-core-type conductors, one core-type neutral conductor and one shield conductor ($n^{UNLV} = 4$). The shield is grounded at both ends while the cable is buried 1m inside the ground. The exact dimensions of this UN LV MTL configuration are reported in [6].
- *UN MV MTL Configuration:* With reference to Fig. 1(d) of [6], the cable arrangement of UN MV MTL configuration comprises the three-phase three- sector-type conductors, one shield conductor and one armor conductor. Similarly to UN LV MTL configuration, both the shield and the armor are grounded at both ends while the cable is buried 1m inside the ground. Due to the shielding of UN MV cables and according to [2], [6], [34], the propagation and transmission analysis can be only focused on the inner set of conductors ($n^{UNMV} = 3$), say the three-phase conductors and the shield. The exact dimensions of this UN MV MTL configuration are given in [6].

Finally, the properties of the ground, which are detailed in [6], are assumed common in distribution BPL networks. Here, it should be noted that these ground properties are suitable for the propagation and transmission of BPL signal across distribution BPL networks that operate in the 1-100MHz frequency range of interest.

2.2 Indicative Distribution BPL Topologies

To define a set of indicative distribution BPL topologies, the simple BPL topology of Fig. 1 is considered. With reference to Fig. 1, the transmitting and receiving ends, which are situated at point A and B of the simple BPL topology, respectively,

are assumed to be matched. The branch terminations, which are connected at positions A'_k , $k=1, \dots, N$, are assumed open circuits [11], [13]-[16], [35]-[38]. The end-to-end connection between transmitting and receiving end (path length) of the simple BPL topology, which is encountered in BPL signal transmission, is equal to $L = \sum_{k=1}^{N+1} L_k$ [38]-[40].

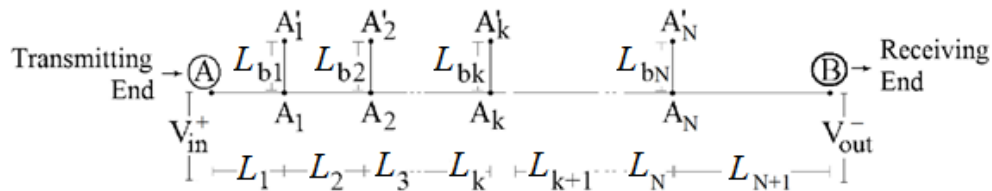


Fig. 1. Simple BPL topology [14], [16].

For comparison reasons, some indicative distribution BPL topologies with the ones of [6], [33] are considered in this paper. In Table 1, five indicative OV distribution BPL topologies of 1000m average path lengths are given as well as the correspondent description, the number of branches, the length of distribution lines and the length of branch lines. Similarly to Table 1, five indicative UN distribution BPL topologies of 200m average path length with their properties are reported in Table 2. Here it should be noted that for given type of distribution power grids, the topologies remain the same; say, BPL topologies of Table 1 remain the same either OV LV or OV MV power grid is considered.

Table 1
OV Distribution BPL Topologies

Topology Name	Topology Description	Number of Branches	Length of Distribution Lines	Length of Branch Lines
Urban case A	Typical overhead urban topology	3	$L_1=500\text{m}$, $L_2=200\text{m}$, $L_3=100\text{m}$, $L_4=200\text{m}$	$L_{b1}=8\text{m}$, $L_{b2}=13\text{m}$, $L_{b3}=10\text{m}$
Urban case B	Aggravated overhead urban topology	5	$L_1=200\text{m}$, $L_2=50\text{m}$, $L_3=100\text{m}$, $L_4=200\text{m}$, $L_5=300\text{m}$, $L_6=150\text{m}$	$L_{b1}=12\text{m}$, $L_{b2}=5\text{m}$, $L_{b3}=28\text{m}$, $L_{b4}=41\text{m}$, $L_{b5}=17\text{m}$
Suburban case	Overhead suburban topology	2	$L_1=500\text{m}$, $L_2=400\text{m}$, $L_3=100\text{m}$	$L_{b1}=50\text{m}$, $L_{b2}=10\text{m}$
Rural case	Overhead rural topology	1	$L_1=600\text{m}$, $L_2=400\text{m}$	$L_{b1}=300\text{m}$
“LOS” case	Overhead Line-of-Sight transmission	0	$L_1=1000\text{m}$	-

Table 2
UN Distribution BPL Topologies

Topology Name	Topology Description	Number of Branches	Length of Distribution Lines	Length of Branch Lines
Urban case A	Typical underground urban topology	3	$L_1=70\text{m}, L_2=55\text{m}, L_3=45\text{m}, L_4=30\text{m}$	$L_{b1}=12\text{m}, L_{b2}=7\text{m}, L_{b3}=21\text{m}$
Urban case B	Aggravated underground urban topology	5	$L_1=40\text{m}, L_2=10\text{m}, L_3=20\text{m}, L_4=40\text{m}, L_5=60\text{m}, L_6=30\text{m}$	$L_{b1}=22\text{m}, L_{b2}=12\text{m}, L_{b3}=8\text{m}, L_{b4}=2\text{m}, L_{b5}=17\text{m}$
Suburban case	Underground suburban topology	2	$L_1=50\text{m}, L_2=100\text{m}, L_3=50\text{m}$	$L_{b1}=60\text{m}, L_{b2}=30\text{m}$
Rural case	Underground rural topology	1	$L_1=50\text{m}, L_2=150\text{m}$	$L_{b1}=100\text{m}$
“LOS” case	Underground Line-of-Sight transmission	0	$L_1=200\text{m}$	-

3. Relationship among BPL Signal Coupling, Transmission and Propagation Distribution BPL Networks

With reference to Fig. 1, the input BPL signal V_m^+ , which is measured at the transmitting end, carries all the required information that needs to be transmitted through the BPL topology while the output BPL signal V_{out}^- , which is measured at the receiving end, should optimally (*i.e.*, if aggravating factors are ignored) be equal to the input BPL signal so that no information is lost. However, aggravating factors that include the attenuation due to the BPL signal propagation, multipath due to the BPL signal transmission and coupling losses influence the measured output BPL signal.

In Figs. 2(a) and 2(b), the general implementation of a coupling scheme module that describes the injection of the input BPL signal onto and the extraction of the output BPL signal from the power lines of BPL topologies, respectively, is illustrated. In fact, different power percentages are allocated among the available conductors that depend on: (i) the participation percentages C_i^{in} , $i=1, \dots, n^G$ of the conductors of the MTL configuration during the BPL signal injection; and (ii) the participation percentages C_i^{out} , $i=1, \dots, n^G$ of the conductors of the MTL configuration during the BPL signal extraction. Note that C_i^{in} , $i=1, \dots, n^G$ and C_i^{out} , $i=1, \dots, n^G$ are the elements of the $n^G \times 1$ input coupling column vector \mathbf{C}^{in} and the $1 \times n^G$ output coupling line vector \mathbf{C}^{out} , respectively, where $[\cdot]^G$ denotes the examined power grid type –either OV MV or UN MV or OV LV or UN LV–.

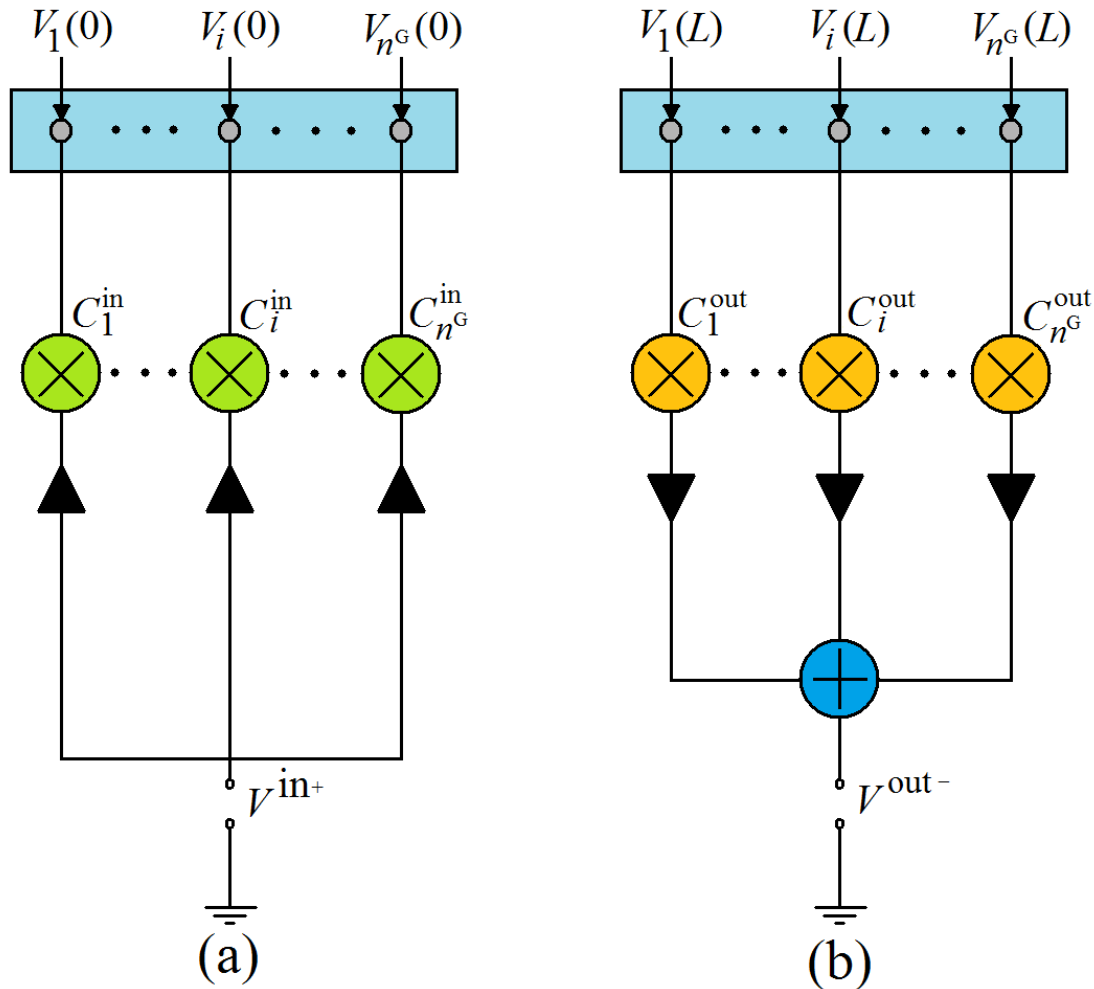


Fig. 2. General implementation of a coupling scheme module [33]. (a) BPL signal injection interface at the transmitting end. (b) BPL signal extraction at the receiving end.

Depending on the element values of \mathbf{C}^{in} and \mathbf{C}^{out} that are restricted by a set of power related constraints analyzed in [33], coupling scheme modules can support three different types of coupling schemes, namely:

1. *Coupling Scheme Type 1*: It consists of Wire-to-Ground (WtG) or Shield-to-Phase (StP) coupling schemes for OV or UN distribution BPL networks, respectively. The signal injection is made in only one conductor at the transmitting end and returns via either the ground for OV distribution cables or the shield for UN distribution cables. The signal extraction is made from the same conductor at the receiving end. $[\mathbf{C}^{\text{in}}]^{\text{WtG}^s/\text{StP}^s}$ and $[\mathbf{C}^{\text{out}}]^{\text{WtG}^s/\text{StP}^s}$ have zero elements except in line s and row s , respectively, where the value is equal to 1. Note that $[\cdot]^{\text{C}}$ denotes the applied coupling scheme. Both CS1 and CS2 modules support this coupling scheme type without performance diversification.
2. *Coupling Scheme Type 2*: It consists of Wire-to-Wire (WtW) or Phase-to-Phase (PtP) coupling schemes for OV or UN distribution BPL networks, respectively. The signal is injected in equal parts between two conductors while it

is extracted from the same conductors. $[\mathbf{C}^{\text{in}}]^{\text{WtW}^{p-q} / \text{PtP}^{p-q}}$ and $[\mathbf{C}^{\text{out}}]^{\text{WtW}^{p-q} / \text{PtP}^{p-q}}$ have zero elements except in lines p and q where the values are different from zero. In terms of these non-zero values, CS1 and CS2 module differentiate each other (see the following analysis).

3. *Coupling Scheme Type 3*: It consists of MultiWire-to-MultiWire (MtM) or MultiPhase-to-MultiPhase (MtM) coupling schemes for OV or UN distribution BPL networks, respectively. The signal is injected among multiple conductors with different participation percentages while the signal is extracted from the same conductor set at the receiving end. For example, when MtM coupling scheme occurs among the three conductors p, q and $r, p, q, r = 1, \dots, n^G$ of MV BPL networks with participation percentages equal to $C_p^{\text{in}}, C_q^{\text{in}}$ and C_r^{in} , respectively, $[\mathbf{C}^{\text{in}}]^{\text{MtM}_{C_p^{\text{in}}-C_q^{\text{in}}-C_r^{\text{in}}^{p-q-r}}$ has zero elements except in lines p, q and r .

At the same rows p, q and $r, [\mathbf{C}^{\text{out}}]^{\text{MtM}_{C_p^{\text{in}}-C_q^{\text{in}}-C_r^{\text{in}}^{p-q-r}}$ receives its non-zero values. This coupling scheme type is only supported by CS2 module.

In accordance with [33] and the general implementation of a coupling scheme module given in Fig. 2, the coupling scheme channel transfer function $H^C\{\cdot\}$ that relates the output BPL signal with the input BPL signal is determined by:

$$H^C\{\cdot\} = \frac{[\mathbf{V}^{\text{out}}]^{\text{C}}}{[\mathbf{V}^{\text{in}}]^{\text{C}}} = [\mathbf{C}^{\text{out}}]^{\text{C}} \cdot \mathbf{H}\{\cdot\} \cdot [\mathbf{C}^{\text{in}}]^{\text{C}} \quad (1)$$

where $\mathbf{H}\{\cdot\}$ is the $n^G \times n^G$ channel transfer function matrix that relates line voltages $\mathbf{V}(z) = [V_1(z) \ \dots \ V_{n^G}(z)]^T$ at the transmitting ($z=0$) and the receiving ($z=L$) ends and is the output of the hybrid model (see [33]). Note that $[\cdot]^T$ denotes the transpose of a matrix. Therefore, the dependence of the coupling scheme channel transfer function on the applied coupling scheme is expressed by the presence of the input and output coupling vector \mathbf{C}^{in} and \mathbf{C}^{out} , respectively, when the channel transfer function is given.

As it concerns the characterization of the elements of the channel transfer function matrix $\mathbf{H}\{\cdot\}$ of eq. (1), its elements $H_{ij}\{\cdot\}, i, j = 1, \dots, n$ with $i = j$ are the co-channel (CC) transfer functions, while those with $i \neq j$ are the cross-channel (XC) transfer functions where $H_{ij}, i, j = 1, \dots, n$ denotes the element of matrix $\mathbf{H}\{\cdot\}$ in row i of column j . All together, $H_{ij}\{\cdot\}, i, j = 1, \dots, n$ are the transfer functions of MIMO channels (either CCs or XCs) whose broadband statistical performance has been examined in [17]. By observing eq. (1), coupling and MIMO channel transfer functions are related through the input and output coupling vector while the broadband performance of coupling channels is investigated and compared against the one of MIMO channels through the broadband performance statistical metrics in this paper.

With reference to the aforementioned coupling scheme types, coupling channels and eq. (1), the differences between CS1 module [3], [6] and CS2 module [33] are focused on the element values of the coupling vectors \mathbf{C}^{in} and \mathbf{C}^{out} that, anyway, describe the operation of CS1 and CS2 module, say:

- *CS1 module*: The main concept of this module is its design and definition simplicity that is preserved through:

$$[\mathbf{C}^{out}] = [\mathbf{C}^{in}]^T \quad (2)$$

Namely, the configuration of BPL injector and extractor remains the same whereas the power flow changes. Therefore, CS1 module can only support coupling scheme type 1 and coupling type scheme 2. As concerns the coupling scheme type 1, the element values of $[\mathbf{C}^{in}]^{WtG^s/StP^s}$ has previously been mentioned. As concerns the coupling scheme type 2, the non-zero values in lines p and q of $[\mathbf{C}^{in}]^{WtW^{p-q}/PtP^{p-q}}$ are equal to 0.5 and -0.5, respectively, following the polarity of the input signal between the conductors. On the basis of eq. (2), the element values of $[\mathbf{C}^{out}]^{WtG^s/StP^s}$ and $[\mathbf{C}^{out}]^{WtW^{p-q}/PtP^{p-q}}$ can be determined for coupling scheme type 1 and 2, respectively. Note that CS1 module creates coupling losses.

- *CS2 module*: The main concept of this module is the minimization of coupling losses that is accomplished by the consideration of \mathbf{C}^{in} and \mathbf{C}^{out} as orthonormal matrices. Namely, apart from the power flow, the configuration of BPL injector and extractor changes. In fact, the element values of \mathbf{C}^{in} and \mathbf{C}^{out} are determined under the principle of energy conservation and eqs (4)-(6) of [33]. With reference to the aforementioned coupling scheme types, CS2 module can support all the three ones. More specifically, as concerns the coupling scheme type 1, CS2 module follows the same definition with CS1 module. As concerns the coupling scheme type 2, CS2 module agrees with the definition of the element values of $[\mathbf{C}^{in}]^{WtW^{p-q}/PtP^{p-q}}$ but $[\mathbf{C}^{out}]^{WtW^{p-q}/PtP^{p-q}}$ has zero elements except in rows p and q where the values are equal to 1 and -1 , respectively. As concerns the coupling scheme type 3, which is supported only by the CS2 module, when MtM coupling scheme occurs among the three conductors p , q and r , $p, q, r=1, \dots, n^G$ with participation percentages equal to C_p^{in} , C_q^{in} and C_r^{in} , respectively, at the transmitting end, $[\mathbf{C}^{in}]^{MtM_{C_p^{in}-C_q^{in}-C_r^{in}}^{p-q-r}}$ has zero elements except in lines p , q , and r where the values are equal to C_p^{in} , C_q^{in} and C_r^{in} , respectively, whereas, at the receiving end, $[\mathbf{C}^{out}]^{MtM_{C_p^{in}-C_q^{in}-C_r^{in}}^{p-q-r}}$ has zero elements except in rows p , q , and r where the values are equal to $|C_p^{in}|/C_p^{in}$, $|C_q^{in}|/C_q^{in}$ and $|C_r^{in}|/C_r^{in}$, respectively.

4. Broadband Performance Statistical Metrics and Regression Approximations of Distribution BPL Networks

In this Section, the broadband performance statistical metrics of [17], which have been applied for the broadband performance assessment of MIMO channels of distribution BPL networks, are here modified in order to assess the broadband performance of various coupling schemes. In fact, the main modification is focused on the replacement of UVD modal channel transfer functions of [17] with the coupling scheme transfer function of eq. (1) as demonstrated in the following analysis.

More particularly, the broadband performance statistical metrics, which are applied in this paper, are the ACG, the RMS-DS, the CB and the SE while the

computation of the discrete impulse response of the coupling scheme transfer function is considered as a prerequisite task. More specifically:

- a. *The discrete impulse response.* Once the coupling scheme channel transfer function $H^C\{\cdot\}$ has already been determined in eq. (1), the discrete coupling scheme channel transfer function H^{C+} that is an important transformation during the computation of broadband performance metrics is given by

$$H^{C+} = \begin{cases} |H_q^{C+}|e^{j\varphi_q^+}, & q = 0, \dots, K-1 \\ 0, & q = K, \dots, J-1 \end{cases} = \begin{cases} H_q^{C+}(f = qf_s), & q = 0, \dots, K-1 \\ 0, & q = K, \dots, J-1 \end{cases} \quad (3)$$

where $F_s = 1/T_s$ is the Nyquist sampling rate, $K \leq J/2$ is the number of subchannels in the BPL signal frequency range of interest, $f_s = F_s/J$ is the flat-fading subchannel frequency spacing. $|H_q^{C+}|$ and φ_q^+ , $q = 0, \dots, J-1$ are the amplitude responses and the phase responses of the discrete coupling scheme channel transfer function, respectively [17], [41]-[43].

Discrete coupling scheme impulse response $h^{C+} = h^{C+}(t = pT_s)$, $p = 0, \dots, J-1$ is obtained as the power of two J -point Inverse Discrete Fourier Transform (IDFT) of the discrete coupling scheme channel transfer function of eq. (3).

- b. *ACG.* ACGs of coupling scheme channels is computed by averaging over frequency [17], [41]-[47]:

$$\overline{|H^{C+}|^2} = \sum_{p=0}^{J-1} |h_p^{C+}|^2 = \frac{1}{J} \sum_{q=0}^{J-1} |H_q^{C+}|^2 \quad (4)$$

- c. *RMS-DS.* The RMS-DS of coupling scheme channels σ_τ^{C+} is determined from [17], [41]-[47]:

$$\sigma_\tau^{C+} = T_s \sqrt{\mu_0^{(2)} - (\mu_0)^2} \quad (5)$$

where

$$\mu_0 = \frac{\sum_{p=0}^{J-1} p |h_p^{C+}|^2}{\sum_{p=0}^{J-1} |h_p^{C+}|^2} \quad (6)$$

$$\mu_0^{(2)} = \frac{\sum_{p=0}^{J-1} p^2 |h_p^{C+}|^2}{\sum_{p=0}^{J-1} |h_p^{C+}|^2} \quad (7)$$

- d. *CB.* It is the range of frequencies over which the normalized autocorrelation function of the channel transfer function is over a certain CB correlation level X (usually set to either 0.9 or 0.7 or 0.5), *i.e.*, the maximum bandwidth in which the subchannels can be approximately considered flat-fading. In accordance with [17], the CB of coupling scheme channels can be determined by:

$$B_c(\Delta f) = \frac{E\left\{H_q^{C+} \cdot [H^{C+}(f = qf_s + \Delta f)]^*\right\}}{E\left\{|H_q^{C+}|^2\right\}}, q = 0, 1, \dots, \left\lfloor (J-2) + \frac{\Delta f}{f_s} \right\rfloor \quad (8)$$

where Δf is the frequency shift, $[\cdot]^*$ denotes the complex conjugate of an element and $\lfloor x \rfloor$ is the largest integer not greater than x . From eq. (8), CB_X is that value of Δf such that $B_c(\Delta f) = X$ while $CB_{0.5}$ is used in this paper.

- e. *Capacity and SE.* In accordance with [33], capacity is defined as the maximum achievable transmission rate that can be reliably transmitted over a BPL topology. Capacity depends on the applied MTL configuration, the BPL topology, the coupling scheme applied, EMI policies adopted and the noise environment. The capacity C for given coupling scheme channel is determined from

$$C = f_s \sum_{q=0}^{K-1} \log_2 \left\{ 1 + \left[\frac{\langle p(q \cdot f_s) \rangle_L}{\langle N(q \cdot f_s) \rangle_L} \cdot |H^{C+}(q \cdot f_s)|^2 \right] \right\} \quad (9)$$

where $\langle \cdot \rangle_L$ is an operator that converts dBm/Hz into a linear power ratio (W/Hz), $p(f)$ is the injected power spectral density limits (IPSD limits) and $N(f)$ is the uniform additive white Gaussian noise (AWGN) PSD level.

Finally, SE is based on the previous capacity computations and refers to the information in bps/Hz that can be reliably transmitted over the used BPL bandwidth for the examined distribution BPL topology. Since capacity computations of this paper are given in 3-88MHz frequency range, spectral efficiency is given by

$$SE = \frac{C}{85\text{MHz}} \quad (10)$$

In accordance with [33], the IPSD limits that are applied are proposed by Ofcom in order to provide a presumption of compliance with FCC Part 15. However, these IPSD limits depend on the type of the distribution power grid (*i.e.*, either OV or UN) and the BPL frequency range (*i.e.*, either 3-30MHz or 30-88MHz). Hence, for given distribution power grid type, the average SE is given by eq. (10) since the capacity computations consider the 3-88MHz frequency range.

Apart from the broadband performance statistical metrics, three regression approaches (*i.e.*, UN1, UN2 and UN3 approach) are applied and computed in this paper in order to describe the behavior of coupling scheme BPL channels. Among the three regression approaches, the first two ones have been introduced in [17] while the last one is first presented in this paper. More specifically:

- *UN1 approach.* UN1 approach linearly approximates the negatively correlated lognormal relation between ACG and RMS-DS of coupling scheme channels of distribution BPL topologies. In this paper, the regression approximation of UN1 approach is compared against the corresponding one of MIMO channels of distribution BPL topologies as demonstrated in [17].
- *UN2 approach.* UN2 approach describes the correlation relation between CB and RMS-DS of coupling scheme channels of distribution BPL topologies through suitable hyperbolic functions. The results of UN2 approach are compared against the respective ones of MIMO channels of distribution BPL topologies of [17]. Since these indicative BPL topologies are carefully selected so as to be the same with those of [17], UN1 and UN2 approaches of this paper concerning the coupling scheme channels are going to be compared against the respective ones of MIMO channels of [17].
- *UN3 approach.* UN3 approach demonstrates the correlation between SE and ACG. With reference to eq. (10), SE depends on the IPSD limits and AWGN PSD noise levels but also on the channel attenuation of the examined distribution BPL

topologies. Here, the relation between SE and channel attenuation is clarified. Furthermore, the impact of the applied coupling scheme module (*i.e.*, CS2 and CS1 module) on the UN3 approach is first investigated through its impact on the coupling transfer functions.

5. Numerical Results and Discussion

The simulations and respective numerical results of this Section aim at assessing the transmission performance of CS2 module against the vintage CS1 module. Extending the capacity observations of [33], the comparison between CS2 and CS1 module is based on the results of the broadband performance statistical metrics of ACG, RMS-DS, CB and SE. Also, the universal role of UN1 and UN2 approaches is examined in distribution BPL networks regardless of the coupling scheme module (*i.e.*, CS2 or CS1 module) or the channel type (*i.e.*, coupling scheme channel or MIMO channel). In addition, the behavior of UN3 approach is first presented and then investigated in terms of the applied coupling scheme module.

For the numerical computations, the indicative OV and UN distribution BPL topologies of Tables 1 and 2 (denoted hereafter as indicative topologies) are considered. With reference to eq. (1), the numerical results focus on the coupling transfer function from the application of CS2 and CS1 modules rather than on the behavior of the channel transfer function matrices since the last issue has thoroughly been analyzed in [3], [6], [11], [14]-[16], [33].

For comparison reasons, the same simulation model properties with [17] concerning the sampling and IDFT settings are here assumed. More specifically, the operating frequency band, the Nyquist sampling rate F_s and flat-fading subchannel frequency spacing f_s are assumed equal to 1-100MHz, 200MHz and 0.1MHz, respectively. Therefore, the number of subchannels K in the BPL signal frequency range of interest and the J -point IDFT are assumed equal to 991 and 2048, respectively [41]-[43].

As the capacity computation model properties are regarded, these are assumed to be the same with [17], [33], namely, the IPSP limits proposed by Ofcom are applied while AWGN PSD levels of -105dBm/Hz and -135dBm/Hz in the case of overhead and underground BPL networks, respectively, are applied in order to describe the noise conditions. For the sake of comparison, 3-88MHz frequency range is only assumed for the case of capacity and SE computations since the aforementioned IPSP limits are so defined.

Finally, as the properties of coupling schemes are concerned, representative coupling schemes of the three coupling scheme types of Sec. III are considered so that a clear transmission performance comparison between CS2 and CS1 module can be presented by simultaneously respecting the manuscript size limitations. Hence, the coupling schemes types of WtG^1/StP^1 , WtW^{2-3}/PtP^{2-3} and $MtM_{0.7_{-0.1_{-0.2}}^{1-2-3}}$ are the representative ones for the coupling scheme type 1, 2 and 3, respectively. Already been mentioned, WtG and WtW coupling schemes are related to OV distribution BPL topologies whereas StP and PtP coupling schemes are related to UN distribution BPL topologies. MtM coupling schemes are common for both OV and UN distribution BPL topologies. Note that during MtM coupling schemes, the fourth conductor, where it exists, is not used. For the representative coupling schemes, the broadband performance

statistical metrics as well as the regression approximations are applied so that their performance and the overall performance of CS2 module can be examined.

5.1 ACG

ACG is a statistical metric that describes the complexity of the examined BPL topologies. The lowest ACG values imply an intense multipath environment where high number of short branches exists. Also, ACG facilitates the comparison between CS2 and CS1 module since their impact during the injection and extraction process of BPL signal is clearly quantified.

In Table 3, ACG of the indicative OV LV and OV MV topologies is reported when CS2 and CS1 modules are considered and the aforementioned representative coupling schemes are applied. Same results with Table 3 are reported for the indicative UN LV and UN MV topologies in Table 4.

Table 3
ACG of the Indicative OV Distribution BPL Topologies for the Representative Coupling Schemes when CS2 and CS1 Modules are Considered

		ACG (dB)					
		WtG ¹		WtW ²⁻³		MtM ¹⁻²⁻³ _{0.7_-0.1_-0.2}	
		CS2	CS1	CS2	CS1	CS2	CS1
Urban case A	LV	-9.53	-9.53	-9.40	-15.42	-9.05	-
	MV	-9.84	-9.84	-9.45	-15.47	-9.09	-
Urban case B	LV	-12.70	-12.70	-12.59	-18.62	-12.19	-
	MV	-13.01	-13.01	-12.54	-18.56	-12.14	-
Suburban case	LV	-8.22	-8.22	-8.08	-14.10	-7.72	-
	MV	-8.54	-8.54	-8.09	-14.11	-7.72	-
Rural case	LV	-6.74	-6.74	-6.54	-12.56	-6.12	-
	MV	-7.06	-7.06	-6.51	-12.53	-6.09	-
“LOS” case	LV	-4.65	-4.65	-4.51	-10.53	-4.17	-
	MV	-4.92	-4.92	-4.48	-10.51	-4.14	-

Table 4
ACG of the Indicative UN Distribution BPL Topologies for the Representative Coupling Schemes when CS2 and CS1 Modules are Considered

		ACG (dB)					
		StP ¹		PtP ²⁻³		MtM ¹⁻²⁻³ _{0.7_-0.1_-0.2}	
		CS2	CS1	CS2	CS1	CS2	CS1
Urban case A	LV	-15.40	-15.40	-16.70	-22.72	-15.97	-
	MV	-25.14	-25.14	-25.14	-31.16	-25.14	-
Urban case B	LV	-19.18	-19.18	-20.47	-26.49	-19.74	-
	MV	-27.08	-27.08	-27.08	-33.10	-27.08	-
Suburban case	LV	-14.42	-14.42	-15.70	-21.72	-14.98	-
	MV	-23.31	-23.31	-23.31	-29.33	-23.31	-
Rural case	LV	-12.20	-12.20	-13.42	-19.44	-12.74	-
	MV	-20.78	-20.78	-20.78	-26.80	-20.78	-
“LOS” case	LV	-9.46	-9.46	-10.59	-16.61	-9.96	-
	MV	-17.95	-17.95	-17.95	-23.97	-17.95	-

From Tables 3 and 4, several interesting remarks concerning the applied coupling schemes and examined coupling scheme modules as well as their interaction can be pointed out. First, ACGs of OV and UN LV and MV topologies remain the same for given BPL topology regardless of the WtG¹ or StP¹ coupling scheme applied. This is a rather logical observation for the coupling schemes of type 1 since $[C^{in}]^{WtG^1/StP^1}$ and $[C^{out}]^{WtG^1/StP^1}$ of CS2 module are equal to the respective coupling vectors of the vintage CS1 module. Anyway, the main differences of CS2 and CS1 module are focused on the coupling scheme type 2 and 3.

As the coupling schemes of type 2 are concerned, CS2 module achieves better ACGs than CS1 module since $[C^{out}]^{WtW^{2-3}/PtP^{2-3}}$ of CS2 module allows the full reconstruction of the output signal in contrast with the half-signal reception of CS1 module due to $[C^{out}]^{WtW^{2-3}/PtP^{2-3}}$. Hence, as it is expected, ACG difference between CS2 and CS1 module remains approximately equal to +6dB and this is numerically validated from the comparison of CS1 and CS2 columns of WtW²⁻³ and PtP²⁻³ coupling schemes in Table 3 and 4, respectively. Although CS2 module can significantly improve ACG of coupling schemes of type 2, WtW and PtP coupling schemes still present slightly worst ACG performance in comparison with the respective one of WtG and StP coupling schemes for given BPL network type.

As the coupling schemes of type 3 are examined, only CS2 module may support these coupling schemes due to its capability to discretely define $[C^{in}]^{WtG^3/StP^3}$ and $[C^{out}]^{WtG^3/StP^3}$. Despite its installation complexity, MtM coupling schemes exploit either the better ACG performance of coupling schemes of type 1 or the better electromagnetic compatibility (EMC) efficiency of coupling schemes of type 2. By appropriately adjusting the participation percentage C_p^{in} , C_q^{in} and C_r^{in} of $[C^{in}]^{MtM^{1-2-3}_{C_p^{in}, C_q^{in}, C_r^{in}}}$,

a trade-off relationship between broadband transmission, capacity performance and EMC can be adjusted through remote monitoring and surveillance.

5.2 RMS-DS

Already been mentioned in [17], RMS-DS is a highly variable statistical performance metric that depends on the power grid type and the examined BPL topology. Similarly to the ACG approach of Sec.5.1A, RMS-DS of the indicative OV LV and OV MV topologies is reported in Table 5 when CS2 and CS1 modules are considered and the aforementioned representative coupling schemes are applied. Same results with Table 5 are reported for the indicative UV LV and UN MV BPL topologies in Table 6.

Similarly to ACG, RMS-DS reflects the complexity of the examined BPL topology but, in contrast with ACG, RMS-DS cannot directly quantify the impact of the applied coupling scheme modules; RMS-DS values are the same for CS2 and CS1 module for given power grid type and BPL topology. However, RMS-DS computation remains critical since its values are necessary for the UN1 and UN2 approximations. In general, RMS-DS presents higher values as the BPL topology complexity increases; say, urban topologies present higher RMS-DS values than those of suburban, rural and “LOS” topologies due to the their aggravated multipath environment [48], [49].

Table 5
RMS-DS of the Indicative OV Distribution BPL Topologies for the Representative Coupling Schemes when CS2 and CS1 Modules are Considered

		RMS-DS					
		(μs)					
		WtG ¹		WtW ²⁻³		MtM ¹⁻²⁻³ _{0.7_-0.1_-0.2}	
		CS2	CS1	CS2	CS1	CS2	CS1
Urban case A	LV	0.56	0.56	0.59	0.59	0.61	-
	MV	0.74	0.74	0.64	0.64	1.01	-
Urban case B	LV	1.11	1.11	1.18	1.18	1.25	-
	MV	1.07	1.07	1.18	1.18	1.28	-
Suburban case	LV	0.53	0.53	0.55	0.55	0.58	-
	MV	0.64	0.64	0.58	0.58	0.84	-
Rural case	LV	1.07	1.07	1.09	1.09	1.12	-
	MV	1.08	1.08	1.10	1.10	1.18	-
“LOS” case	LV	0.09	0.09	0.10	0.10	0.10	-
	MV	0.38	0.38	0.20	0.20	0.61	-

Table 6
RMS-DS of the Indicative UN Distribution BPL Topologies for the Representative Coupling Schemes when CS2 and CS1 Modules are Considered

		RMS-DS					
		(μs)					
		StP ¹		PtP ²⁻³		MtM _{0.7_-0.1_-0.2} ¹⁻²⁻³	
		CS2	CS1	CS2	CS1	CS2	CS1
Urban case A	LV	0.54	0.54	0.57	0.57	0.55	-
	MV	1.21	1.21	1.21	1.21	1.21	-
Urban case B	LV	0.83	0.83	0.84	0.87	0.85	-
	MV	1.45	1.45	1.45	1.45	1.45	-
Suburban case	LV	0.48	0.48	0.48	0.48	0.48	-
	MV	0.79	0.79	0.79	0.79	0.79	-
Rural case	LV	0.53	0.53	0.54	0.54	0.53	-
	MV	0.87	0.87	0.87	0.87	0.87	-
“LOS” case	LV	0.26	0.26	0.29	0.29	0.28	-
	MV	0.60	0.60	0.60	0.60	0.60	-

5.3 CB

Similarly to RMS-DS, CB expresses the maximum bandwidth in which the subchannels can be approximately considered flat-fading in a BPL channel. CB_{0.5} of the indicative OV LV and OV MV topologies is reported in Table 7 when CS2 and CS1 modules are applied and the aforementioned representative coupling schemes are considered. Same results with Table 7 are reported for the indicative UV LV and UN MV BPL topologies in Table 8.

Table 7
CB_{0.5} of the Indicative OV Distribution BPL Topologies for the Representative Coupling Schemes when CS2 and CS1 Modules are Considered

		CB _{0.5}					
		(MHz)					
		WtG ¹		WtW ²⁻³		MtM _{0.7_-0.1_-0.2} ¹⁻²⁻³	
		CS2	CS1	CS2	CS1	CS2	CS1
Urban case A	LV	2.6	2.6	2.6	2.6	2.5	-
	MV	2.7	2.7	2.6	2.6	2.4	-
Urban case B	LV	0.7	0.7	0.7	0.7	0.7	-
	MV	0.8	0.8	0.7	0.7	0.7	-
Suburban case	LV	1.1	1.1	1.1	1.1	1.1	-
	MV	1.1	1.1	1.1	1.1	1.1	-
Rural case	LV	5.7	5.7	3.2	3.2	0.7	-
	MV	6.7	6.7	3.2	3.2	0.2	-
“LOS” case	LV	49.4	49.4	49.4	49.4	49	-
	MV	47.6	47.6	49.3	49.3	46.6	-

Table 8
 $CB_{0.5}$ of the Indicative UN Distribution BPL Topologies for the Representative Coupling Schemes when CS2 and CS1 Modules are Considered

		$CB_{0.5}$					
		(MHz)					
		StP ¹		PtP ²⁻³		MtM ¹⁻²⁻³ _{0.7_-0.1_-0.2}	
		CS2	CS1	CS2	CS1	CS2	CS1
Urban case A	LV	1.3	1.3	1.3	1.3	1.3	-
	MV	0.6	0.6	0.6	0.6	0.6	-
Urban case B	LV	0.8	0.8	0.7	0.7	0.7	-
	MV	0.5	0.5	0.5	0.5	0.5	-
Suburban case	LV	1.3	1.3	1.3	1.3	1.3	-
	MV	1.1	1.1	1.1	1.1	1.1	-
Rural case	LV	21.2	21.2	21.2	21.2	21.2	-
	MV	3.8	3.8	3.8	3.8	3.8	-
“LOS” case	LV	37	37	33.5	33.5	35.6	-
	MV	5.8	5.8	5.8	5.8	5.8	-

Similarly to ACG and RMS-DS, CB depends on the complexity of the examined BPL topology. BPL topologies with aggravated multipath environments require shorter subchannel bandwidths so that their channels can be considered as flat-fading ones. Numerically, 49.4MHz and 0.5MHz are the maximum and minimum flat-fading subchannel bandwidths that are reported in Tables 7 and 8 for the examined representative BPL topologies. Here, it should be noted that flat-fading subchannel frequency spacing f_s is assumed equal to 0.1MHz, thus allowing the flat-fading subchannel frequency consideration either during the computation of the statistical broadband performance metrics of this paper or the capacity computations of [33].

5.4 Capacity and SE

The behavior of the transmission performance metrics of ACG, RMS-DS and CB, which has been highlighted in the previous subsections, is also reflected on the capacity performance metrics. With reference to [33], capacity of the indicative OV LV and OV MV topologies is reported in Table 9 when CS2 and CS1 modules are applied and the aforementioned representative coupling schemes are considered. Here it should be reminded that both capacity performance metrics are computed in the 3-88MHz frequency range due to the frequency range limitations of the applied IPSP limits. Same results with Table 9 are reported for the indicative UV LV and UN MV BPL topologies in Table 10. In Table 11 and 12, SE values are computed for the same cases of Table 9 and 10, respectively.

Table 9
Capacity of the Indicative OV Distribution BPL Topologies for the Representative Coupling Schemes when CS2 and CS1 Modules are Considered

		Capacity (Mbps)					
		WtG ¹		WtW ²⁻³		MtM ¹⁻²⁻³ _{0.7_-0.1_-0.2}	
		CS2	CS1	CS2	CS1	CS2	CS1
Urban case A	LV	606	606	612	463	620	-
	MV	596	596	612	463	622	-
Urban case B	LV	469	469	475	346	484	-
	MV	459	459	476	346	485	-
Suburban case	LV	715	715	721	561	730	-
	MV	705	705	722	562	732	-
Rural case	LV	797	797	803	637	811	-
	MV	787	787	803	638	811	-
“LOS” case	LV	902	902	908	738	916	-
	MV	892	892	909	739	918	-

Table 10
Capacity of the Indicative UN Distribution BPL Topologies for the Representative Coupling Schemes when CS2 and CS1 Modules are Considered

		Capacity (Mbps)					
		StP ¹		PtP ²⁻³		MtM ¹⁻²⁻³ _{0.7_-0.1_-0.2}	
		CS2	CS1	CS2	CS1	CS2	CS1
Urban case A	LV	1849	1849	1805	1635	1830	-
	MV	815	815	815	698	815	-
Urban case B	LV	1634	1634	1590	1420	1615	-
	MV	685	685	685	581	685	-
Suburban case	LV	1953	1953	1909	1739	1934	-
	MV	890	890	890	767	890	-
Rural case	LV	2053	2053	2008	1838	2034	-
	MV	968	968	968	838	968	-
“LOS” case	LV	2152	2152	2108	1938	2133	-
	MV	1049	1049	1049	913	1049	-

Table 11

SE of the Indicative OV Distribution BPL Topologies for the Representative Coupling Schemes when CS2 and CS1 Modules are Considered

		SE (bps/Hz)					
		WtG ¹		WtW ²⁻³		MtM ¹⁻²⁻³ _{0.7_-0.1_-0.2}	
		CS2	CS1	CS2	CS1	CS2	CS1
Urban case A	LV	7.13	7.13	7.20	5.45	7.29	-
	MV	7.01	7.01	7.20	5.45	7.32	-
Urban case B	LV	5.52	5.52	5.59	4.07	5.69	-
	MV	5.40	5.40	5.60	4.07	5.71	-
Suburban case	LV	8.41	8.41	8.48	6.60	8.59	-
	MV	8.29	8.29	8.49	6.61	8.61	-
Rural case	LV	9.38	9.38	9.45	7.49	9.54	-
	MV	9.26	9.26	9.45	7.51	9.54	-
“LOS” case	LV	10.61	10.61	10.68	8.68	10.78	-
	MV	10.49	10.49	10.69	8.69	10.80	-

Table 12

SE of the Indicative UN Distribution BPL Topologies for the Representative Coupling Schemes when CS2 and CS1 Modules are Considered

		SE (bps/Hz)					
		StP ¹		PtP ²⁻³		MtM ¹⁻²⁻³ _{0.7_-0.1_-0.2}	
		CS2	CS1	CS2	CS1	CS2	CS1
Urban case A	LV	21.75	21.75	21.24	19.24	21.53	-
	MV	9.59	9.59	9.59	8.21	9.59	-
Urban case B	LV	19.22	19.22	18.71	16.71	19.00	-
	MV	8.06	8.06	8.06	6.84	8.06	-
Suburban case	LV	22.98	22.98	22.46	20.46	22.75	-
	MV	10.47	10.47	10.47	9.02	10.47	-
Rural case	LV	24.15	24.15	23.62	21.62	23.93	-
	MV	11.39	11.39	11.39	9.86	11.39	-
“LOS” case	LV	25.32	25.32	24.80	22.80	25.09	-
	MV	12.34	12.34	12.34	10.74	12.34	-

From Tables 9-12, it is obvious that CS2 module achieves better spectral exploitation of the allocated BPL frequency band in comparison with the CS1 module in coupling schemes of type 2 and 3. Only by appropriately adjusting the way that the BPL signal power is extracted at the receiving end, average SE improvement of 1.821bps/Hz and 1.718bps/Hz is achieved in OV/WtW and UN/PtP distribution BPL networks, respectively, while the respective capacity improvement is equal to 155Mbps and 146Mbps.

Apart from their special transmission metric attributes, MtM coupling schemes present notable capacity characteristics that can be combined with their EMC adaptability [33]. Here, it should be underlined that only CS2 module supports MtM coupling schemes in distribution BPL networks. Numerically, with reference to Table 11, an average MtM coupling scheme achieves better SE in all the indicative topologies of the OV distribution BPL networks examined. With reference to Table 12, the same average MtM coupling scheme achieves better SE behavior in the vast majority of the UN/PtP distribution BPL topologies examined while its values are comparable even to the ones of the UN/StP distribution BPL topologies. Therefore, MtM can combine the favourable characteristics of both coupling scheme types 1 and 2; say the high SE of coupling scheme type 1 and the EMC strength of coupling scheme type 2. However, the main disadvantage of MtM coupling schemes is their high cost due to the installation of additional BPL repeaters on the distribution OV and UN conductors.

Finally, as the benchmark SE performance of CS2 and CS1 module is concerned, when the coupling schemes of the coupling scheme type 1 are applied, capacity and SE improvements are not observed regardless of the adoption of CS2 or CS1 module.

5.5 UN1 Approach

In [17], the correlation between RMS-DS and ACG has been highlighted with respect to the OV and UN MIMO/LV and MIMO/MV BPL channels, say CC and XC of OV and UN LV and MV BPL topologies. Following this fundamental property of several wireline networks, such as DSL and coaxial ones, regression trend lines of the form $(\sigma_{\tau})_{\mu s} = -v \cdot \left(\overline{|H|^2} \right)_{dB} + w$ have been used in the aforementioned MIMO BPL channels

where $(\sigma_{\tau})_{\mu s}$ is the RMS-DS in μs of the examined BPL channels, $\left(\overline{|H|^2} \right)_{dB}$ is the ACG in dB and v and w are the robust regression parameters. UN1_{MIMO} approach, which has been proposed in [17], is characterized by a set of robust regression parameters v and w that comes from the least squares fitting method being applied to the ACG / RMS-DS values of MIMO BPL channels regardless of the power grid type, BPL topology and MIMO channel type.

RMS-DS / ACG regression curves, which come from the linear regression approximations of different measurement campaign data, have been extensively proposed in the BPL literature for various BPL network types (e.g., in-home, in-ship, in-car, OV LV and OV MV BPL networks) [41], [50]-[53]. UN1 approach is compared against other well validated approximations of the BPL literature that deals with the coupling channels of various BPL networks; say, ANT approach and GAL approach as given by [46] and [41]-[43], respectively. Analytically, the robust regression parameters of each approach are reported in Table 13. In the same Table, the robust regression parameters v and w of

$UN1_{CS2}$ approach are computed for all the BPL topologies regardless of the power grid type when WtG^1 , StP^1 , WtW^{2-3} , PtP^{2-3} and $MtM_{0.7-0.1-0.2}^{1-2-3}$ of CS2 module are applied in accordance with Tables 3-6. Similarly to $UN1_{CS2}$ approach, the robust regression parameters v and w of $UN1_{CS1}$ approach are computed for all the BPL topologies regardless of the power grid type when WtG^1 , StP^1 , WtW^{2-3} and PtP^{2-3} of CS1 module are applied in accordance with Tables 3-6.

In Fig. 3, except for the simulation data of Tables 3-6, the set of regression trend lines of Table 13, say ANT, GAL, $UN1_{MIMO}$, $UN1_{CS1}$ and $UN1_{CS2}$ approaches, are also illustrated.

Table 13
Robust Regression Parameters v and w of the Different RMS-DS / ACG Approaches

	ANT	GAL	$UN1_{MIMO}$	$UN1_{CS1}$	$UN1_{CS2}$
v ($\mu\text{s}/\text{dB}$)	-0.0197	-0.0075	-0.01029	-0.0227	-0.0242
w (μs)	0	0.183	0.59	0.3659	0.4378

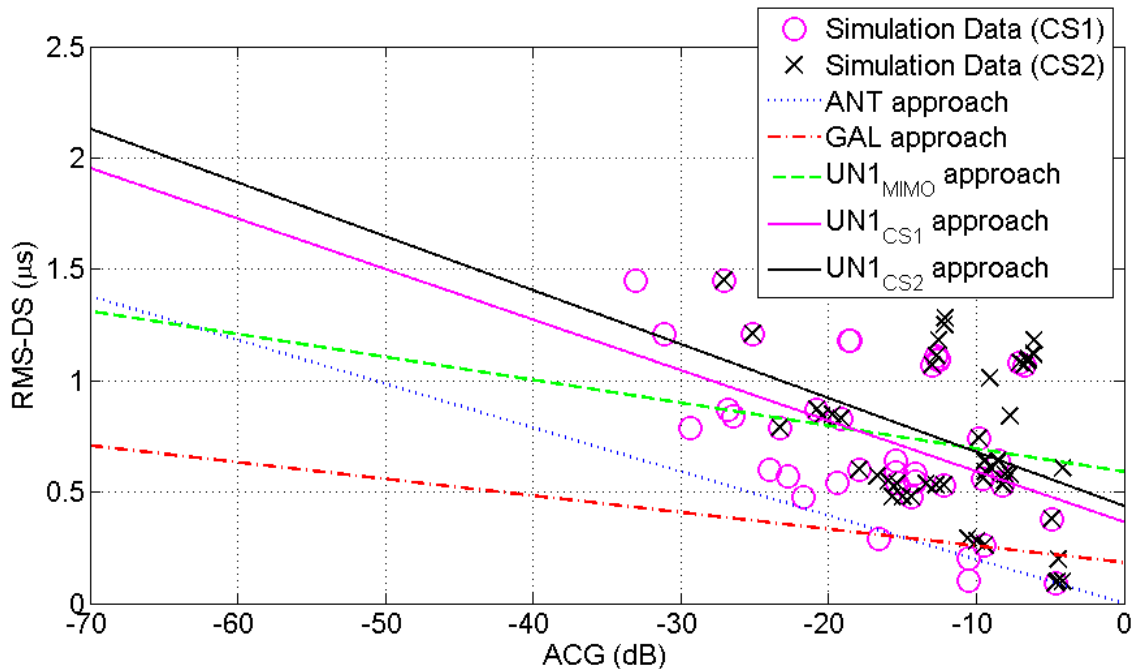


Fig. 3. Scatter plot of RMS-DS versus ACG for simulated coupling scheme OV and UN MV and LV BPL channels and various regression approaches.

From Fig. 3, several interesting remarks concerning the performance of regression approximations can be pointed out, namely:

- Either MIMO or coupling scheme channels are examined, ACG and RMS-DS of OV and UN LV and MV BPL channels are negatively correlated lognormal random variables. This fact is validated by the negative slopes of all regression lines that approximate simulation data in Fig. 3.
- The set of UN1 regression lines, say $UN1_{MIMO}$, $UN1_{CS1}$ and $UN1_{CS2}$ approaches, better approximates the simulation in comparison with ANT and GAL approaches. This is due to the fact that the set of UN1 regression lines is based on simulation data of distribution BPL networks rather on other various types of BPL networks (indoor, in-vehicle, etc).
- The differences among UN1 regression lines remain low enhancing the role of UN1 regression lines as a unified regression approach [17]. More specifically:
 - The small differences between $UN1_{MIMO}$ approach and $UN1_{CSx}$ approaches, $x=1,2$ are due to the different origin of the processed simulation data; the former approach is based on the approximation of MIMO channels while the latter approaches approximate simulation data of coupling scheme channels. Hence, the impact of signal coupling is reflected on the differences of the aforementioned approaches.
 - The differences between $UN1_{CS1}$ and $UN1_{CS2}$ approaches can be considered as negligible while they come from the versatility of coupling scheme types supported by CS2 module. In comparison with the supported coupling schemes by CS1 module, CS2 module mainly affects the performance of coupling schemes of type 2, *i.e.*, WtW and PtP coupling schemes, while coupling schemes of type 3, *i.e.*, MtM coupling schemes, are only supported by CS2 module. Since coupling schemes of type 1 remain the same, the difference between $UN1_{CS1}$ and $UN1_{CS2}$ approaches can be considered as the weighted mean average of the supported coupling scheme types; for example, if RMS-DS is assumed to be equal to $1\mu s$, the difference between the AVG of $UN1_{CS1}$ and $UN1_{CS2}$ approach is equal to 4.7dB, that is near to the two thirds of the +6dB ACG difference between CS2 and CS1 module mentioned in Sec.VA where two thirds corresponds to the number of coupling scheme types affected by CS2 module.

5.6 UN2 Approach

UN2 approach describes the fundamental correlation between CB and RMS-DS. In [17], this fundamental property of OV and UN LV and MV MIMO BPL channels has been reported and has been described through an appropriate hyperbolic trend curves set while the efficiency of $UN2_{MIMO}$ approach has been computed with respect to suitable simulation data of MIMO channels.

Similarly to RMS-DS / ACG regression curves, RMS-DS / CB hyperbolic trend curves have widely been used in various BPL network types [50], [52], [53]. In fact, the regression hyperbolic trend curves of the form $(\sigma_{\tau})_{\mu s} = y \cdot (CB_{0.5})_{MHz}^{-1}$ are also used in UN2 approach where y is the robust regression parameter. In this paper, the same form of regression hyperbolic trend curves are going to be used for the assessment of coupling

scheme BPL channels when CS2 and CS1 modules are adopted. By using robust linear least square error fitting between the trend and the simulation data of the OV and UN LV and MV BPL coupling scheme channels as reported in Tables 5-8, the parameter y of corresponding UN2_{CS1} and UN2_{CS2} approaches can be calculated. Analytically, the robust regression parameter y of each approach is reported in Table 11.

In Fig. 4, except for the simulation data of Tables 5-8, the set of regression trend curves of Table 10, say UN2_{MIMO}, UN2_{CS1} and UN2_{CS2} approaches, are illustrated.

Table 14
Robust Regression Parameter y of the Different RMS-DS / CB_{0.5} Approaches

	UN2 _{MIMO}	UN2 _{CS1}	UN2 _{CS2}
y ($\mu\text{s} \cdot \text{MHz}$)	0.4155	0.7912	0.6131

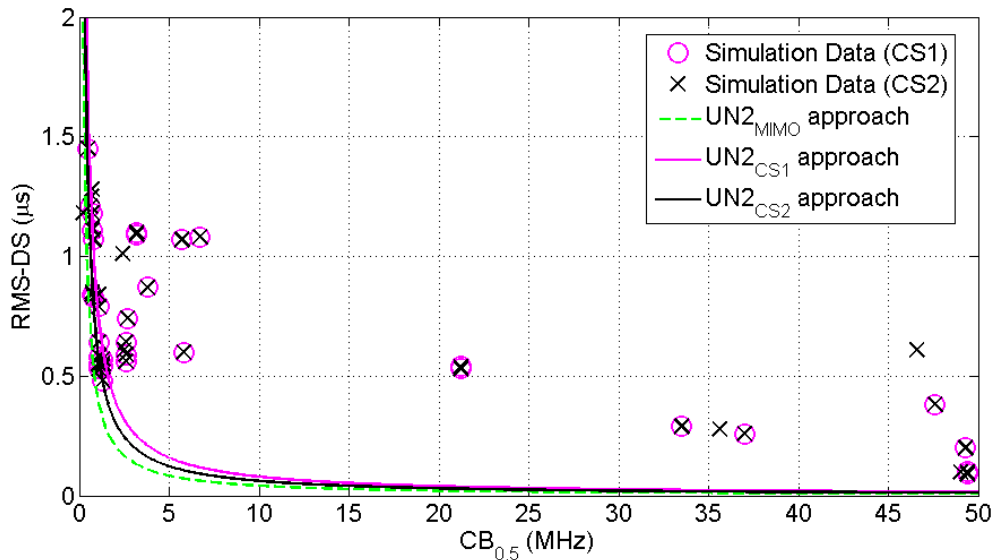


Fig. 4. Scatter plot of RMS-DS versus CB_{0.5} for simulated coupling scheme OV and UN LV and MV BPL channels and various regression approaches.

From Fig. 4, additional observations regarding the performance of regression approximations can be given, namely:

- CB and RMS-DS remain inversely related each other either in MIMO or in coupling scheme channels of distribution BPL networks. In both cases, appropriate hyperbolic functions can approximate CB and RMS-DS simulation data.
- Differences among UN2_{MIMO}, UN2_{CS1} and UN2_{CS2} approaches remain marginal despite the high variability of CB / RMS-DS simulation. The main divergences of UN2 approach curves are focused on the rural and “LOS” topologies of

distribution BPL networks whose RMS-DSs remain high due to the long average path lengths of distribution BPL networks.

- Due to the low differences of UN2_{MIMO}, UN2_{CS1} and UN2_{CS2} approaches, each of the UN2 approaches can sustain a unified consideration of the CB / RMS-DS correlation of either MIMO or coupling scheme channels.

5.7 UN3 Approach

UN3 approach, which is first presented in this paper, achieves to correlate the average SE and ACG of a distribution BPL topology. With respect to eq. (9), capacity significantly depends on the channel attenuation of the examined distribution BPL topology across the frequency range of interest but not only on this. In this paper, the different coupling scheme modules that are benchmarked do influence the coupling transfer function and, thus, its ACG. In order to highlight: (i) the SE dependence on the ACG when IPSD limits and noise PSD levels are assumed to be common; (ii) the role of the coupling scheme modules; and (iii) the SE dependence diversification on the IPSD limits and noise PSD levels when OV and UN distribution BPL networks are assumed, UN3 approach is here proposed following the definition of UN1 approach. In this subsection, UN3 approach examines the aforementioned correlation when CS2 and CS1 modules are applied.

UN3 approach is assumed to be described by regression trend lines of the form $(SE)_{\text{bps/Hz}} = -a \cdot \left(\overline{|H|^2} \right)_{\text{dB}} + \beta$ where $(SE)_{\text{bps/Hz}}$ is the average SE given in Tables 11 and 12 for OV and UN distribution BPL networks, respectively, while a and β are the robust regression parameters that come from the least squares fitting method. In order to investigate the SE performance diversification due to the different IPSD limits and noise PSD levels that are used in OV and UN distribution networks, two different regression trend lines of UN3 approach are presented for each coupling scheme module; say, one regression trend line for the OV distribution networks (*i.e.*, UN3^{OV} approach) and another one for the UN distribution networks (*i.e.*, UN3^{UN} approach). Analytically, the robust regression parameters of each approach per coupling scheme module are reported in Table 15. Note that a and β of each column of Table 15 are computed for all

Table 15
Robust Regression Parameter α and β of the Different SE / ACG Approaches

	UN3 _{CS1-OV}	UN3 _{CS1-UN}	UN3 _{CS2-OV}	UN3 _{CS2-UN}
α bps/(dB·Hz)	0.4472	0.8627	0.6434	1.1154
β (bps/Hz)	12.396	34.356	13.546	37.363

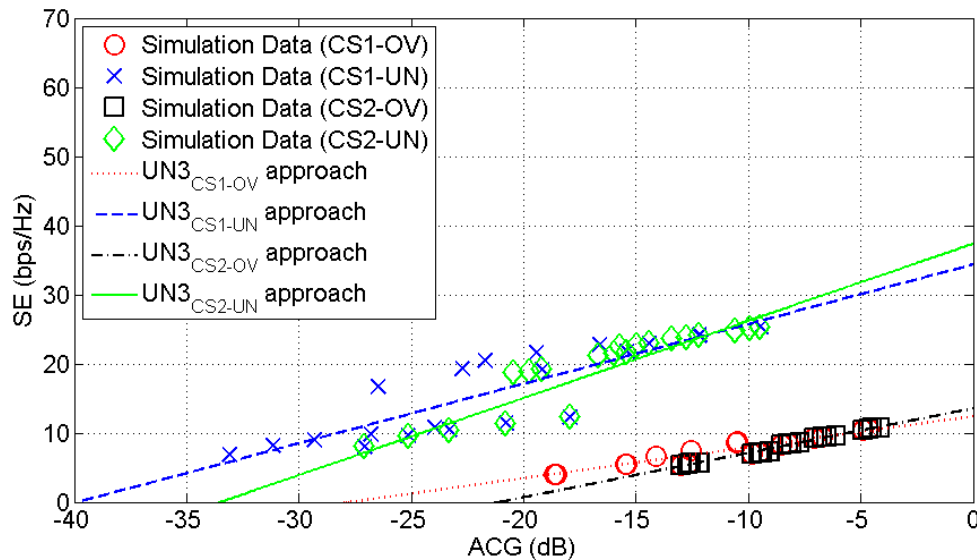


Fig. 5. Scatter plot of SE versus ACG for simulated coupling scheme OV and UN LV and MV BPL channels and various regression approaches and coupling scheme modules.

the BPL topologies of the examined power grid type (*i.e.*, either OV or UN) when WtG^1 , StP^1 , WtW^{2-3} , PtP^{2-3} and $MtM_{0.7_{-0.1_{-0.2}}^{1-2-3}}$ of the applied coupling scheme module (*i.e.*, either CS2 or CS1 module) are used in accordance with Tables 11 and 12.

In Fig. 5, except for the simulation data of Tables 11 and 12, the set of regression trend curves of Table 15, say $UN3_{CS1-OV}$, $UN3_{CS1-UN}$, $UN3_{CS2-OV}$ and $UN3_{CS2-UN}$ approaches, are illustrated.

From Fig. 5, several interesting observations concerning the correlation between SE and ACG can be made:

- For the same ACG value, UN distribution BPL networks present higher SE in comparison with OV distribution BPL networks. This is due to the fact that UN environment is a more protected environment concerning: (i) its transmitted EMI to the other radioservices that operate at the same frequency operation band; and (ii) the EMI that receives from the aforementioned radioservices. Therefore, higher IPSD limits are applied in UN distribution BPL networks due to the previous first reason while lower noise PSD is presented in UN distribution BPL networks due to the previous second reason. The favourable operation of UN distribution BPL networks is reflected on the significant β difference between UN and OV distribution BPL networks (see also Table 15) for given coupling scheme module.
- Coupling schemes of type 1 produce pairs of SE / ACG values that coincide when CS1 and CS2 module are applied. When coupling schemes of type 2 are examined, CS2 module has as an output SE / ACG points that are located at more upper right positions in comparison with the respective ones of CS1 module when a certain distribution BPL topology is examined. This has as an effect higher inclinations

- of UN_{3CS2-OV} and UN_{3CS2-UN} curves in comparison with UN_{3CS1-OV} and UN_{3CS1-UN} ones, respectively (see also α of Table 15).
- Despite the differences between UN_{3CS2-OV} and UN_{3CS1-OV} curves, whichever of these two curves can offer an approximate estimation of SE and, thus, capacity when the ACG of an overhead distribution BPL topology is available. Similarly to OV distribution BPL networks, UN_{3CS2-UN} and UN_{3CS1-UN} curves can facilitate the approximate SE estimation when ACG of a UN distribution BPL topology is given.

5.8 UN1, UN2 and UN3 Approaches – The Impact of CS2 Module

UN1 and UN2 approaches have been computed either for MIMO or for coupling scheme channels of the OV and UN LV and MV BPL topologies. Especially, in the case of coupling scheme channels, the two different available coupling scheme modules (*i.e.*, CS1 and CS2 module) have also been applied and assessed.

As UN1 approach is concerned, UN_{1MIMO}, UN_{1CS1} and UN_{1CS2} approaches differ from other well validated RMS-DS / ACG approaches of the BPL literature since these approaches are exclusively computed with respect to suitable simulation data of distribution BPL networks. Actually, UN_{1MIMO}, UN_{1CS1} and UN_{1CS2} approaches present small differences among them due to the different nature of the examined simulation data; UN_{1MIMO} approach comes from the regression analysis of MIMO channel simulation data while UN_{1CS1} and UN_{1CS2} modules also take into consideration the impact of the coupling scheme module and coupling scheme channels. Finally, the impact of CS2 module, which can support more coupling scheme types and more efficient coupling schemes in comparison with CS1 module, is schematically demonstrated through the horizontal curve shift of UN_{1CS1} and UN_{1CS2} approaches.

As UN2 approach is regarded, UN_{2MIMO}, UN_{2CS1} and UN_{2CS2} approaches slightly differ each other due to the form of the regression hyperbolic trend curves regardless of the nature of the examined simulated data. Extensively been used in the BPL literature, the regression hyperbolic trend curves seem to better describe MIMO and coupling scheme channels of urban and suburban distribution BPL topologies rather than corresponding channels of “LOS” and rural distribution BPL topologies.

On the basis of the newly proposed UN3 approach, an approximate SE and capacity estimation can be available if an estimate of the average ACG of a distribution BPL network is assumed. Furthermore, this approximation of SE and capacity can be offered with adequate accuracy for OV distribution BPL networks even if the applied coupling scheme is not known; this is due to the fact that UN_{3CS2-OV} and UN_{3CS1-OV} curves give relatively close results. The same observations can be made for UN distribution BPL networks.

Synoptically, taking under consideration the relatively small differences among UN1, UN2 and UN3 approaches and their universal consideration of the BPL character as described in [17], UN_{1CS2}, UN_{2CS2}, UN_{3CS2-OV} and UN_{3CS2-UN} approaches can be further promoted as the basis towards the common statistical handling of: (i) OV and UN LV and MV BPL topologies; (ii) different MIMO BPL channels; (iii) different BPL channels supported by CS1 and CS2 scheme modules; and (iv) different BPL channels of various coupling schemes.

6. Conclusions

This paper has focused on the assessment of the application of CS2 module in OV and UN LV and MV BPL topologies in terms of four well-known broadband performance metrics (*i.e.*, ACG, RMS-DS, CB and SE). The results of the aforementioned broadband performance metrics when CS2 modules is applied have been compared against respective ones of CS1 module.

The investigation of the statistical metric comparison results reveal that CS2 module offers significant advantages in comparison with the vintage CS1 module. Indeed, CS2 module supports a plethora of new adaptive coupling schemes (*i.e.*, coupling schemes of the coupling scheme type 3) whose performance can be adjusted in accordance with the needs for higher broadband performance and EMC. Also, CS2 module offers better ACGs for the coupling schemes of the coupling scheme type 2 in comparison with CS1 module. ACG improvement of the coupling schemes of the coupling scheme type 2 is reflected on respective capacity and SE results. Since WtW / PtP coupling scheme channels become almost capacity equivalent to WtG / StP coupling scheme channels, the already-known better EMC performance of WtW / PtP coupling scheme channels against WtG / StP ones can influence the BPL system architecture design concerning the selection of suitable coupling schemes.

As the UN1, UN2 and UN3 approaches of CS2 module are concerned, the fundamental properties of the negative correlation between RMS-DS / ACG, the hyperbolic correlation between RMS-DS / CB and the positive correlation between SE / ACG have been validated in OV and UN LV and MV BPL coupling scheme channels. It has been proven that $UN1_{CS2}$, $UN1_{CS1}$ and $UN1_{MIMO}$ approach curves have small and affordable differences among them, thus allowing the consideration of $UN1_{CS2}$ approach curves as a benchmark curve for the OV and UN LV and MV BPL channels regardless of their type (*i.e.*, MIMO channels, CS1 module coupling scheme channels or CS2 module coupling scheme channels). For the UN2 approach curves, the differences among $UN2_{CS2}$, $UN2_{CS1}$ and $UN2_{MIMO}$ approach curves are even smaller than UN1 approach curves difference due to the mathematical form of the approach. Again, $UN2_{CS2}$ approach curves can be applied to efficiently describe coupling scheme and MIMO channels of OV and UN distribution BPL networks. Finally, for the UN3 approach curves, it has been proven that $UN3_{CS2-OV}$ and $UN3_{CS1-OV}$ present small differences between them thus permitting the consideration of $UN3_{CS2-OV}$ approach curves as an estimation tool for the SE and capacity for the OV and UN LV and MV BPL channels regardless of their type (*i.e.*, CS1 module coupling scheme channels or CS2 module coupling scheme channels). The same assumption is valid in UN distribution BPL networks when $UN3_{CS2-UN}$ approach curve is applied.

CONFLICTS OF INTEREST

The author declares that there is no conflict of interests regarding the publication of this paper.

References

- [1] T. A. Papadopoulos, A. I. Chrysochos, E. O. Kontis, R. N. Papadopoulos, and G. K. Papagiannis, "Measurement-based hybrid approach for ringdown analysis of power systems," *IEEE Transactions on Power Systems*, vol. 31, no. 6, pp. 4435–4446, 2016.
- [2] A. G. Lazaropoulos, "Review and Progress towards the Capacity Boost of Overhead and Underground Medium-Voltage and Low-Voltage Broadband over Power Lines Networks: Cooperative Communications through Two- and Three-Hop Repeater Systems," *ISRN Electronics*, vol. 2013, Article ID 472190, pp. 1-19, 2013.
- [3] A. G. Lazaropoulos, "Review and Progress towards the Common Broadband Management of High-Voltage Transmission Grids: Model Expansion and Comparative Modal Analysis," *ISRN Electronics*, vol. 2012, Article ID 935286, pp. 1-18, 2012.
- [4] S. Galli, A. Scaglione, and Z. Wang, "For the grid and through the grid: the role of power line communications in the smart grid," in *Proc. IEEE*, vol. 99, no. 6, pp. 998–1027, Jun. 2011.
- [5] A. N. Milioudis, G. T. Andreou, and D. P. Labridis, "Detection and Location of High Impedance Faults in Multiconductor Overhead Distribution Lines Using Power Line Communication Devices," *IEEE Trans. Smart Grid.*, vol. 6, no. 2, pp. 894–902, Mar. 2015.
- [6] A. G. Lazaropoulos, "Towards Modal Integration of Overhead and Underground Low-Voltage and Medium-Voltage Power Line Communication Channels in the Smart Grid Landscape: Model Expansion, Broadband Signal Transmission Characteristics, and Statistical Performance Metrics (Invited Paper)," *ISRN Signal Processing*, vol. 2012, Article ID 121628, pp. 1-17, 2012. . [Online]. Available: <http://downloads.hindawi.com/journals/isrn/2012/121628.pdf>
- [7] A. G. Lazaropoulos, "Deployment Concepts for Overhead High Voltage Broadband over Power Lines Connections with Two-Hop Repeater System: Capacity Countermeasures against Aggravated Topologies and High Noise Environments," *Progress in Electromagnetics Research B*, vol. 44, pp. 283-307, 2012.
- [8] C. Cano, A. Pittolo, D. Malone, L. Lampe, A. M. Tonello, and A. G., Dabak, "State of the art in power line communications: From the applications to the medium," *IEEE Journal on Selected Areas in Communications*, vol. 34, no. 7, pp. 1935-1952, 2016.
- [9] M. S. P. Facina, H. A. Latchman, H. V. Poor, and M. V. Ribeiro, "Cooperative In-Home Power Line Communication: Analyses Based on a Measurement Campaign," *IEEE Trans. Commun.*, vol. 64, no. 2, pp. 778–789, Feb. 2016.
- [10] G. Prasad, L. Lampe, and S. Shekhar, "In-Band Full Duplex Broadband Power Line Communications," *IEEE Trans. Comm.*, vol. 64, no. 9, pp. 3915–3931, Sep. 2016.
- [11] A. G. Lazaropoulos and P. G. Cottis, "Transmission characteristics of overhead medium voltage power line communication channels," *IEEE Trans. Power Del.*, vol. 24, no. 3, pp. 1164–1173, Jul. 2009.
- [12] M. Antoniali, F. Versolatto, and A. M. Tonello, "An Experimental Characterization of the PLC Noise at the Source," *IEEE Trans. Power Del.*, vol. 31, no. 3, pp. 1068–1075, Jun. 2016.

- [13] R. Lefort, R. Vauzelle, V. Courtecuisse, N., Idir, and A. M. Poussard, "Influence of the MV/LV Transformer Impedance on the Propagation of the PLC Signal in the Power Grid," *IEEE Trans. Power Del.*, vol. 32, no. 3, pp. 1339–1349, Jun. 2017.
- [14] A. G. Lazaropoulos and P. G. Cottis, "Capacity of overhead medium voltage power line communication channels," *IEEE Trans. Power Del.*, vol. 25, no. 2, pp. 723–733, Apr. 2010.
- [15] A. G. Lazaropoulos and P. G. Cottis, "Broadband transmission via underground medium-voltage power lines—Part I: transmission characteristics," *IEEE Trans. Power Del.*, vol. 25, no. 4, pp. 2414–2424, Oct. 2010.
- [16] A. G. Lazaropoulos and P. G. Cottis, "Broadband transmission via underground medium-voltage power lines—Part II: capacity," *IEEE Trans. Power Del.*, vol. 25, no. 4, pp. 2425–2434, Oct. 2010.
- [17] A. G. Lazaropoulos, "Broadband over Power Lines Systems Convergence: Multiple-Input Multiple-Output Communications Analysis of Overhead and Underground Low-Voltage and Medium-Voltage BPL Networks (Invited Paper)," *ISRN Power Engineering*, vol. 2013, Article ID 517940, pp. 1-30, 2013. [Online]. Available: <http://www.hindawi.com/isrn/power.engineering/2013/517940/>
- [18] T. A. Papadopoulos, C. G. Kaloudas, A. I. Chrysochos, and G. K. Papagiannis, "Application of Narrowband Power-Line Communication in Medium-Voltage Smart Distribution Grids," *IEEE Trans. Power Del.*, vol. 28, no. 2, pp. 981–988, Apr. 2013.
- [19] N. Pavlidou, A. J. Han Vinck, J. Yazdani, and B. Honary, "Power line communications: state of the art and future trends," *IEEE Commun. Mag.*, vol. 41, no. 4, pp. 34–40, Apr. 2003.
- [20] M. Gebhardt, F. Weinmann, and K. Dostert, "Physical and regulatory constraints for communication over the power supply grid," *IEEE Commun. Mag.*, vol. 41, no. 5, pp. 84–90, May 2003.
- [21] A. G. Lazaropoulos, "Towards Broadband over Power Lines Systems Integration: Transmission Characteristics of Underground Low-Voltage Distribution Power Lines," *Progress in Electromagnetics Research B*, vol. 39, pp. 89-114, 2012.
- [22] G. Jee, C. Edison, R. Das Rao, and Y. Cern, "Demonstration of the technical viability of PLC systems on medium- and low-voltage lines in the United States," *IEEE Commun. Mag.*, vol. 41, no. 5, pp. 108–112, May 2003.
- [23] A. G. Lazaropoulos, "Broadband transmission and statistical performance properties of overhead high-voltage transmission networks," *Hindawi Journal of Computer Networks and Commun.*, 2012, article ID 875632, 2012.
- [24] A. G. Lazaropoulos, "Green Overhead and Underground Multiple-Input Multiple-Output Medium Voltage Broadband over Power Lines Networks: Energy-Efficient Power Control," *Springer Journal of Global Optimization*, vol. 2012 / Print ISSN 0925-5001, pp. 1-28, Oct. 2012.
- [25] A. G. Lazaropoulos, "Overhead and Underground MIMO Low Voltage Broadband over Power Lines Networks and EMI Regulations: Towards Greener Capacity Performances," *Elsevier Computers and Electrical Engineering*, in press. [Online]. Available: <http://www.sciencedirect.com/science/article/pii/S0045790613000293>
- [26] A. G. Lazaropoulos, "Capacity Performance of Overhead Transmission Multiple-Input Multiple-Output Broadband over Power Lines Networks: The Insidious Effect of Noise and the Role of Noise Models (Invited Paper),"

- Trends in Renewable Energy*, vol. 2, no. 2, pp. 61-82, Jan. 2016. [Online]. Available: <http://futureenergysp.com/index.php/tre/article/view/23>
- [27] A. G. Lazaropoulos, "Power Systems Stability through Piecewise Monotonic Data Approximations – Part 1: Comparative Benchmarking of L1PMA, L2WPMA and L2CXCV in Overhead Medium-Voltage Broadband over Power Lines Networks," *Trends in Renewable Energy*, vol. 3, no. 1, pp. 2 – 32, Jan. 2017. [Online]. Available: <http://futureenergysp.com/index.php/tre/article/view/29/34>
- [28] A. G. Lazaropoulos, "Power Systems Stability through Piecewise Monotonic Data Approximations – Part 2: Adaptive Number of Monotonic Sections and Performance of L1PMA, L2WPMA and L2CXCV in Overhead Medium-Voltage Broadband over Power Lines Networks," *Trends in Renewable Energy*, vol. 3, no. 1, pp. 33 – 60, Jan. 2017. [Online]. Available: <http://futureenergysp.com/index.php/tre/article/view/30/35>
- [29] A. G. Lazaropoulos, "Improvement of Power Systems Stability by Applying Topology Identification Methodology (TIM) and Fault and Instability Identification Methodology (FIIM) – Study of the Overhead Medium-Voltage Broadband over Power Lines (OV MV BPL) Networks Case," *Trends in Renewable Energy*, vol. 3, no. 2, pp. 102 – 128, Apr. 2017. [Online]. Available: <http://futureenergysp.com/index.php/tre/article/view/34/pdf>
- [30] A. G. Lazaropoulos, "Measurement Differences, Faults and Instabilities in Intelligent Energy Systems – Part 1: Identification of Overhead High-Voltage Broadband over Power Lines Network Topologies by Applying Topology Identification Methodology (TIM)," *Trends in Renewable Energy*, vol. 2, no. 3, pp. 85 – 112, Oct. 2016.
- [31] A. G. Lazaropoulos, "Wireless Sensor Network Design for Transmission Line Monitoring, Metering and Controlling: Introducing Broadband over PowerLines-enhanced Network Model (BPLeNM)," *ISRN Power Engineering*, vol. 2014, Article ID 894628, 22 pages, 2014. doi:10.1155/2014/894628. [Online]. Available: <http://www.hindawi.com/journals/isrn.power.engineering/2014/894628/>
- [32] A. G. Lazaropoulos, "Wireless Sensors and Broadband over PowerLines Networks: The Performance of Broadband over PowerLines-enhanced Network Model (BPLeNM) (Invited Paper)," *ICAS Publishing Group Transaction on IoT and Cloud Computing*, vol. 2, no. 3, pp. 1-35, 2014. [Online]. Available: <http://citeseerx.ist.psu.edu/viewdoc/download;jsessionid=741EE7C15693046FFFF5E9749149F579?doi=10.1.1.679.8217&rep=rep1&type=pdf>
- [33] A. G. Lazaropoulos, "New Coupling Schemes for Distribution Broadband over Power Lines (BPL) Networks," *Progress in Electrom. Research B (PIERB)*, vol. 71, pp. 39-54, 2016.
- [34] A. G. Lazaropoulos, "A Panacea to Inherent BPL Technology Deficiencies by Deploying Broadband over Power Lines (BPL) Connections with Multi-Hop Repeater Systems," *Bentham Recent Advances in Electrical & Electronic Engineering*, vol. 10, no. 1, pp. 30-46, 2017.
- [35] P. Amirshahi and M. Kavehrad, "High-frequency characteristics of overhead multiconductor power lines for broadband communications," *IEEE J. Sel. Areas Commun.*, vol. 24, no. 7, pp. 1292–1303, Jul. 2006.
- [36] T. Sartenaer, "Multiuser communications over frequency selective wired channels and applications to the powerline access network" Ph.D. dissertation, Univ. Catholique Louvain, Louvain-la-Neuve, Belgium, Sep. 2004.

- [37] P. Amirshahi, "Broadband access and home networking through powerline networks" Ph.D. dissertation, Pennsylvania State Univ., University Park, PA, May 2006.
- [38] OPERA1, D44: Report presenting the architecture of plc system, the electricity network topologies, the operating modes and the equipment over which PLC access system will be installed, IST Integr. Project No 507667, Dec. 2005.
- [39] DLC+VIT4IP, D1.2: Overall system architecture design DLC system architecture. FP7 Integrated Project No 247750, Jun. 2010.
- [40] OPERA1, D5: Pathloss as a function of frequency, distance and network topology for various LV and MV European powerline networks. IST Integrated Project No 507667, Apr. 2005.
- [41] S. Galli, "A novel approach to the statistical modeling of wireline channels," *IEEE Trans. Commun.*, vol. 59, no. 5, pp. 1332–1345, May 2011.
- [42] S. Galli, "A simplified model for the indoor power line channel," in *Proc. IEEE Int. Symp. Power Line Communications and Its Applications*, Dresden, Germany, Mar./Apr. 2009, pp. 13–19.
- [43] S. Galli, "A simple two-tap statistical model for the power line channel," in *Proc. IEEE Int. Symp. Power Line Communications and Its Applications*, Rio de Janeiro, Brazil, Mar. 2010, pp. 13–19.
- [44] F. Versolatto and A. M. Tonello, "Analysis of the PLC channel statistics using a bottom-up random simulator," in *Proc. IEEE Int. Symp. Power Line Communications and Its Applications*, Rio de Janeiro, Brazil, Mar. 2010, pp. 236–241.
- [45] A. M. Tonello, F. Versolatto, and C. Tornelli, "Analysis of impulsive UWB modulation on a real MV test network," in *Proc. IEEE Int. Symp. Power Line Communications and Its Applications*, Udine, Italy, Apr. 2011, pp. 18–23.
- [46] M. Antoniali, A. M. Tonello, M. Lenardon, and A. Qualizza, "Measurements and analysis of PLC channels in a cruise ship," in *Proc. IEEE Int. Symp. Power Line Communications and Its Applications*, Udine, Italy, Apr. 2011, pp. 102–107.
- [47] A. M. Tonello and F. Versolatto, "Bottom-up statistical PLC channel modeling—Part II: inferring the statistics," *IEEE Trans. Power Delivery*, vol. 25, no. 4, pp. 2356–2363, Oct. 2010.
- [48] M. Tlich, A. Zeddami, F. Moulin, and F. Gauthier, "Indoor power-line communications channel characterization up to 100 MHz—Part I: one parameter deterministic model," *IEEE Trans. Power Del.*, vol. 23, no. 3, pp. 1392–1401, July 2008.
- [49] M. Tlich, A. Zeddami, F. Moulin, and F. Gauthier, "Indoor power-line communications channel characterization up to 100 MHz—Part II: Time-Frequency Analysis," *IEEE Trans. Power Del.*, vol. 23, no. 3, pp. 1402–1409, July 2008.
- [50] A. M. Tonello, A. Pittolo, and M. Girotto, "Power line communications: Understanding the channel for physical layer evolution based on filter bank modulation," *IEICE Transactions on Communications*, vol. 97, no. 8, pp. 1494–1503, 2014.
- [51] J. A. Cortés, F.J. Cañete, L. Díez, and J. L. G. Moreno, "On the Statistical Properties of Indoor Power Line Channels: Measurements and Models," *Proc. Int. Symp. on Power Line Commun. and Its App. (ISPLC)*, pp.271–276, April 2011.

- [52] M. Tlich, A. Zeddami, A. Moulin, and F. Gauthier, "Indoor PowerLine Communications Channel Characterization up to 100 MHz - Part II: Time-Frequency Analysis," *IEEE Trans. on Power Del.*, vol. 23, no. 3, pp. 1402–1409, Jul. 2008.
- [53] F. V. A. Pittolo, M. De Pianta and A. Tonello, "In vehicle plc: In-car and in-ship channel characterization," *IEEE Vehicular Technology Magazine*, Aug. 2015.

Article copyright: © 2018 Athanasios G. Lazaropoulos. This is an open access article distributed under the terms of the [Creative Commons Attribution 4.0 International License](https://creativecommons.org/licenses/by/4.0/), which permits unrestricted use and distribution provided the original author and source are credited.



Enhancement of the Rooftop Photovoltaic Array Characteristic Interconnected by the Grid under Partial Shading Condition by using Cascaded DC/DC Converter [WITHDRAWN]

Ahmed M. Mahmoud^{1*}, Salah M. Saafan², Ahmed M. Attalla³ and Hamdy Elgohary³

1: MS. Student, Department of electrical power and machines, Faculty of Engineering- Ain Shams University, Cairo, Egypt

2: Dr., Electric and Computer Engineering Department, Higher Technological Institute (HTI), 10th of Ramadan City, Egypt

3: Professor Dr., Department of electrical power and machines, Faculty of Engineering- Ain Shams University, Cairo, Egypt

Received March 5, 2018; Accepted April 2, 2018; Published April 12, 2018

This article was withdrawn by the Editor-in-Chief, because it's found to be a duplicated submission of authors' publication in another journal:

Ahmed M. Mahmoud, Salah M. Saafan, Ahmed M. Attalah. (2018) Enhancement of the rooftop Photovoltaic array characteristic interconnected by the grid under partial shading condition by using cascaded DC/DC converter. International Journal of Power Systems, 3, 42-52

Sustainable Management of Spent Hydroprocessing Catalyst

Changyan Yang^{1,2}, Jinlong Wu¹, Wei Wang¹, Bo Li¹, Bo Zhang^{1*}, Yigang Ding¹

1: Key Laboratory for Green Chemical Process of Ministry of Education, Hubei Key Laboratory of Novel Chemical Reactor and Green Chemical Technology, School of Chemical Engineering and Pharmacy, Wuhan Institute of Technology, Hubei, China

2: Hubei Key Laboratory for Processing and Application of Catalytic Materials, Huanggang Normal University, Hubei, China

Received February 6, 2018; Accepted May 2, 2018; Published May 3, 2018

Increasing demand for high-quality transportation fuels and stringent environmental standards have resulted in the significantly increased quantity of spent hydroprocessing catalysts, which require the sustainable management. To minimize the generation of hazardous wastes, the spent hydroprocessing catalysts can be regenerated via oxidative regeneration or reactivated via the rejuvenation process. If the catalytic activity cannot be restored, it can be utilized as a source of other useful materials, and/or metals in the spent catalyst are recovered. Finally, the stabilized residues shall be disposed by using an environmentally sound method.

Keywords: Sustainable Management; Spent Hydroprocessing Catalyst; Oxidative Regeneration; Rejuvenation; Metals Reclamation

Introduction

Increasing demand for high-quality transportation fuels and stringent environmental standards have resulted in the significant growth of the use of hydroprocessing catalysts globally. It is expected that the amount of spent hydroprocessing catalysts produced will be 200,000 tons annually with an anticipated 5% annual increase [1]. Therefore, the sustainable management of these spent catalyst wastes will reduce the pollution to the environment and increase the economic efficiency of the hydrogenation process.

Hydroprocessing catalysts generally include hydrotreating and hydrocracking catalysts. The most used hydrotreating catalysts are molybdate (Mo) supported on alumina (Al_2O_3) and promoted by cobalt (Co), nickel (Ni) or tungsten (W), while hydrocracking catalysts are bifunctional, and consisting of active metals (like Mo, Pt, and Ru) supported on a zeolite (e.g., ZSM-5). The catalyst life varies for different applications: 1-2 years for hydroprocessing of atmospheric gas oils or vacuum gas oils, 0.5-1 year for hydrotreating resid, 5-10 years for a naphtha hydrotreater using straight run feed [2], and ~2 years for hydrotreating bio-feedstock [3, 4].

When the performance of the catalysts cannot meet the desired level, they will be unloaded and examined for its regenerateness. After regeneration, the regenerated spent hydroprocessing catalysts will be re-evaluated. Catalysts of a good quality are pooled and re-sulfided for reusing, while catalysts with a lower quality could be reused in less critical

*Corresponding author: bzhang_wh@foxmail.com

applications. For the spent catalyst has lost its regenerateness, the metal in the spent catalyst will be recycled to the maximum extent. The residues are disposed by using an environmentally sound method.

Oxidative Regeneration

Oxidative regeneration is mainly used to burn off the coke deposited on the spent hydrotreating catalysts and transform metal sulfides back into their oxides. But it could not recover the structural properties to the same level as the fresh catalysts. Typically, the spent catalyst should not contain more than 2-3 wt% of metal contaminants (mostly Ni and V) to be suitable for oxidative regeneration [5].

This regeneration process is affected by multiple factors including O₂ supply, the composition of the coke, and mass transfer. Air generally provides a good O₂ source. However, the uncontrolled temperature increase may lead to sintering of the catalyst. Under certain circumstances, diluted air may be more suitable.

The temperature is the most critical factor. It is found that a complete removal requires burning at the high temperature of ~450°C, if burning the sulfided spent CoMo catalysts [6]. Oxidation of sulfidic sulfur and organic sulfur resulted in the release of SO₂ at 250°C and 450°C, respectively. Oxidation of carbon also happens at ~450°C [7]. More severe oxidation conditions are needed for the NiW catalyst, because of the lower oxidation activity of NiO and WO₃ compared to Co₃O₄ and MoO₃ [8]. The removal of sulfidic sulfur from the spent NiW catalysts as SO₂ happened at 227-327°C and the removal of carbon as CO₂ or CO occurred at 377-577°C.

The shapes of the catalysts establish the mass transfer limitations, which may be minimized by grinding the deactivated catalyst to a fine particle size [9, 10].

The oxidative regeneration can be carried out in situ or ex situ. The conventional in-situ technique burns off the coke and re-sulfides the catalyst in the hydrotreating reactors. Regeneration is performed by injecting a stream of diluted air with nitrogen or steam to remove coke and reversible poisons like sulfur and nitrogen by oxidizing them at temperatures between 450-550°C into gaseous CO, CO₂, SO_x, and NO_x. The process parameters such as air concentration and temperature are carefully controlled to prevent runaway combustion [11]. Following regeneration, sulfiding converts the metal oxides impregnated onto the catalyst support into the corresponding metal sulfides, and forms H₂S that can enter the process water to be removed. According to environmental regulations, acidic gases must be neutralized, and the neutralization process is time-consuming and requires injection systems, trained operators, and time. Forth more, in-situ regeneration requires long unit downtime and gives poor activity recovery due to uneven gas flow [12].

The ex situ (also called off-site) oxidative regeneration has been widely accepted by the petroleum refining industry in the 1990s, because it provides benefits on safety, time savings, and less environmental problems caused by generating SO_x and CO_x. Better activity recovery can be achieved by the ex situ regeneration, because it allows performing more than one cycle with the same catalyst batch [13]. The reactor corrosion due to the formation of acidic gases is eliminated. The chance for accidents, hot spots, and reactor malfunction is lower. Dedicated catalyst specific regeneration procedures can be applied, and the fines can be removed by screening. The costs of the oxidative ex situ regeneration are around 20% of the fresh catalyst price [14].

Rejuvenation

The rejuvenation of spent catalysts, also known as reactivation or reactivation, is additional processes that may be required. Oxidative regeneration is typically performed on older generation Type I catalysts, with recovered activity in the range of 70-85% of fresh activity, depending on the degree of metals contamination and surface area. For more recent generation catalysts containing the highly active Type II sites, the oxidative regeneration of Type II catalysts only results in a mediocre activity recovery. One possible reason for this low-activity recovery is that these catalysts have not been exposed to the temperatures that are required to restore their activities. The rejuvenation process developed by Porocel [15] consists of two steps: an initial thermal regeneration to remove the carbon and sulfur, followed by a proprietary chemical treatment to remove the inactive crystalline compound such as β -CoMoO₄ or NiMoO₄, re-disperse the metals, and restore the Type II active sites for maximum activity recovery. These treatments typically use some oxygen containing compounds that play the role of chelating agents and thus may help re-disperse the metals [16]. Rejuvenation of the spent catalyst may restore greater than 90% of fresh catalyst activity and provide the spent catalysts that meet certain physical and chemical criteria.

Reuse of the Spent Catalysts

Reuse of a regenerated spent catalyst to maximize the catalyst life is the key to the sustainable management. The regenerated catalysts may be suitable for less demanding refinery operations. Typically, the regenerated gas oil hydrotreating catalyst might be used for hydrotreating of kerosene, and the regenerated Kerosene hydrotreating catalyst can be applied for naphtha hydrotreating [17].

It's also possible to use at least a small portion of spent catalysts for the preparation of useful materials like fused alumina, Anorthite glass-ceramics, and abrasive material [18]. Depending on the remaining porosity and surface area, spent catalysts may still have potential especially, in some gas-solid applications, *e.g.*, used as a H₂S clean-up sorbent [19].

This kind of catalyst management services could provide sustainability to the global catalyst inventory through a pool where each site or unit will take the required catalyst quantity corresponding to their need.

Metals Reclamation

When the spent catalyst reaches the end-of-cycle, *i.e.*, the desired level of activity could not be restored, or the mechanical properties would strongly deteriorate during regeneration. Metals reclamation could remove toxic components and make further dispose of residues possible [20].

There are two types of reclamation processes: hydrometallurgy and pyrometallurgy. The hydrometallurgical reclamation involves the solubilization of metals via roasting, followed by a selective leaching of metals of interest [21]. Literature

regarding the hydrometallurgical reclamation of metals is extensive, and has been reviewed by Furimsky [21] and Marafi and Stanislaus [18, 22].

The pyrometallurgical process starts with melting dry catalysts in a furnace at temperatures around 1200-1500°C [23]. Heavy metals sink to the bottom as alloys containing the alumina or silica support, which are further separated from the slag. Pyrometallurgical processes for recovering metals (like Pt and Pd) in hydrocracking catalysts involve chlorination at high temperatures (900-950°C) for recovery of platinum and other metals as volatile chlorides, which is followed by heating at high temperatures (800°C) in a gas flow containing water [24].

CONCLUSIONS

As the energy demand continues to rise and the environmental regulations are more stringent, the increasing quantity of spent hydroprocessing catalysts requires the sustainable management, which has a goal of minimizing the generation of hazardous wastes. The spent hydroprocessing catalysts can be regenerated via oxidative regeneration and re-sulfided or reactivated via the rejuvenation process, if it meets the requirements of the regenerateness. If the catalytic activity cannot be restored, it can be utilized to make other useful materials, and/or metals in the spent catalyst are recovered. Finally, the stabilized residues of spent hydroprocessing catalysts can be disposed in landfills.

ACKNOWLEDGMENTS

We are grateful for the support from the School of Chemical Engineering and Pharmacy at the Wuhan Institute of Technology.

CONFLICTS OF INTEREST

The authors declare that there is no conflict of interests regarding the publication of this paper.

REFERENCES

- [1] Chiranjeevi, T., Pragma, R., Gupta, S., Gokak, D. T., and Bhargava, S. (2016). Minimization of Waste Spent Catalyst in Refineries. *Procedia Environmental Sciences*, 35, 610-617.
- [2] Dufresne, P. (2007). Hydroprocessing catalysts regeneration and recycling. *Applied Catalysis A: General*, 322, 67-75.
- [3] Zhang, B., and Seddon, D. (2018). *Hydroprocessing Catalysts and Processes: The Challenges for Biofuels Production*, World Scientific Publishing, Singapore.
- [4] Zhang, B., and Wang, Y. (2013). *Biomass Processing, Conversion, and Biorefinery*, Nova Science Publishers, Inc., New York.

- [5] Eijsbouts, S. (1999). Life cycle of hydroprocessing catalysts and total catalyst management. *Studies in Surface Science and Catalysis*, 127, 21-36.
- [6] Yoshimura, Y., and Furimsky, E. (1986). Oxidative regeneration of hydrotreating catalysts. *Applied Catalysis*, 23(1), 157-171.
- [7] Furimsky, E., and Yoshimura, Y. (1987). Mechanism of oxidative regeneration of molybdate catalyst. *Industrial & Engineering Chemistry Research*, 26(4), 657-662.
- [8] Yoshimura, Y., Sato, T., Shimada, H., Matsubayashi, N., Imamura, M., Nishijima, A., Yoshitomi, S., Kameoka, T., and Yanase, H. (1994). Oxidative Regeneration of Spent Molybdate and Tungstate Hydrotreating Catalysts. *Energy & Fuels*, 8(2), 435-445.
- [9] Massoth, F. E. (1967). Oxidation of Coked Silica-Alumina Catalyst. *Industrial & Engineering Chemistry Process Design and Development*, 6(2), 200-207.
- [10] Mickley, H. S., Nestor, J. W., and Gould, L. A. (1965). A kinetic study of the regeneration of a dehydrogenation catalyst. *The Canadian Journal of Chemical Engineering*, 43(2), 61-68.
- [11] Leprince, P. (2001). *Petroleum Refining. Vol. 3 Conversion Processes*, Editions Technip.
- [12] Vukovic, J., and Neuman, D. (2004). Ex-Situ Catalyst Treatments Reduce Refinery Emissions and Unit Downtime: Update on the Economic and Environmental Benefits of TRICAT's Ex-situ Regeneration and Pre-Activation Technologies. *5th EMEA Catalyst Technology Conference* Cannes, France.
- [13] Dufresne, P., Valeri, F., and Abotteen, D. S. (1996). Continuous developments of catalyst off-site regeneration and presulfiding. *Studies in Surface Science and Catalysis*, 100, 253-262.
- [14] Eijsbouts, S., Battiston, A. A., and van Leerdam, G. C. (2008). Life cycle of hydroprocessing catalysts and total catalyst management. *Catalysis Today*, 130(2-4), 361-373.
- [15] Porocel (2017). Catalyst Rejuvenation. <http://www.porocel.com/14-rejuvenation-catalyst-services/>. (accessed on 5/1/2018)
- [16] Stanislaus, A., Marafi, M., and Absi-Halabi, M. (1993). Studies on the rejuvenation of spent catalysts: effectiveness and selectivity in the removal of foulant metals from spent hydroprocessing catalysts in coked and decoked forms. *Applied Catalysis A: General*, 105(2), 195-203.
- [17] Marafi, M. (2008). Spent Catalyst Waste Minimization and Utilization. <http://thefutureenergy.org/wp-content/uploads/2018/02/2008Spent-Catalyst-Waste-Minimization-and-Utilization.pdf>. (accessed on 5/1/2018)
- [18] Marafi, M., and Stanislaus, A. (2008). Spent catalyst waste management: A review: Part I—Developments in hydroprocessing catalyst waste reduction and use. *Resources, Conservation and Recycling*, 52(6), 859-873.
- [19] Furimsky, E. (1997). Activity of spent hydroprocessing catalysts and carbon supported catalysts for conversion of hydrogen sulphide. *Applied Catalysis A: General*, 156(2), 207-218.
- [20] Trimm, D. L. (1989). Deactivation, Regeneration and Disposal of Hydroprocessing Catalysts. *Studies in Surface Science and Catalysis*, 53, 41-60.
- [21] Furimsky, E. (1996). Spent refinery catalysts: Environment, safety and utilization. *Catalysis Today*, 30(4), 223-286.

- [22] Marafi, M., and Stanislaus, A. (2008). Spent hydroprocessing catalyst management: A review: Part II. Advances in metal recovery and safe disposal methods. *Resources, Conservation and Recycling*, 53(1), 1-26.
- [23] Marafi, M., Stanislaus, A., and Furimsky, E. (2010). Chapter 11 - Metal Reclamation from Spent Hydroprocessing Catalysts. In: *Handbook of Spent Hydroprocessing Catalysts*, Elsevier, Amsterdam, pp: 269-315. DOI: 10.1016/B978-0-444-53556-6.00011-2
- [24] Marafi, M., and Furimsky, E. (2017). Hydroprocessing Catalysts Containing Noble Metals: Deactivation, Regeneration, Metals Reclamation, and Environment and Safety. *Energy & Fuels*, 31(6), 5711-5750.

Article copyright: © 2018 Changyan Yang, Jinlong Wu, Wei Wang, Bo Li, Bo Zhang and Yigang Ding. This is an open access article distributed under the terms of the [Creative Commons Attribution 4.0 International License](https://creativecommons.org/licenses/by/4.0/), which permits unrestricted use and distribution provided the original author and source are credited.





CALL FOR PAPERS

Trends in Renewable Energy

ISSN Print: 2376-2136 ISSN online: 2376-2144

<http://futureenergysp.com/index.php/tre/>

Trends in Renewable Energy (TRE) is an open accessed, peer-reviewed semi-annual journal publishing reviews and research papers in the field of renewable energy technology and science. The aim of this journal is to provide a communication platform that is run exclusively by scientists. This journal publishes original papers including but not limited to the following fields:

- ✧ Renewable energy technologies
- ✧ Catalysis for energy generation, Green chemistry, Green energy
- ✧ Bioenergy: Biofuel, Biomass, Biorefinery, Bioprocessing, Feedstock utilization, Biological waste treatment,
- ✧ Energy issues: Energy conservation, Energy delivery, Energy resources, Energy storage, Energy transformation, Smart Grid
- ✧ Environmental issues: Environmental impacts, Pollution
- ✧ Bioproducts
- ✧ Policy, etc.

We publish the following article types: peer-reviewed reviews, mini-reviews, technical notes, short-form research papers, and original research papers.

The article processing charge (APC), also known as a publication fee, is fully waived for the Trends in Renewable Energy.

Call for Editorial Board Members

We are seeking scholars active in a field of renewable energy interested in serving as volunteer Editorial Board Members.

Qualifications

Ph.D. degree in related areas, or Master's degree with a minimum of 5 years of experience. All members must have a strong record of publications or other proofs to show activities in the energy related field.

If you are interested in serving on the editorial board, please email CV to editor@futureenergysp.com.